

Novel effects of glycosylation loss and anaesthetics on Kv1.2 channels

By

Daniel Oluwamayowa Fajonyomi

A thesis submitted in partial fulfillment of the requirements for the degree of

Master of Science

Department of Pharmacology

University of Alberta

© Daniel Oluwamayowa Fajonyomi, 2020

ABSTRACT

Slow gating regulation is an extrinsic regulatory mechanism that inhibits the activation of Kv1.2 channels. Physiological factors modulating slow gating regulation are incompletely understood and the interplay between slow gating regulation and Kv1.2 channel pharmacology is unexplored. In chapter 3, I investigated how N-glycosylation influences Kv1.2 sensitivity to slow gating regulation. Using site-directed mutagenesis, I generated glycosylation deficient Kv1.2 channels by mutating the Kv1.2 N-glycosylation site at asparagine (N) 207. Using whole-cell patch-clamp electrophysiology, I characterized the activation properties of glycosylation deficient Kv1.2 channels in mammalian cell lines. I found the activation of glycosylation deficient Kv1.2 channels was strikingly inhibited compared to wild-type Kv1.2, and further investigated whether this arose from direct effects on channel gating, or an interaction with Kv1.2 slow gating. Manipulations that attenuate slow gating regulation relieved the inhibited activation of these channels. Specifically, the Thr252Arg mutation, previously shown to attenuate slow gating regulation, also weakened the slow gating features of glycosylation deficient Kv1.2 channels. Activating prepulses caused accelerated activation of glycosylation deficient channels, consistent with activity-dependent relief of slow gating. Furthermore, co-expression with a recently described Kv1.2 regulatory partner, Slc7a5, abolished slow gating regulation in both WT and glycosylation deficient Kv1.2. Finally, I showed glycosylation deficient channels and WT Kv1.2 channels exhibit similar activation properties in *Xenopus* oocytes using two-electrode voltage clamp, in contrast to the apparent differences between these channels in mammalian cell lines, illustrating that the inhibited activation of glycosylation deficient channels is likely not an intrinsic property. Taken together, these results demonstrate that glycosylation deficient Kv1.2 exhibits enhanced sensitivity to slow gating regulation.

I also investigated the influence of slow gating regulation on Kv1.2 pharmacology by testing the response of various Kv1.2 mutants to the general anaesthetic propofol. Propofol modulation of

Kv1.2 mutants was measured using whole-cell patch clamp electrophysiology of cell lines with intact mechanisms of slow gating regulation. Propofol exerted a combination of inhibitory and potentiating effects on Kv1.2 channels. Propofol inhibited Kv1.2 current magnitudes and caused a time-dependent decay of Kv1.2 currents consistent with open state block of Kv1.2 channels. However, Kv1.2 channel mutants showed differing sensitivities to these inhibitory effects, correlated to their propensity for slow gating regulation. Superimposed on these inhibitory effects, propofol shifted the voltage-dependence of Kv1.2 to more negative voltages and accelerated Kv1.2 channel activation kinetics. These findings suggest these potentiating effects are due to propofol-mediated disruption of the slow gating regulation of Kv1.2 channels. Overall, this thesis demonstrates that post-translational modifications of Kv1.2 can influence their sensitivity to extrinsic regulatory mechanisms, highlight the impact of extrinsic regulatory mechanisms on ion channel pharmacology, and describe the first instance of modulation of slow gating regulation of Kv1.2 by a small molecule (propofol).

PREFACE

This thesis is an original work by Daniel Fajonyomi. No part of this thesis has been previously published. Slc7a5 modulation of WT Kv1.2 described in Chapter 3 was measured and analyzed by Victoria Baronas. The two-electrode voltage clamp experiments in Chapter 3 were performed together with Jingru Li. Daniel Fajonyomi performed all other experiments and analysed the data. Daniel Fajonyomi performed all experiments and data analysis in Chapter 4.

ACKNOWLEDGEMENTS

I would like to thank my supervisor Harley Kurata for the opportunity to perform this research. Your patience, guidance, and commitment to my development during my graduate studies have made it a better experience than I could have imagined. I would also like to thank my committee members, Amy Tse and Frances Plane, for their advice and support. I would like to thank all the lab mates I have worked with during my time in the Kurata lab - Damayantee Das, Jingru Li, Jasmine Maghera, Richard Kanyo, Shawn Lamothe, Nazlee Sharmin, Camilla Lund, Tarek Ammar, Victoria Baronas, Caroline Wang, Runying Yang, and Yubin Hao. I am very grateful for all the support each of you gave me. I would also like to thank the friends who have been there all the way, I value and appreciate you all. Finally, thank you to my parents for making this possible.

TABLE OF CONTENTS

ABSTRACT.....	ii
PREFACE.....	iv
ACKNOWLEDGEMENTS.....	v
TABLE OF CONTENTS.....	vi
LIST OF FIGURES.....	ix
LIST OF ABBREVIATIONS.....	x
Chapter 1: Introduction.....	1
Section 1.1: Voltage-gated potassium channels-An overview.....	1
Section 1.2: Architecture of Voltage-gated potassium channels.....	1
1.2.1: Selectivity filter.....	5
1.2.2: S6 bundle crossing.....	6
1.2.3: Glycosylation of Kv channels.....	6
Section 1.3: Voltage-dependent gating of Kv channels.....	7
1.3.1: Motion of the Kv channel voltage sensor.....	8
1.3.2: Electromechanical coupling in Kv channels.....	9
1.3.3: N- and C-type inactivation.....	9
Section 1.4: Localization and function of Kv1.2 channels.....	11
1.4.1: Central nervous system.....	11
1.4.2: Peripheral nervous system.....	14
1.4.3: Cardiovascular system.....	15
Section 1.5: Regulation of Kv1.2 channels.....	15
1.5.1: Interacting regulatory proteins.....	15
1.5.2: Slow gating regulation.....	19
1.5.3: Post-translational modifications.....	21
1.5.4: Lipids.....	23
Section 1.6: Pharmacology of Kv1.2 channels.....	24
1.6.1: General anaesthetics.....	24
1.6.2: Peptide toxins.....	25
1.6.3: 4-Aminopyridine.....	27
Section 1.7: Scope of thesis investigation.....	27
Chapter 2: Materials and Methods.....	28

2.1.1: Mutagenesis and expression.....	28
2.1.2: Cell culture	28
2.1.3: Whole-cell patch clamp recordings.....	29
2.1.4: Two-electrode voltage clamp recordings	29
2.1.5: Wash-in experiments	30
2.1.6: Electrophysiology data analysis	30
Chapter 3: Glycosylation loss increases the sensitivity of Kv1.2 channels to slow gating regulation	32
Section 3.1: Introduction	32
Section 3.2: Results.....	34
3.2.1: Slow activation kinetics of glycosylation deficient Kv1.2 mutants.....	34
3.2.2: Activation properties of Kv1.2[N207A/Q] channels implicate slow gating regulation	36
3.2.3: Slow gating of glycosylation mutants is attenuated by the T252R mutation	36
3.2.4: Altered use-dependent activation properties in glycosylation deficient channels	38
3.2.5: Slow activation is not an intrinsic property of glycosylation deficient Kv1.2 channels.....	40
3.2.6: Slc7a5 competes with slow gating regulation in Kv1.2 channels	42
3.2.7: Reducing conditions attenuate Slc7a5 effects on glycosylation mutants	47
3.2.8: Slow gating regulation is absent in <i>Xenopus laevis</i> oocytes	49
3.2.9: Delayed deactivation kinetics of glycosylation deficient channels	50
Section 3.3: Discussion	52
3.3.1: Interaction between Slc7a5 and slow gating regulation	53
3.3.2: Previously reported effects of glycosylation loss on Kv1.2 channels.....	54
Chapter 4: Propofol exerts contrasting functional effects on Kv1.2 channels and interacts with slow gating regulation	56
Section 4.1: Introduction	56
Section 4.2: Results.....	57
4.2.1: Kv1.2 currents progressively decay in propofol	57
4.2.2: Propofol inhibits Kv1.2 channel peak currents.....	61
4.2.3: Propofol potentiates Kv1.2 channel activation	62
4.2.4: Propofol potentiates Kv1.2 channels by modifying slow gating regulation	67
Section 4.3: Discussion	68
4.3.1: Propofol inhibition of Kv1.2 channels.....	69
4.3.2: Propofol inhibits Kv1.2 channels by an open channel block mechanism	69
4.3.3: Modification of slow gating regulation by propofol	70

4.3.4: Previously reported effects of propofol on Kv1.2 channels	71
4.3.5: Exploring roles for Kv1.2 channels in anesthesia.	72
Chapter 5: General discussion & Conclusion	74
5.1.1: Glycosylation loss promotes slow gating inhibition	75
5.1.2: Modification of ion channel glycosylation <i>in-vivo</i>	76
5.1.3: Biophysical effects of glycosylation on voltage-gated ion channels	77
5.1.4: Inhibited activation of glycosylation deficient Kv1.2 channels is not consistent with an intrinsic biophysical mechanism	78
5.1.5: Mechanism of increased slow gating inhibition in glycosylation deficient channels...	79
5.1.6: Novel effects of propofol on Kv1.2 channels.....	80
5.1.7: Impact of slow gating regulation on Kv1.2 pharmacology	83
5.1.8: Conclusion	84
BIBLIOGRAPHY	85

LIST OF FIGURES

Figure 1.1: Schematic depiction of the transmembrane topology of an individual Kv channel α -subunit	2
Figure 1.2: Inverted teepee structure of the stereotypical Kv channel pore.	4
Figure 1.3: Hypothetical model of Kv1.2 slow gating regulation.....	21
Figure 1.4: Illustration of the Kv1.2 extracellular N207 glycosylation site on the S1-S2 linker and the Thr252 site on the intracellular S2-S3 linker.	23
Figure 3.1: Glycosylation deficient Kv1.2 channels have prominent slow activation kinetics.....	35
Figure 3.2: Slow gating of Kv1.2[N207A] channels is attenuated by the T252R mutation.....	38
Figure 3.3: Enhanced use-dependent activation in Kv1.2[N207A] channels.....	40
Figure 3.4: Pre-pulse potentiation of Kv1.2[N207A] channel activation.	42
Figure 3.5: Slc7a5 competes with the slow gating mechanism in wild-type Kv1.2 channels.	44
Figure 3.6: Slc7a5 antagonizes slow gating regulation of Kv1.2[N207A] channels.	46
Figure 3.7: The Slc7a5 effect on Kv1.2 channels is diminished in reducing conditions.....	48
Figure 3.8: Slow gating of Kv1.2 channels is absent in <i>Xenopus laevis</i> oocytes.....	50
Figure 3.9: Glycosylation deficient Kv1.2 channels exhibit delayed deactivation kinetics.	51
Figure 4.1: Kv1.2 channel currents progressively decay in propofol.	59
Figure 4.2: Propofol inhibits Kv1.2 channel peak currents.	62
Figure 4.3: Propofol hyperpolarized the GV relationships of Kv1.2 channels.....	64
Figure 4.4: Propofol hyperpolarized the activation $V_{1/2}$ of all cells.	66
Figure 4.5: Depolarized activation $V_{1/2}$ values in control correlate with large $V_{1/2}$ shifts in propofol.	68
Figure 5.1: Factors modulating occupancy of the fast and slow gating modes.	75
Figure 5.2: Model of Kv1.2 potentiation by propofol.	82

LIST OF ABBREVIATIONS

4-AP: 4-Aminopyridine
AIS: Axon initial segment
BC: Basket cells
cDNA: Complementary DNA
CHO: Chinese Hamster Ovary cell line
DMSO: Dimethyl sulfoxide
DNA: Deoxyribonucleic acid
DRG: Dorsal root ganglion
DTT: Dithiothreitol
ER: Endoplasmic Reticulum
GABA: Gamma (γ)-aminobutyric acid
HEK 293: Human embryonic kidney 293 cell line
HERG: Human Ether-à-go-go-Related Gene
Hz: Hertz
IC₅₀: Concentration required to achieve half maximal inhibition
K⁺: Potassium ion
Kv: Voltage-gated potassium ion channel
Kv α : Voltage-gated potassium ion channel alpha (α)-subunit
Kv β : Voltage-gated potassium ion channel beta (β)-subunit
LM: Mouse fibroblast cell line
mAChR: M1 muscarinic acetylcholine receptor
mM: Millimolar
MNTB: Medial nucleus of the trapezoid body
ms: Millisecond
mV: Millivolt
M Ω : Megaohm
N-glycosylation: Asparagine (N) linked glycosylation
nA: Nanoamp
NADPH: Nicotinamide adenine dinucleotide phosphate
NADH: Nicotinamide adenine dinucleotide
Nav: Voltage-gated sodium ion channel
nM: Nanomolar

pA: Picoamp
PCR: Polymerase chain reaction
PD: Pore domain
pH: potential of hydrogen
PIP₂: Phosphatidylinositol 4,5-bisphosphate
RNA: Ribonucleic acid
s: Second
TEA⁺: Tetraethylammonium ion
TEVC: Two-electrode voltage clamp
TIM barrel: Triose phosphate isomerase barrel
μM: Micromolar
v/v: Volume per volume
V_{1/2}: Half-voltage of activation
VSD: Voltage-sensing domain
WT: Wild type
σ-1 receptor: Sigma-1 receptor
τ: Time constant
τ_m: Membrane time constant

Amino acid	Three letter Abbreviation	Single letter abbreviation
Alanine	Ala	A
Arginine	Arg	R
Asparagine	Asn	N
Aspartic acid	Asp	D
Cysteine	Cys	C
Glutamine	Gln	Q
Glutamic acid	Glu	E
Glycine	Gly	G
Histidine	His	H
Isoleucine	Ile	I
Leucine	Leu	L
Lysine	Lys	K
Methionine	Met	M
Phenylalanine	Phe	F
Proline	Pro	P
Serine	Ser	S
Threonine	Thr	T
Tryptophan	Trp	W
Tyrosine	Tyr	Y
Valine	Val	V

Chapter 1: Introduction

Section 1.1: Voltage-gated potassium channels-An overview

Voltage-gated potassium ion channels (Kv channels) are transmembrane proteins with ion selective pores that facilitate the movement of potassium ions through plasma membranes in the direction of their electrochemical gradient (Yellen, 1998). Kv channels are expressed in a variety of cells and tissues, including excitable cells of the brain, heart, pancreas, and muscle. (Chandy et al., 2004; Ranjan et al., 2019; Vallon et al., 2005; Wulff et al., 2009). Opening and closing of Kv channels is controlled primarily by voltage (Yellen, 1998), however, additional unrecognized mechanisms that influence their gating likely exist. The movement of cationic potassium ions from the intracellular environment to the extracellular environment following the opening of Kv channels results in hyperpolarization of the membrane potential (Wulff et al., 2009). Thus in excitable cells, Kv channels contribute to membrane repolarization following an action potential, and influence the shape and frequency of action potentials (Robbins and Tempel, 2012; Wulff et al., 2009).

Section 1.2: Architecture of Voltage-gated potassium channels

Kv channels are tetrameric structures composed of four pore-forming alpha (α)-subunits that assemble to form a functional channel (MacKinnon, 1991). In mammals, there are forty pore-forming Kv channel α -subunits, encoded by individual genes (Ranjan et al., 2019). The Kv channel α -subunits are classified into twelve voltage-gated potassium ion channel subfamilies based on sequence similarity termed Kv1-Kv12 (Ranjan et al., 2019). Only α -subunits belonging to the same subfamily can assemble to form Kv channels (Covarrubias et al., 1991). For example, Kv1 subfamily α -subunits can only form Kv channel tetramers with other Kv1 subfamily α -subunits and do not assemble with Kv2 subfamily α -subunits (Christie et al., 1990;

Covarrubias et al., 1991; Li et al., 1992). The T1 domain, in the N-terminal region of Kv channel α -subunits, controls the specificity of Kv channel assembly (Figure 1.1) (Shen and Pfaffinger, 1995; Shen et al., 1993). Sequences in the T1 domain regulate the recognition and assembly of Kv channel α -subunits (Shen and Pfaffinger, 1995). Incompatibility between the T1 domain sequences of α -subunits belonging to different Kv channel subfamilies is likely the basis of the specificity of Kv channel assembly (Shen and Pfaffinger, 1995).

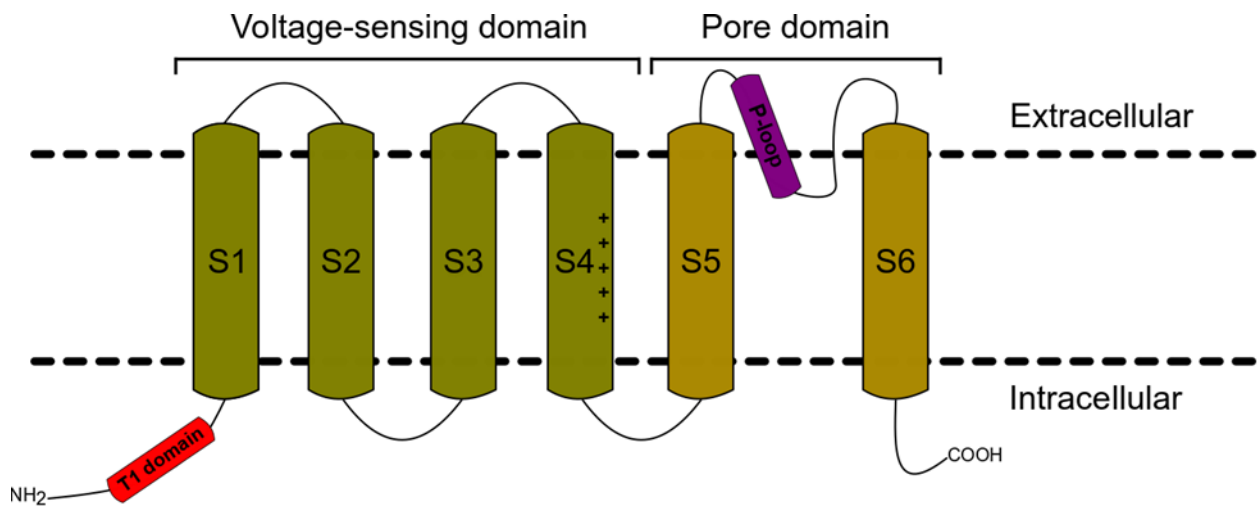


Figure 1.1: Schematic depiction of the transmembrane topology of an individual Kv channel α -subunit

Kv channel α -subunits possess six transmembrane segments termed S1-S6, the voltage-sensing domain (VSD) is formed by S1-S4 (olive) and the pore domain (PD) is formed by S5 and S6 (light brown) and the P-loop (purple). The T1 domain on the N-terminus (red) regulates α -subunit assembly while the P-loop contains the signature sequence and forms the selectivity filter.

Each Kv channel α -subunit consists of six transmembrane segments termed S1-S6 (Figure 1.1) (Kuang et al., 2015). The S1-S4 transmembrane segments form the voltage-sensing domain of Kv channels (Figure 1.1) (Kuang et al., 2015; Labro and Snyders, 2012). The S4 transmembrane segment has positively charged arginine and lysine residues interspersed by two hydrophobic residues in a highly conserved triplet pattern, such that there is a positively charged residue in every third position (Kuang et al., 2015; Swartz, 2008). The S1-S3 transmembrane segments also contribute to voltage-dependent gating. Negatively charged

residues in the S1-S3 segments stabilize the positive charges in the S4 segment which is hypothesized to aid S4 movement (Blunck and Batulan, 2012; Kuang et al., 2015; Swartz, 2008). The pore domain of Kv channels is formed by the S5 and S6 segments, together with a re-entrant loop called the P-loop which links these helices (Figure 1.1) (Barros et al., 2019; Sands et al., 2005). The S5, P-loop, and S6 sections from each of the four α -subunits assemble to form a central ion conduction pore whose structure is described as an inverted teepee (Figure 1.2) (Barros et al., 2019; Doyle et al., 1998; Kuang et al., 2015; Sands et al., 2005). At the cytoplasmic end of the pore, the C termini of the four S6 segments form a bundle crossing called the S6 gate or “bundle crossing” which prevents access to the pore when channels are closed (Figure 1.2) (Blunck and Batulan, 2012; Labro and Snyders, 2012). Beyond the S6 gate is a wide and central water-filled cavity that leads to the selectivity filter at the extracellular end of the pore (Figure 1.2) (Doyle et al., 1998; Heginbotham et al., 1994).

Extracellular

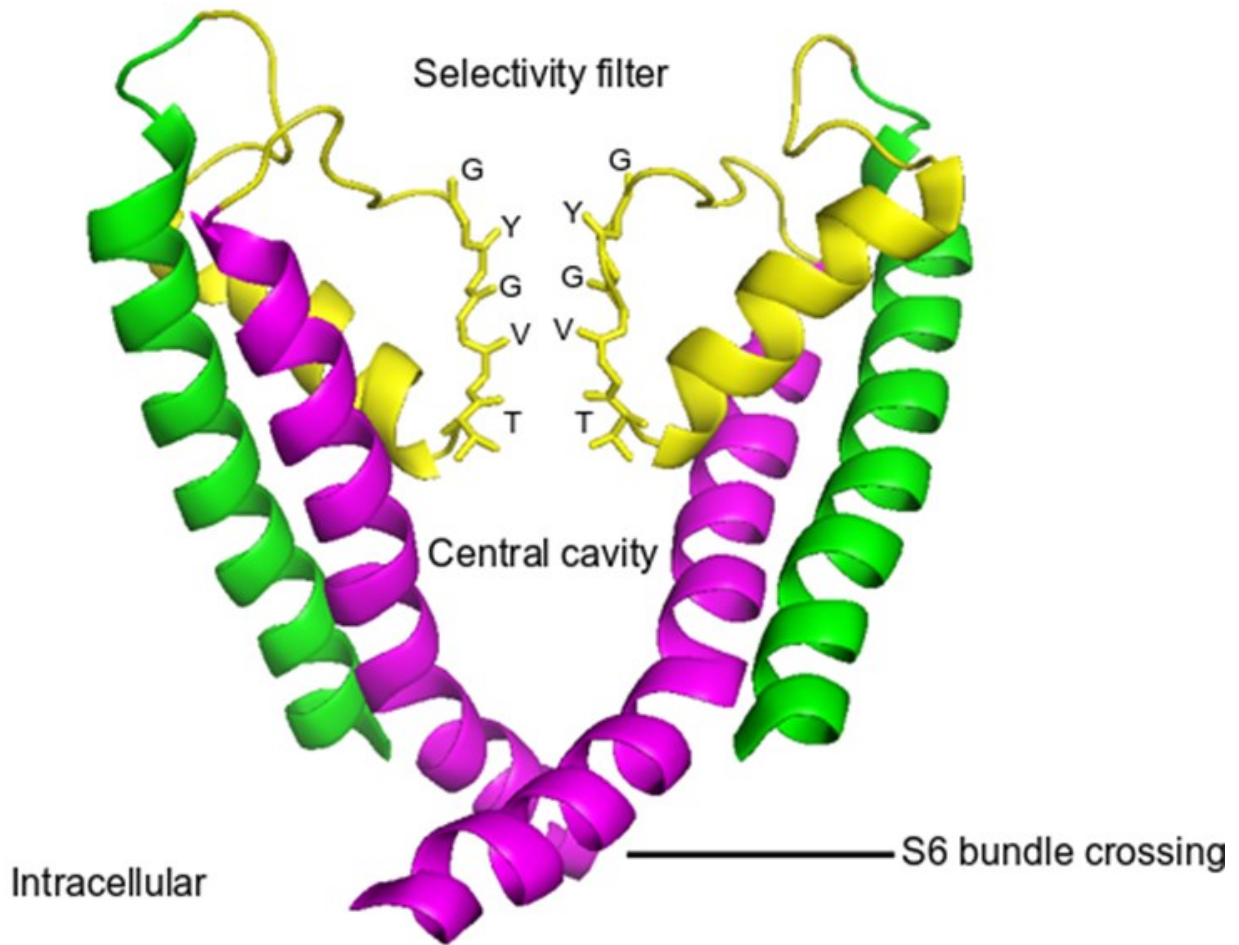


Figure 1.2: Inverted teepee structure of the stereotypical Kv channel pore.

Atomic resolution structure of the pore-forming domain of Kv1.2, with 2 subunits (Front and Rear) omitted for clarity. The structure shows the S5 (green), P-loop (yellow), and S6 (magenta) sections of the two α -subunits. The kink in the S6 transmembrane segment is visible. The backbone carbonyl oxygen atoms of the TVGYG signature sequence are shown pointing into the pore and are labeled, threonine contributes a carbonyl oxygen and a hydroxyl oxygen to the filter. The location of the S6 gate or bundle crossing is also labeled. Structure adapted from PDB file 3LUT, a structural model of Kv1.2 (Chen et al., 2010).

1.2.1: Selectivity filter

The selectivity filter is a narrow structure formed by the P-loops extending towards the pore and is responsible for potassium ion selectivity in Kv channels (Doyle et al., 1998; Kim and Nimigean, 2016). It contains the conserved signature sequence of potassium ion channels, TXGYG, in Kv1.2 channels this sequence is TVGYG (Figure 1.2) (Heginbotham et al., 1994; Kim and Nimigean, 2016; Labro and Snyders, 2012). The backbone carbonyl oxygens of the TVGYG sequence and the side chain hydroxyl oxygen of threonine point towards the pore and form four evenly spaced potassium ion binding sites (Kim and Nimigean, 2016). Each potassium ion binding site accommodates a single dehydrated potassium ion (Armstrong, 2003; Kim and Nimigean, 2016; Kuang et al., 2015). Thus, potassium ions in the water-filled central cavity must dehydrate to pass through the selectivity filter (Armstrong, 2003; Kim and Nimigean, 2016; Kuang et al., 2015). The oxygen atoms in the selectivity filter are arranged to mimic the hydration of potassium ions in water, which minimizes the energy cost of potassium ions dehydrating to enter the filter (Armstrong, 2003; Doyle et al., 1998; Kuang et al., 2015).

The arrangement of oxygen atoms in the selectivity filter also functions to exclude the passage of cations such as sodium ions through the pore (Armstrong, 2003; Doyle et al., 1998; Kim and Nimigean, 2016). Their hydration shell is not mimicked by the oxygen atoms in the selectivity filter thus entry into the filter is energetically unfavorable (Armstrong, 2003; Doyle et al., 1998; Kim and Nimigean, 2016). The selectivity filter is hypothesized to exclude anions by electrostatic repulsion from the electronegative end of carbonyl dipoles in the filter (Armstrong, 2003).

Potassium ions move through the selectivity filter in a single file and only two potassium ions are present in the filter at a time (Kuang et al., 2015). The electrochemical gradient of potassium controls the direction of net potassium flux through the selectivity filter, and electrostatic repulsion between nearby potassium ions in the selectivity filter accelerates the exit of ions (Armstrong, 2003; Kim and Nimigean, 2016; Kuang et al., 2015). As a result of the selectivity

filter properties, potassium ion channels are approximately 10,000 times more selective for potassium ions over sodium ions, and potassium ions conduct through the pore at a rate near the diffusion limit (Kuang et al., 2015).

1.2.2: S6 bundle crossing

In Kv channels, the cytoplasmic entrance to the pore is blocked by a bundle crossing formed by the S6 transmembrane helices (Figure 1.2) (Labro and Snyders, 2012). The S6 segment in Kv channels has a conserved PXP motif where X is a hydrophobic amino acid (Labro et al., 2003). Proline tends to bend helices, causing the S6 segment to adopt a “bent” or “kinked” structure (Figure 1.2) (Labro et al., 2003; Labro and Snyders, 2012). The PXP motif contributes to a flexible hinged region that allows for movement of the S6 in response to channel opening and closing (Labro et al., 2003; Labro and Snyders, 2012). Mutation of the prolines in the PXP motif to other amino acids results in non-functional channels or channels with altered gating properties (Labro et al., 2003; Labro and Snyders, 2012). In the closed state, the S6 bundle crossing forms a tight constriction that acts as a hydrophobic seal and prevents entry of potassium ions into the pore (del Camino and Yellen, 2001; Labro and Snyders, 2012; Long et al., 2005a). However, when Kv channels open, the S6 constriction widens and permits pore access (del Camino and Yellen, 2001; Labro and Snyders, 2012; Long et al., 2005a).

1.2.3: Glycosylation of Kv channels

Glycosylation is a crucial post-translational modification of proteins that occurs mainly in the endoplasmic reticulum and Golgi apparatus of cells (Moremen et al., 2012; Spiro, 2002). There are 4 known types of glycosylation in vertebrates which are classified based on the nature of the glycan-protein linkage: N-glycosylation, O-glycosylation, C-glycosylation, and Glypiation (Moremen et al., 2012; Spiro, 2002). In N-glycosylation, glycans are attached to asparagine side chains on proteins through an amide bond (Moremen et al., 2012). O-glycosylation refers to

glycans attached to the hydroxyl side chains of serine, threonine, tyrosine, or hydroxylysine (Moremen et al., 2012; Spiro, 2002). In C-glycosylation, also referred to as C-mannosylation, the C1 carbon of mannose is attached to the C2 carbon of Tryptophan's indole ring in a carbon-carbon bond (Moremen et al., 2012; Spiro, 2002). In glypiation, a glycosylphosphatidylinositol is attached to the C-terminal end of proteins, typically to an amino acid residue with small side chains such as alanine and cysteine (Spiro, 2002). Almost fifty percent of human proteins are glycosylated with N-glycosylation being the most common type (Moremen et al., 2012).

Glycosylation affects the stability and surface expression of several Kv channel types (Napp et al., 2005; Petrecca et al., 1999; Thayer et al., 2016; Watanabe et al., 2015, 2003). Glycosylation is required for surface expression in Kv channels such as HERG (Petrecca et al., 1999), however, surface expression can still occur in the absence of glycosylation such as with Kv1.2 (Watanabe et al., 2007). Glycosylation also influences the gating properties of Kv channels such as Kv1.2 and may play a role in the regulation of Kv channel gating (Napp et al., 2005; Watanabe et al., 2007, 2003). The results in this thesis indicate glycosylation may play a role in Kv1.2 regulation by accessory proteins.

Section 1.3: Voltage-dependent gating of Kv channels

Interaction between positive charges on the S4 transmembrane segment and the membrane electric field is the basis of Kv channel voltage-dependent gating (Kuang et al., 2015; Swartz, 2008). The positive charges on S4 translocate through the membrane electric field in response to voltage changes (Kuang et al., 2015). However, the motions of the S4 segment and the mechanisms that couple this motion to S6 gate opening and closing are incompletely understood.

1.3.1: Motion of the Kv channel voltage sensor

There are several models for the motion of S4 following voltage changes. In the helical screw model, the S4 segment is drawn towards the intracellular environment by the electrostatic force of the negative resting membrane potential (Catterall, 2010). Depolarization alters this electrostatic interaction resulting in the vertical movement of the S4 segment towards the extracellular environment, rotating as it moves through the membrane (Catterall, 2010). In contrast, the paddle model describes a region of S3, S3b, and S4 as a voltage-sensor paddle (Jiang et al., 2003b). At rest, the paddle is close to the intracellular environment due to the negative resting membrane potential and is positioned almost horizontally (Jiang et al., 2003b, 2003a). On depolarization, the paddle moves a large distance across the membrane to its extracellular position, tilting to a more vertical orientation (Jiang et al., 2003b, 2003a). In the transporter model tilting of the S4 segment with minimal movement through the membrane occurs in response to voltage changes (Chanda et al., 2005). Over the years, and with the ongoing emergence of high resolution structures of ion channels, these diverse models of S4 movement have been consolidated into a single consensus model (Kuang et al., 2015). In this consensus model, negative charges in the S1-S3 transmembrane segments form pair-wise interactions with positive charges in the S4 segment (Kuang et al., 2015; Yarov-Yarovoy et al., 2006). These interactions stabilize the positive charges in S4 (Kuang et al., 2015). On channel activation, the S4 segment undergoes conformational changes that are posited to be a combination of rotation, vertical translations, and a tilt in position (Kuang et al., 2015; Vargas et al., 2011; Yarov-Yarovoy et al., 2006). The S4 segment is also posited to transition from an α -helix to a 3_{10} helical conformation that allows the S4 to extend and twist to maintain interactions with the negative charges in the S1-S3 transmembrane segments (Kuang et al., 2015; Vargas et al., 2011).

1.3.2: Electromechanical coupling in Kv channels

Current knowledge prevents detailed elucidation of the mechanisms that couple S4 movement to pore opening. However, it is clear that the S4 moves in response to voltage changes, and that this movement is transduced to the S6 gate by the S4-S5 linker (Blunck and Batulan, 2012; Vardanyan and Pongs, 2012). The S4-S5 linker is an alpha-helical structure that links the S4 and S5 segments and physically interacts with the C-terminus of the S6 segment from the same alpha-subunit (Long et al., 2005b). The S6 helix possesses a bend, created by the conserved PXP motif, that allows the C-terminus of S6 to run parallel to the membrane and create a platform for the S4-S5 linker (Long et al., 2005b). Mutations and chimeric replacements in the regions of the S4-S5 linker and S6 C-terminus that are in close contact often leads to non-functional Kv channels or channels with aberrant coupling between voltage changes and pore opening, highlighting the importance of this interaction in voltage-dependent gating (Blunck and Batulan, 2012; Haddad and Blunck, 2011; Lu et al., 2002; Vardanyan and Pongs, 2012). For several Kv channels, all four S4 segments must activate before the pore opens in a concerted step (Blunck and Batulan, 2012; Jensen et al., 2012; Labro and Snyders, 2012). However, in some Kv channels such as KCNQ1, all S4 segments do not need to activate before pore opening and potassium ion conduction occurs (Osteen et al., 2012; Westhoff et al., 2019).

1.3.3: N- and C-type inactivation

The inactivated state is a non-conducting channel state distinct from the open and closed gating states (Kuang et al., 2015; Rasmusson et al., 1998). There are two broadly recognized mechanisms of inactivation, N-type inactivation and C-type inactivation (Kuang et al., 2015). N-type inactivation is a rapid form of inactivation where the cytoplasmic entry to the pore is physically blocked following pore opening, preventing the entry of potassium ions (Kuang et al., 2015). This is often referred to as a ball and chain mechanism, as the blocking particle is

thought of as a mobile 'ball' tethered to the channel by a flexible peptide 'chain' (Kim and Nimigean, 2016; Zagotta et al., 1990). Some rapidly inactivating Kv channels such as Kv1.4 possess an N-terminal region that forms an inactivation ball directly tethered to the channel (Fan et al., 2012; Kim and Nimigean, 2016; Rettig et al., 1994). However, in other delayed rectifier Kv channels such as Kv1.1 and Kv1.2, rapid N-type inactivation can be conferred by association with Kv-beta ($Kv\beta$) subunits that possess an inactivation ball (Long et al., 2005a; Rettig et al., 1994; Stühmer et al., 1989).

In contrast to N-type inactivation, C-type inactivation is a slower form of inactivation that is proposed to occur due to conformational changes in the selectivity filter and the extracellular side of the pore (Kurata and Fedida, 2006). This proposition is supported by several observations. C-type inactivation is inhibited by high extracellular potassium ion concentrations and extracellular application of the pore blocker TEA⁺ (Baukrowitz and Yellen, 1995; Kurata and Fedida, 2006). The presence of K⁺ or TEA⁺ ions in the pore is believed to prevent the conformational changes that underlie C-type inactivation by promoting occupancy of an ion binding site in the selectivity filter (Baukrowitz and Yellen, 1995; Kurata and Fedida, 2006). Conversely, intracellular application of quaternary ammonium blockers and N-type inactivation promote C-type inactivation, likely by preventing occupancy of the selectivity filter binding site controlling C-type inactivation (Baukrowitz and Yellen, 1996; Kurata and Fedida, 2006). Furthermore, a structure of the bacterial potassium ion channel KcsA in low potassium concentration shows the oxygen atoms in the KCSA selectivity filter adopt a non-conducting state in this condition (Zhou et al., 2001). However, this structural arrangement has not been directly linked with C-type inactivation (Kurata and Fedida, 2006).

Section 1.4: Localization and function of Kv1.2 channels

Kv1.2 channels belong to the Kv1 subfamily of voltage-gated potassium ion channels (Shamotienko et al., 1997). They can be homotetramers composed of four identical Kv1.2 α -subunits or heterotetramers containing other Kv1 subfamily α -subunits (Coleman et al., 2002; Shamotienko et al., 1997). Kv1.2 channels are expressed in the central nervous system, the peripheral nervous system, and the cardiovascular system (Coleman et al., 2002; Rasband et al., 2001; Roberds and Tamkun, 1991; Wang et al., 1994, 1993). Due to their activation at subthreshold voltages, and slow time course of activation and inactivation, Kv1.2 channels primarily regulate excitability by setting the action potential threshold (Dodson and Forsythe, 2004; Robbins and Tempel, 2012). However, heteromerization with other Kv1 subfamily α -subunits such as Kv1.4 and association with regulators such as Kv β proteins provides functional diversity to Kv1.2 channels by altering their gating properties (Coleman et al., 2002; Ranjan et al., 2019; Rettig et al., 1994; Rhodes et al., 1995; Sheng et al., 1995). The importance of Kv1.2 channels in regulating excitability is highlighted by the fact that mutations in Kv1.2 cause severe epilepsies and ataxias in humans (Corbett et al., 2016; Hundallah et al., 2016; Pena and Coimbra, 2015; Syrbe et al., 2015).

1.4.1: Central nervous system

Myelinated axons

Myelinated axons in several brain regions exhibit high expression of Kv1.2 channels in their juxtaparanodes, located near the nodes of Ranvier, and in their axon initial segments (Arancibia-Carcamo and Attwell, 2014; Robbins and Tempel, 2012; Wang et al., 1994, 1993). The axon initial segment (AIS) is considered the initiation site of action potentials, as the high concentration of voltage-gated sodium channels at the AIS enables action potential initiation (Robbins and Tempel, 2012). Kv1.2 channels are localized to the AIS in multiple cell types by

the membrane-associated guanylate kinase PSD-93, where they play a key role in regulating action potential initiation and firing (Dodson et al., 2002; Kole et al., 2007; Lorincz and Nusser, 2008; Ogawa et al., 2008; Robbins and Tempel, 2012). Kv1.2 channels are clustered to the juxtaparanodes of myelinated axons by the cell adhesion molecule TAG-1 and the neurexin protein Caspr2 (Poliak et al., 2003; Traka et al., 2003). Kv1.2 channels at the juxtaparanode are thought to regulate internodal excitability, and an increase in Kv1.2 activity at the juxtaparanode could be involved in the loss of action potential propagation observed in demyelinating conditions (Arancibia-Carcamo and Attwell, 2014).

Cerebral Cortex

Kv1.2 channels are widely distributed in the cerebral cortex. They are expressed in the neuropil of the cortex; the axon initial segment (AIS) and apical dendrites of layer V pyramidal neurons; the AIS of layer II/III pyramidal neurons, and in the AIS of cortical GABAergic interneurons (Lorincz and Nusser, 2008; Sheng et al., 1994). Kv1.2 channels in the AIS of cortical neurons likely act to shape action potentials. The expression pattern of Kv1.2 channels in the AIS of layer II/III pyramidal neurons appears to correlate with the expression of Nav1.6, the dominant voltage-gated sodium channel type at this site (Lorincz and Nusser, 2008). Studies with pharmacological blockers of Kv1 channels in layer V pyramidal neurons have demonstrated a role for AIS Kv1.2 channels in modulating action potential duration (Katz et al., 2018; Kole et al., 2007; Lorincz and Nusser, 2008; Shu et al., 2007).

Hippocampus

Kv1.2 channels are expressed in several regions of the human hippocampus, typically as heteromeric channels with Kv1.1 (Willis et al., 2018). The CA2/3 stratum pyramidale, dentate gyrus hilus, and CA1 stratum oriens show the highest Kv1.2 expression (Willis et al., 2018). Kv1.2 expression has also been established in the CA1 stratum radiatum and the molecular

layer of the dentate gyrus (Willis et al., 2018). Studies in animal models provide additional information on the subcellular localization of Kv1.2 in these regions. Kv1.2 channels in the molecular layer of the dentate gyrus are localized to the axons and axon terminals of perforant path neurons, originating in the entorhinal cortex (Monaghan et al., 2001; Wang et al., 1994; Willis et al., 2018). Kv1.2 channels in the CA1 stratum radiatum are expressed in the axons and axon terminals of Schaffer collaterals (Monaghan et al., 2001; Willis et al., 2018). In CA3, Kv1.2 is localized to the axon terminals of mossy fibers which synapse with CA3 pyramidal neurons (Sheng et al., 1994), and to the axon initial segment of CA3 pyramidal neurons (Lorincz and Nusser, 2008). Hippocampal Kv1.2 channels contribute to a dendrotoxin sensitive, low threshold, and slowly inactivating potassium current called the D-type current which is involved in regulating burst firing of hippocampal neurons (Chen and Johnston, 2004; Hyun et al., 2013; Metz et al., 2007).

Cerebellum

Approximately 80% of the Kv1.2 channels in the cerebellum are heteromers mixed with a Kv1.1 α -subunit (Koch et al., 1997). Kv1.2 channels are found in complex with Kv1.1 in the axon terminals of cerebellar basket cells (Kole et al., 2015; Wang et al., 1993). Basket cell axon terminals make contact with the axon initial segment (AIS) of Purkinje neurons, the sole efferent output from the cerebellar cortex, in a structure called the pinceau (Iwakura et al., 2012; Kole et al., 2015; Southan and Robertson, 1998). As the AIS is the site of action potential initiation, basket cells regulate the ultimate output of Purkinje neurons (Southan and Robertson, 1998). Kv1.2 channels are also localized to the cell bodies and dendrites of Purkinje neurons (Sheng et al., 1994). Studies with pharmacological blockers of Kv1.2 containing channels have indicated a potential role of Kv1.2 in suppressing Purkinje hyperexcitability (Khavandgar et al., 2005; McKay et al., 2005).

Brainstem

Kv1.2 channels in the brainstem play a crucial role in sound source localization. In the auditory brainstem pathway, a medial nucleus of the trapezoid body (MNTB) neuron receives excitatory glutamatergic input from a large synapse, the calyx of Held, formed by the axon terminal of a globular bushy cell (Kopp-Scheinflug et al., 2008). The pattern of action potentials in this network transmits information pivotal for localizing sounds (Dodson et al., 2002). Homomeric Kv1.2 channels and heteromeric Kv1.1/Kv1.2 channels are expressed presynaptically to the calyx of Held, in bushy cell axons (Dodson et al., 2003; Ishikawa et al., 2003). The activation of Kv1.2 channels in bushy cell axons prevents hyperexcitability and maintains the temporal precision of action potentials that reach the calyx (Dodson et al., 2003; Ishikawa et al., 2003). Kv1.2/Kv1.1 channels are also expressed in the axon initial segment of MNTB neurons (Dodson et al., 2002). Their localization in the AIS of MNTB neurons ensures that each excitatory postsynaptic potential from the calyx produces a single action potential in the target MNTB neuron, further acting to preserve the pattern of action potential firing in this network (Dodson et al., 2002).

1.4.2: Peripheral nervous system

Myelinated afferent axons of medium to large diameter dorsal root ganglion (DRG) neurons express Kv1.2 channels in their juxtaparanodes, typically as heteromers with Kv1.1 (Kv1.2/Kv1.1) or with Kv1.1 and Kv1.4 (Kv1.2/Kv1.1/Kv1.4) (Fan et al., 2014; Rasband et al., 2001). Downregulation of Kv1.2 channel expression in medium and large DRG neurons raises the resting membrane potential, reduces the threshold for action potentials, and increases action potential frequency (Zhao et al., 2013), suggesting Kv1.2 channels in these neurons are key regulators of excitability. Reduced Kv1.2 channel expression in DRG neurons is observed in injury models of neuropathic pain and linked to DRG neuron hyperexcitability, a causative factor of neuropathic pain (Fan et al., 2014; Kim et al., 2002; Rasband et al., 2001; Zhao et al., 2013).

The reduced expression of Kv1.2 channels following DRG injury may be due to injury-induced methylation of KCNA2, the gene encoding Kv1.2, by the DNA methyltransferase DNMT3a which suppresses KCNA2 expression (Zhao et al., 2017).

1.4.3: Cardiovascular system

The highest Kv1.2 expression is found in the central nervous system. However, Kv1.2 channels are also expressed, albeit at lower levels, in the atria and ventricles of the heart, and the aorta (Roberds and Tamkun, 1991). In atrial myocytes, Kv1.2 channels underlie the $I_{K,DTX}$ cardiac current, one of the cardiac delayed-rectifier currents that contribute to the repolarization of atrial myocytes following an action potential (Bou-Abboud and Nerbonne, 1999; Nerbonne, 2000). Kv1.2 channels are also expressed in vascular smooth muscle cells in heteromeric complexes (Frances et al., 2005). These Kv1.2 heteromeric channels regulate vasomotor tone by contributing to the control of the resting membrane potential (Kerr et al., 2001; Knot and Nelson, 1995; Plane et al., 2005; Yuan et al., 1998).

Section 1.5: Regulation of Kv1.2 channels

This section explores the regulatory mechanisms that influence Kv1.2 channels. The regulatory mechanisms discussed in this section likely underrepresent the regulatory signals of Kv1.2 channels but demonstrate the profound effects regulators have on Kv1.2 channel function.

1.5.1: Interacting regulatory proteins

Kv β

Kv β proteins are cytoplasmic accessory proteins of Kv channels. They bind to Kv channels in the endoplasmic reticulum via the T1 domain, located in the N-terminus of Kv channel α -subunits (Gulbis et al., 2000; Torres et al., 2007). Kv β and Kv α subunits assemble in a 1:1 ratio,

thus a tetrameric Kv channel will be associated with four Kv β subunits (Torres et al., 2007). The Kv β proteins that have been identified are Kv β 1, Kv β 2, Kv β 3, and their splice variants (Pongs and Schwarz, 2010). Kv β 1 and Kv β 2 have the splice variants Kv β 1.1-1.3 and Kv β 2.1-2.2, respectively (Pongs and Schwarz, 2010).

Kv β proteins alter the surface expression, deactivation kinetics, activation kinetics, and inactivation properties of Kv channels (Pongs and Schwarz, 2010). However, the ability of Kv β proteins to exert these effects varies depending on the Kv β protein splice variant and Kv α subunit type (Pongs and Schwarz, 2010). Arguably the most notable gating effect of Kv β proteins is their ability to confer rapid N-type inactivation to typically non-inactivating Kv channels. This effect is specific to Kv β 1 and Kv β 3 proteins which possess an N-terminal inactivation region that is absent in Kv β 2 (Long et al., 2005a; Majumder et al., 1995; Rettig et al., 1994). Immunoprecipitation studies in mammalian brains and cell lines indicate Kv1.2 homomeric and heteromeric channels associate with Kv β 1 and Kv β 2, while effects of Kv β 3 on Kv1.2 gating have been demonstrated (Bähring et al., 2004; Coleman et al., 2002; Nakahira et al., 1996; Rhodes et al., 1995). Co-expression with Kv β 1 confers N-type inactivation to typically non-inactivating Kv1.2 channels and significantly increases their surface expression (Accili et al., 1997; Peters et al., 2009). Kv β 2, the most abundant Kv β subunit in the brain, promotes Kv1.2 surface expression, stability, and N-glycosylation *in-vitro*, but does not induce N-type inactivation (Rhodes et al., 1995; Shi et al., 1996). Kv β 3 also confers N-type inactivation to Kv1.2 channels but does not appear to increase their surface expression (Bähring et al., 2004). The effects of Kv β proteins on Kv1.2 surface expression are mediated by co-translational association with Kv1.2 which occurs early in the biosynthetic pathway (Shi et al., 1996).

Studies examining the sequence, structure, and binding properties of the Kv β proteins have determined they belong to the aldo-keto reductase enzyme superfamily (Gulbis et al., 2000; McCormack and McCormack, 1994; Tipparaju et al., 2007; Weng et al., 2006). Aldo-keto

reductases are a superfamily of enzymes that catalyze the reduction of aldehyde or ketone groups to alcohols using NADPH or NADH as cofactors (Barski et al., 2008). The conserved core sequence of Kv β proteins shows homology to aldo-keto reductase protein sequences, and examination of the Kv β 2 structure reveals Kv β proteins possess a TIM barrel containing a catalytic site, similar to aldo-keto reductases (Gulbis et al., 1999; McCormack and McCormack, 1994; Pongs and Schwarz, 2010). Furthermore, similar to aldo-keto reductases, Kv β proteins can utilize NADPH as a cofactor in catalytic reactions; in fact, the presence of NADPH increases the rate of Kv1 channel inactivation when Kv β proteins are present (Tipparaju et al., 2007; Weng et al., 2006). Interestingly, Kv β proteins exhibit properties that would indicate a physiological function typical of aldo-keto reductases, and yet they are regulators of Kv channels. This theme of unconventional proteins regulating Kv1.2 channels features prominently throughout this section.

Slc7a5

Slc7a5 (or LAT1) is a broadly expressed transmembrane transporter with a canonical role in the transport of neutral amino acids (Scalise et al., 2018). Co-expression of Slc7a5 also generates profound effects on Kv1.2 expression and gating (Baronas et al., 2018; Sharmin et al., 2020). Co-expression of Slc7a5 with Kv1.2 significantly reduces total Kv1.2 protein expression and the density of Kv1.2 currents measured in electrophysiological experiments, with some current recovery observed following prolonged hyperpolarization (Baronas et al., 2018; Sharmin et al., 2020). In terms of its consequences on Kv1.2 gating, Slc7a5 co-expression hyperpolarizes the activation half-voltage of Kv1.2 channels by ~50 mV and promotes C-type inactivation (Baronas et al., 2018; Sharmin et al., 2020). These gating effects are suspected to be mediated by interactions with the Kv1.2 voltage sensor (Sharmin et al., 2020). The regulation of Kv1.2 by Slc7a5 could play a role in neurological conditions. Mutations in Slc7a5 that have been associated with autism spectrum disorder and motor deficits attenuate the effects of Slc7a5 on

Kv1.2 gating (Baronas et al., 2018; Tărlungeanu et al., 2016). Additionally, Kv1.2 mutations associated with epilepsy and ataxia increased Kv1.2 sensitivity to the effects of Slc7a5 (Baronas et al., 2018).

Sigma-1 receptor

The sigma-1 (σ -1) receptor is a chaperone and signalling modulator protein that is primarily resident in the mitochondria-associated ER membrane (Kourrich et al., 2013, 2012). Following binding and activation by agonists such as cocaine, σ -1 receptors can translocate from the mitochondria-associated ER membrane to other cellular regions such as the plasma membrane (Kourrich et al., 2013, 2012; Su et al., 2010). σ -1 receptors interact with Kv1.2 channels in the nucleus accumbens shell, and this interaction is thought to be involved in cocaine addiction (Delint-Ramirez et al., 2020; Kourrich et al., 2012). Behavioural sensitization to cocaine is associated with the reduced firing of medium spiny neurons in the nucleus accumbens shell (Delint-Ramirez et al., 2020; Kourrich et al., 2013; Mu et al., 2010). Cocaine increases the formation of σ -1 receptor-Kv1.2 complexes and upregulates the surface expression of Kv1.2 channels in the nucleus accumbens shell, resulting in elevation of Kv1.2-mediated K⁺ currents (Delint-Ramirez et al., 2020; Kourrich et al., 2013). Knockdown of σ -1 receptor expression prevents the increase in Kv1.2 surface expression following cocaine administration (Kourrich et al., 2013). Elevated Kv1.2 currents following cocaine administration may contribute to cocaine-induced hypoexcitability of medium spiny neurons (Delint-Ramirez et al., 2020; Kourrich et al., 2013). The σ -1 receptor has also been postulated to act as a modulator of Kv1.2 slow gating due to its effects on the activation properties of Kv1.2 channels (Abraham et al., 2019). However, σ -1 receptor overexpression has considerably smaller gating effects on Kv1.2 relative to previous reports on slow gating (Baronas et al., 2017, 2015b, 2015a; Rezazadeh et al., 2007).

1.5.2: Slow gating regulation

HEK 293, CHO, and Ltk- mammalian cell lines expressing Kv1.2 channels exhibit quite variable activation kinetics and voltage-dependence of channel gating (Rezazadeh et al., 2007). Widely variable half-activation voltage ($V_{1/2}$) values ranging from -35 mV to +40 mV have been recorded in separate studies (Baronas et al., 2017; Rezazadeh et al., 2007). Examination of their gating properties revealed Kv1.2 channels gate along two gating modes with distinctive gating properties, a *fast gating mode* characterized by *fast activation kinetics* and *hyperpolarized GV relationships*, and a *slow gating mode* characterized by relatively *slow activation kinetics* and *depolarized GV relationships* (Rezazadeh et al., 2007). This creates overall variation in gating properties for cells expressing Kv1.2 channels, produced by differences in the population of slow and fast channels from cell to cell (Rezazadeh et al., 2007). In this thesis, the phenomenon of Kv1.2 channel inhibition by the slow gating mode is referred to as slow gating or slow gating regulation.

Previous studies have identified manipulations that modulate Kv1.2 slow gating. The application of depolarizing prepulses to slow mode Kv1.2 channels accelerates their activation kinetics and shifts their activation half-voltage towards the hyperpolarized voltages characteristic of fast mode gating (Baronas et al., 2015a; Rezazadeh et al., 2007). The potentiating effect of activating prepulses on Kv1.2 channels reflects activity dependent relief from slow gating inhibition (Baronas et al., 2015a; Rezazadeh et al., 2007). Conversely, slow gating recovers when channels are held closed by hyperpolarized voltages (Rezazadeh et al., 2007). This prepulse potentiation effect demonstrates it is possible to interconvert Kv1.2 channels between the slow and fast gating modes, and that the slow gating phenotype is not intrinsic to Kv1.2 channels (Baronas et al., 2015a; Rezazadeh et al., 2007). Pre-pulse potentiation of Kv1.2 channels translates to use-dependent increases in Kv1.2 currents in response to brief repetitive depolarizations (Baronas et al., 2015a). As a result, slow gating regulation has also been

referred to as use-dependent activation (Baronas et al., 2015a). These gating features are unique to Kv1.2 channels among the Kv1 family and have also been reported in primary hippocampal neuron cultures derived from rats (Baronas et al., 2015a).

Mutations of Kv1.2 threonine 252 and extracellular reducing conditions also modulate slow gating regulation (Figure 1.3). The mutation of Kv1.2 threonine 252, located in the intracellular S2-S3 linker of Kv1.2, to charged or bulky amino acids such as arginine or phenylalanine, can abolish slow gating entirely (Baronas et al., 2015a, 2015b; Rezazadeh et al., 2007). Conversely, reducing agents such as DTT and TCEP promote the slow gating mode (Baronas et al., 2017). Kv1.2 channels exposed to reducing agents exhibit prominent use-dependence, considerably decelerated activation kinetics, and extremely depolarized activation half-voltages (ranging from approximately +50 mV to +80 mV) (Baronas et al., 2017). The effect of reducing agents on Kv1.2 channels is insensitive to mutation of Kv1.2 transmembrane cysteines, suggesting this effect is not due to modification of Kv1.2 cysteines by reducing agents (Baronas et al., 2017).

The mechanisms underlying Kv1.2 slow gating regulation are unknown. However, the observations regarding this mechanism discussed in this section led to the hypothesis that Kv1.2 slow gating is mediated by an extrinsic, transmembrane, redox-sensitive regulatory molecule that unbinds from Kv1.2 channels following activation, and rebinds when channels are closed, acting to stabilize the closed state (Figure 1.3) (Baronas et al., 2017, 2015b). This hypothesis is depicted schematically in Figure 1.3. The likely involvement of a transmembrane protein is indicated by the fact that slow gating regulation is attenuated by mutations at Thr252 in the *intracellular* S2-S3 linker, but is also promoted by *extracellular* reducing conditions (Baronas et al., 2017, 2015a). This suggests that the regulatory process is mediated by features on both the extracellular and intracellular sides of the plasma membrane. However, the possibility exists that additional signaling components are involved (Baronas et al., 2017). Slow gating regulation could act to inhibit excitability *in-vivo* (Baronas et al., 2015a, 2015b). Use-

dependent activation may produce increases in Kv1.2 currents during periods of repeated action potential firing *in-vivo*, resulting in hyperpolarization of the membrane and suppressing the generation of action potentials (Baronas et al., 2015a, 2015b).

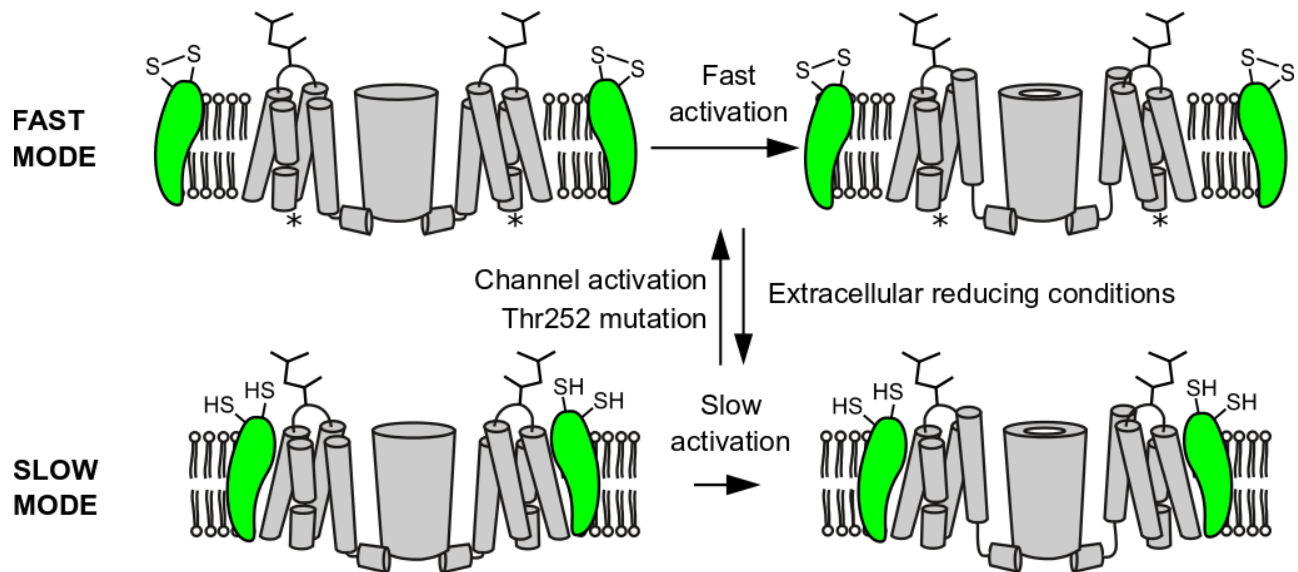


Figure 1.3: Hypothetical model of Kv1.2 slow gating regulation

Kv1.2 transmembrane segments are depicted in grey, together with a hypothetical transmembrane protein that acts as a slow gating regulator. Kv1.2 channels are either bound to the slow gating regulator in the “slow” mode or unbound from the regulator in the “fast” mode. In the slow mode, Kv1.2 channel opening is inhibited due to binding of the slow gating regulator, and channel activation is slow. Conversely, fast mode channels are unbound from the regulator and activate rapidly. Channel activation causes this regulator to unbind, switching Kv1.2 channels from the “slow” gating mode to the “fast” gating mode. Conversely, this regulator can rebind to Kv1.2 channels in the closed state, underlying recovery of slow gating when channels are held closed. Extracellular reducing conditions are sensed by the slow gating regulator (possibly by a vital disulfide bond as depicted), increasing its affinity for Kv1.2 and promoting occupancy of the slow gating mode. Mutation of Thr252 in the S2-S3 linker, indicated by the asterisk, is proposed to alter the binding site of the regulator, resulting in weakened interaction of the regulator with Kv1.2 channels and increased occupancy of the fast gating mode (Baronas et al., 2017, 2015b).

1.5.3: Post-translational modifications

Phosphorylation

Kv1.2 channels in mammalian brains are extensively phosphorylated (Yang et al., 2007). The phosphorylation state of Kv1.2 channels is a key regulator of their surface expression and interaction with other proteins. This is illustrated by M1 muscarinic acetylcholine receptor (mAChR) regulation of Kv1.2 expression and currents. Activation of G-coupled M1 mAChRs decreases Kv1.2 currents via an endocytotic mechanism dependent on tyrosine kinase phosphorylation of Kv1.2 channels (Hattan et al., 2002; Huang et al., 1993; Nesti et al., 2004). M1 mAChR mediated suppression of Kv1.2 currents requires RhoA, a GTPase protein involved in actin regulation and endocytosis (Cachero et al., 1998; Stirling et al., 2009). RhoA activation triggers Kv1.2 endocytosis and significantly decreases Kv1.2 currents, an effect that is attenuated by mutation of a Kv1.2 phosphorylation site at Tyrosine 132 (Cachero et al., 1998; Stirling et al., 2009). M1 mAChR activation also results in the phosphorylation of tyrosine residues in the Kv1.2 C-terminus, this phosphorylation curtails the interaction between Kv1.2 and cortactin, an actin regulating protein that binds to the C-terminus of Kv1.2 channels (Hattan et al., 2002). Further illustrating the role of phosphorylation in the surface expression of Kv1.2 channels, mutation of Kv1.2 serine residues 440 and 441, which are phosphorylated in human brains, inhibits Kv1.2 currents and surface expression in heterologous cell lines (Yang et al., 2007).

Glycosylation

Kv1.2 channels are N-glycosylated at a single glycosylation site at asparagine (N) 207 on their S1-S2 linker (Figure 1.4) (Thayer et al., 2016). Interestingly, all Kv1 family proteins are glycosylated on their S1-S2 linker except for Kv1.6, which is non-glycosylated (Shi and Trimmer, 1999; Thayer et al., 2016). Glycosylated Kv1.2 channels in rat brains possess complex glycan trees with sialic acid residues (Shi and Trimmer, 1999). However, the Kv1.2 glycan structure can vary when channels are expressed in heterologous cell lines (Shi and Trimmer, 1999; Thayer et al., 2016). The glycosylation state of Kv1.2 channels is coupled to their surface

expression. Loss of Kv1.2 glycosylation decreases the surface expression of Kv1.2 channels and increases their degradation rate (Thayer et al., 2016; Watanabe et al., 2007; Zhu et al., 2009). Glycosylation state may also influence Kv1.2 gating. Non-glycosylated Kv1.2 channels, generated by mutating the N207 site, are reported to exhibit modestly slower activation and deactivation kinetics, which combine to generate a depolarized shift in their activation $V_{1/2}$ when expressed in CHO cells (Watanabe et al., 2007). These effects were attributed to the loss of negatively charged sialic acids that would be present in the glycosylated Kv1.2 sugar tree (Watanabe et al., 2007). In this thesis, I demonstrate that glycosylation loss also increases sensitivity to regulation by the slow gating regulatory mechanism.

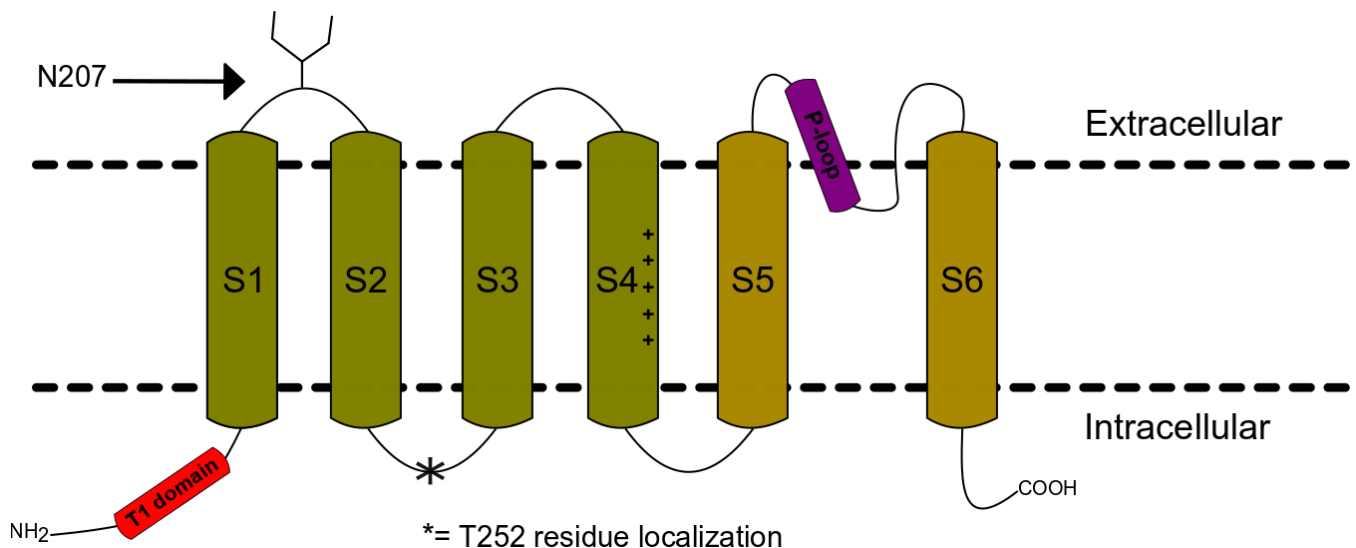


Figure 1.4: Illustration of the Kv1.2 extracellular N207 glycosylation site on the S1-S2 linker and the Thr252 site on the intracellular S2-S3 linker.

1.5.4: Lipids

Phosphatidylinositol 4,5-bisphosphate (PIP₂)

Phosphatidylinositol 4,5-bisphosphate (PIP₂) is the most abundant phosphoinositide lipid found in the plasma membrane and influences the function of Kv1.2 channels (Kruse and Hille, 2013).

The depletion of PIP₂ reduces the current amplitude of Kv1.2 channels, decelerates their deactivation, and produces a hyperpolarizing shift in their activation V_{1/2} (Kruse and Hille, 2013; Rodriguez-Menchaca et al., 2012). PIP₂ perfusion reverses these effects (Rodriguez-Menchaca et al., 2012). PIP₂ is believed to simultaneously restrain the movement of Kv1.2 voltage-sensors and stabilize the open state of Kv1.2 pores via interactions with positively charged amino acids on Kv1.2 (Rodriguez-Menchaca et al., 2012). The loss of these interactions may underlie the effects of PIP₂ depletion on Kv1.2 gating (Rodriguez-Menchaca et al., 2012). The regulation of Kv1.2 channels by PIP₂ is pertinent to the function of Kv1.1/Kv1.2 channels in spiral ganglion neurons, the primary cochlear afferents (Smith et al., 2015). Kv1.1/Kv1.2 channels in spiral ganglion neurons regulate rapid adaptation, a mechanism that contributes to the maintenance of the temporal precision of action potentials (Smith et al., 2015). The depletion of PIP₂ inhibits Kv1.1/Kv1.2 channels and prevents rapid adaptation, suggesting regulation of Kv1.2 channels by PIP₂ is vital to this mechanism (Smith et al., 2015).

Section 1.6: Pharmacology of Kv1.2 channels

This thesis examines the effects of the alkylphenol anesthetic propofol on Kv1.2 channels, demonstrating novel functional effects of propofol on Kv1.2 channel gating. This section provides an overview of chemicals and peptides that act on Kv1.2 channels, their effects, and their identified mechanisms of action.

1.6.1: General anaesthetics

Volatile inhalation and intravenous general anaesthetics can modulate the activity of Kv channels including Kv1.2. The effect of anaesthetics on Kv1.2 channel activity can result in channel potentiation or inhibition depending on the anaesthetic (Li et al., 2018). The inhaled anaesthetic sevoflurane potentiates heterologously expressed Kv1.2 channels with no inhibitory

effects (Barber et al., 2012; Liang et al., 2015; Lioudyno et al., 2013; Woll et al., 2017). At physiologically relevant concentrations, sevoflurane increases the maximum conductance of WT Kv1.2 channels by ~13% and produces a -4 mV hyperpolarized shift in their activation $V_{1/2}$ (Barber et al., 2012; Liang et al., 2015; Lioudyno et al., 2013). Sevoflurane is postulated to hyperpolarize the activation $V_{1/2}$ of Kv1.2 by binding to a cavity formed by the S4-S5 linker and S6 segment and promoting electromechanical coupling of Kv1.2 activation (Woll et al., 2017). This is supported by experiments demonstrating mutation of the leucine 317 residue in the S4-S5 linker of Kv1.2 channels diminishes the effect of sevoflurane on their activation $V_{1/2}$ (Woll et al., 2017). However, this mutation does not affect the sevoflurane-induced increase of Kv1.2 maximum conductance, leading to the suggestion that potentiating effects of sevoflurane occur by separate mechanisms (Liang et al., 2015; Woll et al., 2017). The effect of sevoflurane on the maximum conductance is suggested to be a result of interactions with residues near the external pore region of Kv1.2 (Liang et al., 2015; Woll et al., 2017). Isoflurane, another inhalation anaesthetic, potentiates the conductance of Kv1.2 channels by ~11.5% in *Xenopus laevis* oocytes (Liang et al., 2015). Anaesthetics such as chloroform, halothane, n-butanol, and propofol have been examined for activity on WT Kv1.2 channels expressed in *Xenopus laevis* oocytes (Bu et al., 2018; Liang et al., 2015). Except for n-butanol which inhibits Kv1.2 currents at high concentrations, these anaesthetics showed minimal or no inhibitory or potentiating effects (Bu et al., 2018; Liang et al., 2015).

1.6.2: Peptide toxins

Scorpion toxins

Scorpion toxins are structurally related peptides 23-43 amino acids in length that can act as potent blockers of Kv channels (Miller, 1995; Rodríguez de la Vega et al., 2003). Low nanomolar concentrations of the scorpion toxins charybdotoxin, maurotoxin, and tityustoxin-K

alpha effectively inhibit currents from heterologously expressed Kv1.2 channels (Visan et al., 2004; Werkman et al., 1993, 1992). IC₅₀ values of 1.7 nM, 0.7 nM, and 0.21 nM, respectively, have been recorded in experiments with mammalian cell lines (Visan et al., 2004; Werkman et al., 1993, 1992). These toxins produce a concentration-dependent block of Kv1.2 channel currents with minimal or no recorded effects on their activation kinetics and activation half-voltage (Castle et al., 2003; Sprunger et al., 1996; Visan et al., 2004; Werkman et al., 1993, 1992). Charybdotoxin however has been shown to accelerate the deactivation kinetics of Kv1.2 channels expressed in *X. laevis* oocytes (Sprunger et al., 1996). Scorpion toxins inhibit potassium channel currents by binding to sites around the external opening of the pore and physically preventing potassium ion conduction (Avdonin et al., 2000; MacKinnon and Miller, 1989, 1988; Visan et al., 2004; Werkman et al., 1993).

Dendrotoxins

Dendrotoxins are 57-60 amino acid proteins isolated from the venom of mamba snakes (Harvey, 1997). They are homologous to Kunitz serine protease inhibitors but lack significant antiprotease activity (Harvey, 1997). The dendrotoxins are potent blockers of Kv1.1, Kv1.2, and Kv1.6 channels, whereas other Kv channel types are relatively insensitive (Rettig et al., 1992; Stühmer et al., 1989; Swanson et al., 1990). This property of dendrotoxins has been utilized to characterize *in-vivo* Kv channels (Dodson et al., 2002; Scott et al., 1990; Wang et al., 1999). Currents from heterologously expressed Kv1.2 channels are potently and reversibly inhibited by alpha (α)-dendrotoxin and dendrotoxin-I in a concentration-dependent manner (Hopkins et al., 1994; Robertson, 1996; Stühmer et al., 1989; Werkman et al., 1992). IC₅₀ values of 4 nM and 0.13 nM have been reported for α -dendrotoxin and dendrotoxin-I, respectively, in experiments with *X. laevis* oocytes (Hopkins et al., 1994; Stühmer et al., 1989). Dendrotoxins block Kv channels by associating with residues in the external pore mouth, likely in the P-loop, and

physically preventing the conduction of potassium ions, similar to scorpion toxins (Hopkins et al., 1994; Hurst et al., 1991; Tytgat et al., 1995).

1.6.3: 4-Aminopyridine

4-AP inhibits Kv1.2 channel currents in a reversible and concentration-dependent manner, although the reported IC_{50} values for this block vary (Hart et al., 1993; Kerr et al., 2001; Russell et al., 1994; Stühmer et al., 1989). The opening of Kv1.2 channels is required for 4-AP block, indicating 4-AP inhibition requires pore access and occurs via an open channel block mechanism (Russell et al., 1994). The block of Kv channels by 4-AP restores conduction in demyelinated neurons (Blight, 1989). Consequently, 4-AP has been utilized to manage neurological symptoms in spinal cord injury and demyelinating conditions such as multiple sclerosis (Blight, 2011, 1989; Segal et al., 1999).

Section 1.7: Scope of thesis investigation

The gating of Kv1.2 channels is modulated by slow gating regulation, one of several recognized and unrecognized regulatory mechanisms of voltage-gated ion channels. In chapter 3, I describe the increased sensitivity of Kv1.2 channels to slow gating regulation after glycosylation loss. In chapter 4, I describe a combination of novel potentiating and inhibitory effects of the general anaesthetic propofol on Kv1.2 channels and the influence of slow gating regulation on these effects of propofol. Overall, this thesis addresses gaps in our understanding of the factors that tune the modulation of ion channels by regulatory mechanisms and the implications of regulatory mechanisms on ion channel pharmacology.

Chapter 2: Materials and Methods

2.1.1: Mutagenesis and expression

Kv1.2 mutagenesis was done using a two-step overlapping PCR method as described previously (Baronas et al., 2017). Mutagenic primers for the N207A and N207Q mutations were:

N207A 5': CAC CTA TTC CGC CAG CAC CAT TG

N207A 3': CAA TGG TGC TGG CGG AAT AGG TG

N207Q 5': CAC CTA TTC CCA AAG CAC CAT TG

N207Q 3': CAA TGG TGC TTT GGG AAT AGG TG

The Kv1.5N/Kv1.2[N207A] chimera was generated using standard PCR and compatible restriction digestion and ligation of the N-terminus of human Kv1.5 (amino acid #1-243), and the transmembrane domains and C-terminus of rat Kv1.2 (amino acid #156-499). The fragments of Kv1.2 and Kv1.5 were joined at a BspEI restriction site that is present in Kv1.5, as described previously (Rezazadeh et al., 2007). Construction of mCherry-Slc7a5 was described previously (Baronas et al., 2018). All constructs were expressed in the pcDNA3.1(-) vector (Invitrogen) and verified by diagnostic restriction digestion and Sanger sequencing (University of Alberta Applied Genomics Core). DNA for the constructs of interest was transiently transfected into mouse LM (*tk-*) fibroblast cells for whole-cell patch clamp experiments using jetPRIME transfection reagent (Polyplus).

2.1.2: Cell culture

Mouse LM (*tk-*) fibroblast cells (ATCC, referred to as LM cells throughout the study) were used for all whole-cell patch clamp experiments. LM cells were maintained in culture at 37 °C in a 5% CO₂ incubator in Dulbecco's Modified Eagle Medium supplemented with 10% FBS and 1% penicillin/streptomycin. Cells were typically seeded in standard 12 or 24 well culture dishes and

transfected 12 hours after seeding. Transfection efficiency was approximately 20%. Transfected cells were split onto glass coverslips for experiments and recordings were obtained 24-48 hours post-transfection. Co-transfection with fluorescent proteins was used to select cells for electrophysiological recording.

2.1.3: Whole-cell patch clamp recordings

Patch clamp pipettes were manufactured from soda lime capillary glass (Fisher) using a Sutter P-97 puller (Sutter Instrument) and were not coated before recordings. Pipettes had a tip resistance between 1-4 M Ω when filled with standard recording solutions. Recordings were sampled at 10 kHz and filtered at 5 kHz. The typical cell capacitance and series resistance in whole-cell recordings were between 10 to 20 pF and 2 to 4 M Ω , respectively. The maximum cell capacitance and series resistance were 26 pF and 5 M Ω . The estimated membrane time constant (τ_m), based on the maximal cell capacitance and series resistance, is 130 μ s prior to any series resistance compensation. Manual capacitance compensation and series resistance compensation was between 75%-85%. Recordings were stored on a computer hard drive using Clampex 10 software (Molecular Devices). Bath solution had the following composition: 135 mM NaCl, 5 mM KCl, 1 mM CaCl₂, 1 mM MgCl₂, 10 mM HEPES, and was adjusted to pH 7.4 with NaOH. Pipette solution had the following composition: 135 mM KCl, 5 mM K-EGTA, 10 mM HEPES and was adjusted to pH 7.3 using KOH. Chemicals were purchased from Sigma-Aldrich or Fisher. Holding potential for all recordings is -80 mV unless otherwise stated.

2.1.4: Two-electrode voltage clamp recordings

For two-electrode voltage clamp experiments in *Xenopus laevis* oocytes, complementary RNA was transcribed from Kv1.2 cDNAs of interest using the mMessage mMachine T7 kit (Invitrogen). WT Kv1.2, Kv1.2[N207A], and Kv1.2[T252R] in pcDNA3.1(-) were linearized with BglII and transcribed using the T7 primer. Stage V–VI *Xenopus laevis* oocytes were prepared as

previously described (Shih et al., 1998) and injected with mRNA. Voltage-clamped potassium currents were recorded in a modified Ringer's solution composed of: 116 mM NaCl, 2 mM KCl, 1 mM MgCl₂, 0.5 mM CaCl₂, and 5 mM HEPES (pH 7.4), using an OC-725C voltage clamp (Warner). Glass microelectrodes were backfilled with 3 M KCl and had resistances of 0.1–1 MΩ. Recordings were filtered at 5 kHz and digitized at 10 kHz using a Digidata 1440A controlled by pClamp 10 software. Holding potential for all recordings was -80 mV unless otherwise stated.

2.1.5: Wash-in experiments

Propofol (2,6-Diisopropylphenol, 97%) was obtained from Alfa Aesar. The drug was dissolved in DMSO to achieve a stock concentration of 400 mM. Propofol solution for wash-in experiments was made by dissolving propofol stock in bath solution to achieve the desired concentrations. The control solution for wash-in experiments with propofol consisted of DMSO dissolved in bath solution. The DMSO to bath solution ratio in the control solution was equal to the propofol stock to bath solution ratio in the propofol solution. For wash-in experiments with DMSO as test, the control solution was bath solution alone. 0.10% v/v DMSO solution (vehicle control) was prepared by diluting DMSO into bath solution at a 1/1000 ratio. The final concentration of DMSO in all solutions was ≤ 0.10% v/v. All solutions were prepared on the same day experiments were performed and mixed by vortex for 5 minutes prior to use. Test solutions were perfused into the bath for 2-3 minutes prior to test recordings. All solutions were perfused via pressure-driven flow at room temperature.

2.1.6: Electrophysiology data analysis

Conductance–voltage relationships were normalized to the peak conductance and fit with a Boltzmann equation (Equation 1):

$$(1) G = 1/(1 + e^{-(V-V_{1/2})/k})$$

where V is the voltage applied, $V_{1/2}$ is the half-maximal activation voltage, and k is a slope factor reflecting the voltage range over which an e -fold change in open probability (P_o) is observed.

The sum of two Boltzmanns was occasionally required due to conductance-voltage relationships with both slow and fast gating components. In those cases, this form of the Boltzmann equation was used (Equation 2):

$$(2) G = A/(1 + e^{-(V-V_{1/2,a})/k,a}) + (1 - A)/(1 + e^{-(V-V_{1/2,b})/k,b})$$

where A is the proportion of the curve exhibiting the fast gating component, and $1-A$ the slow.

Time constants (τ) of channel activation were obtained by fitting current traces with a single (Equation 3) or double (Equation 4) exponential equation using Clampfit. A sum of two exponentials was often required due to the presence of clearly distinct slow and fast activation components for some channels:

$$(3) A(t) = A(1 - e^{-t/\tau}) + C$$

$$(4) A(t) = A_{slow}(1 - e^{-t/\tau_{slow}}) + A_{fast}(1 - e^{-t/\tau_{fast}}) + C$$

where $A(t)$ is the current at time (t) from the start of the depolarization, A is the maximum current corresponding to either the slow or fast component, and C is a constant. The fractional slow component of gating was calculated as:

$$(5) \text{Fractional slow component} = \frac{A_{slow}}{A_{slow} + A_{fast} + C}$$

Chapter 3: Glycosylation loss increases the sensitivity of Kv1.2 channels to slow gating regulation

Section 3.1: Introduction

The general principles underlying the function of voltage-gated ion channels have been described in detail for certain model channel types, however, our understanding of their regulation by accessory proteins and signaling pathways is less complete. This knowledge gap limits our ability to fully characterize the properties of voltage-gated ion channels, as accessory regulatory proteins with significant effects on channel function have been established for all major voltage-gated ion channel types (Buraei and Yang, 2010; Calhoun and Isom, 2014; Davies et al., 2007; Pongs and Schwarz, 2010). Previously, our group has explored unrecognized mechanisms of ion channel regulation using Kv1.2 channels as a model system. Kv1.2 was the first mammalian voltage-gated channel with a structure reported at atomic resolution, and this information has provided the basis for development of a detailed understanding of voltage-dependent regulation of ion channels (Long et al., 2007, 2005a).

Previous reports have demonstrated considerable variability of Kv1.2 channel gating properties, specifically highly variable activation kinetics and activation $V_{1/2}$ values (see page 18) (Baronas et al., 2015a; Rezazadeh et al., 2007). This is due to Kv1.2 channels exhibiting variable occupancy of at least two gating modes, a *fast gating mode* characterized by *fast activation kinetics* and *hyperpolarized GV relationships*, and a *slow gating mode* characterized by relatively *slow activation kinetics* and *depolarized GV relationships* (Baronas et al., 2015a; Rezazadeh et al., 2007). Cell to cell variations in the proportion of channels in the slow vs fast

gating modes produce the variable activation properties of Kv1.2 channels (Rezazadeh et al., 2007). A summary of the conditions that modulate slow gating regulation as well as a hypothetical model for this mechanism are presented in Figure 1.3.

In this chapter, the effects of glycosylation loss on Kv1.2 channel sensitivity to slow gating regulation are examined. Kv1.2 channels are N-glycosylated at residue N207 in the extracellular S1-S2 linker. In native mammalian tissue the Kv1.2 glycosylation tree is complex with sialic acid residues (Shi and Trimmer, 1999; Thayer et al., 2016; Watanabe et al., 2007; Zhu et al., 2009). Glycosylation is coupled to Kv1.2 expression at the cell surface (Thayer et al., 2016; Watanabe et al., 2007; Zhu et al., 2009). In addition to an effect on surface expression, altered gating properties of glycosylation deficient Kv1.2 channel mutants have been previously described. Mutation of Kv1.2 N207 to a glutamine (Kv1.2[N207Q]) slowed the activation kinetics of Kv1.2 channels and depolarized the Kv1.2 activation half-voltage (Watanabe et al., 2007). The gating effects of the Kv1.2[N207Q] mutation in the Watanabe et al. (2007) study motivated us to investigate whether Kv1.2 glycosylation affects its regulation by the fast and slow gating modes. Using electrophysiological approaches, I have characterized the gating properties of glycosylation deficient Kv1.2 channels and demonstrated the significant sensitivity of these properties to manipulations known to target slow gating. Utilizing the sensitivity of glycosylation deficient Kv1.2 mutants to slow gating regulation, I have extended observations on slow gating in this chapter and will demonstrate interaction of slow gating regulation with Kv1.2 pharmacology in the subsequent chapter. Overall, this chapter reveals that glycosylation plays a role in the sensitivity of Kv1.2 channels to slow gating regulation. Specifically, loss of glycosylation profoundly increases inhibition of Kv1.2 channels by slow gating.

Section 3.2: Results

3.2.1: Slow activation kinetics of glycosylation deficient Kv1.2 mutants

Glycosylation deficient Kv1.2 channels were generated by mutating the Kv1.2 N207 residue in the S1-S2 linker to alanine (A) and glutamine (Q). The N207 site is the sole glycosylation site of Kv1.2 channels (Watanabe et al., 2007; Zhu et al., 2009). Currents recorded from LM cells expressing Kv1.2[N207A] and Kv1.2[N207Q] glycosylation deficient channels exhibited dramatically slowed activation kinetics compared to currents from cells expressing WT Kv1.2 channels (Figure 3.1). The difference in activation kinetics is illustrated by exemplar current traces in Figure 3.1A. The activation time course of Kv1.2[N207A] in response to a +10 mV depolarization is slower than currents from WT Kv1.2 exhibiting either the fast gating phenotype (i.e. rapid activation kinetics) or the slow gating phenotype (i.e. slowed activation kinetics) (Figure 3.1A&B). Previous reports on slow gating regulation observed a population of WT Kv1.2 cells with fast activation time courses, and a population of WT Kv1.2 cells with biphasic activation time courses, due to varying proportions of fast and slow activation components (Rezazadeh et al., 2007). The slow component in these reports was attributed to slow gating regulation (Rezazadeh et al., 2007). In our experiments, we observed WT Kv1.2 cells with exclusively fast activation time courses that were fit with a single exponential equation. In addition, WT Kv1.2 cells exhibiting biphasic activation with slow and fast activation components, were fit with a double exponential equation. Kv1.2[N207A] and Kv1.2[N207Q] currents typically exhibited exclusively slow or biphasic activation time courses. The slow and fast activation components for all currents recorded and their respective time constants were distinguishable.

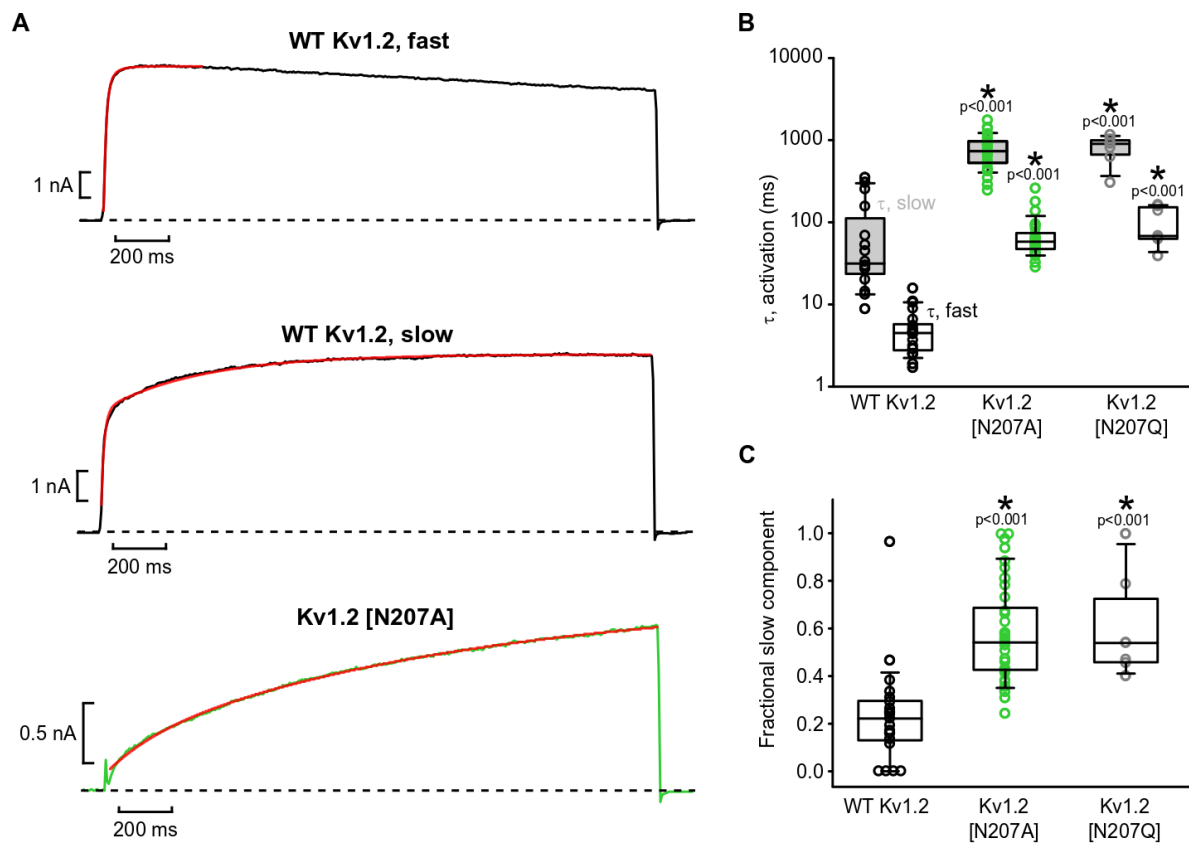


Figure 3.1: Glycosylation deficient Kv1.2 channels have prominent slow activation kinetics.

(A) Exemplar whole-cell recordings of WT Kv1.2 and Kv1.2[N207A] channels expressed in LM cells (2 s depolarization to +10 mV, holding potential of -80 mV). Exponential fits for each current trace are shown in red. WT Kv1.2 exhibits variable activation gating kinetics - samples of a 'fast' cell and a cell exhibiting the 'slow' gating mode are illustrated. (B) Time constants of activation (τ , activation (ms)) for WT Kv1.2 (n=21), Kv1.2[N207A] (n=33), and Kv1.2[N207Q] (n=7) channels. Activating currents were elicited using the protocol described above. The currents were fit with either a single exponential function (Equation 3) or the sum of two exponential functions (double exponential) (Equation 4), to obtain activation time constants for the slow (grey box plots; τ , slow) and fast (white box plots; τ , fast) activation components. (C) The fractional contribution of the slow activation time constant was determined for each cell using Equation 5. A one-way ANOVA (non-parametric Kruskal-Wallis), followed by a post-hoc Dunn's test was used to compare fast and slow time constants between WT Kv1.2 and Kv1.2[N207A/Q]. Significant differences are indicated by * with the associated P value shown.

For currents elicited from cells expressing WT Kv1.2 channels, the median activation time constants (τ , activation) for the slow and fast components were 31 ms (τ , slow) and 5 ms (τ , fast). Kv1.2[N207A] and Kv1.2[N207Q] channels activated with considerably slower kinetics (Figure 3.1B). The median activation time constants for Kv1.2[N207A] channels were 734 ms (τ , slow) and 58 ms (τ , fast). For Kv1.2[N207Q] channels, the activation time constants were 903

ms (τ , slow) and 68 ms (τ , fast). The fractional contribution of the slow activation component to the total current magnitude was also calculated for each cell (Figure 3.1C). The slow component constitutes a significantly greater proportion of the currents from Kv1.2[N207A/Q] channels compared to WT Kv1.2 channels (Figure 3.1C). Thus, Kv1.2[N207A/Q] channels exhibit generally slower activation time constants (Figure 3.1B) and a prominent slow activation component (Figure 3.1C) compared to WT Kv1.2 channels, resulting in very slow activation kinetics.

3.2.2: Activation properties of Kv1.2[N207A/Q] channels implicate slow gating regulation

We observed cell to cell variations in the activation time constants and the fractional contribution of the slow component for glycosylation deficient channels, similar to WT Kv1.2 (Figure 3.1B&C), and consistent with other reports of slow gating (Rezazadeh et al., 2007). The persistence of this variation, and the markedly slow activation of these mutants, prompted further investigation into the involvement of slow gating regulation in their altered activation kinetics. Thus, manipulations previously reported to modify Kv1.2 slow gating regulation were applied to Kv1.2 glycosylation deficient channels. An overview of slow gating regulation and its identified modifiers is provided in the introduction (see page 18 and Figure 1.3). Experiments were performed with Kv1.2[N207A] channels as the Kv1.2[N207A] and Kv1.2[N207Q] mutations had identical functional consequences.

3.2.3: Slow gating of glycosylation mutants is attenuated by the T252R mutation

Mutation of the Kv1.2 T252 residue in the S2-S3 linker to an arginine (R) significantly attenuates sensitivity to the slow gating mode (Baronas et al., 2015b, 2015a; Rezazadeh et al., 2007). Therefore, we tested the effects of the T252R mutation on Kv1.2[N207A] channels (Figure 3.2).

The median activation time constants for Kv1.2[T252R] channels were 43 ms (τ , slow) and 5 ms (τ , fast) (Figure 3.2B), compared to 31 ms (τ , slow) and 5 ms (τ , fast) for WT Kv1.2 channels (Figure 3.1B). The introduction of the T252R mutation to Kv1.2[N207A] channels significantly accelerated their activation kinetics and attenuated the prominent slow activation component (Figure 3.2). Activation time constants at +10 mV were determined for all channels as described in Figure 3.1. The median activation time constants for Kv1.2[T252R] [N207A] channels were 98 ms (τ , slow) and 20ms (τ , fast), compared to 734 ms (τ , slow) and 58 ms (τ , fast) for Kv1.2[N207A] channels (Figure 3.2B). Furthermore, the fractional contribution of the slow activation component was dramatically attenuated in Kv1.2[T252R] [N207A] channels compared to Kv1.2[N207A] channels (Figure 3.2C). Overall, this demonstrates that introduction of the T252R mutation to Kv1.2[N207A] channels relieves their slow activation kinetics and considerably reduces the fractional contribution of the slow component. The effects of the T252R mutation on these parameters provides a direct link between slow gating regulation and the inhibited activation kinetics of glycosylation deficient Kv1.2 channels.

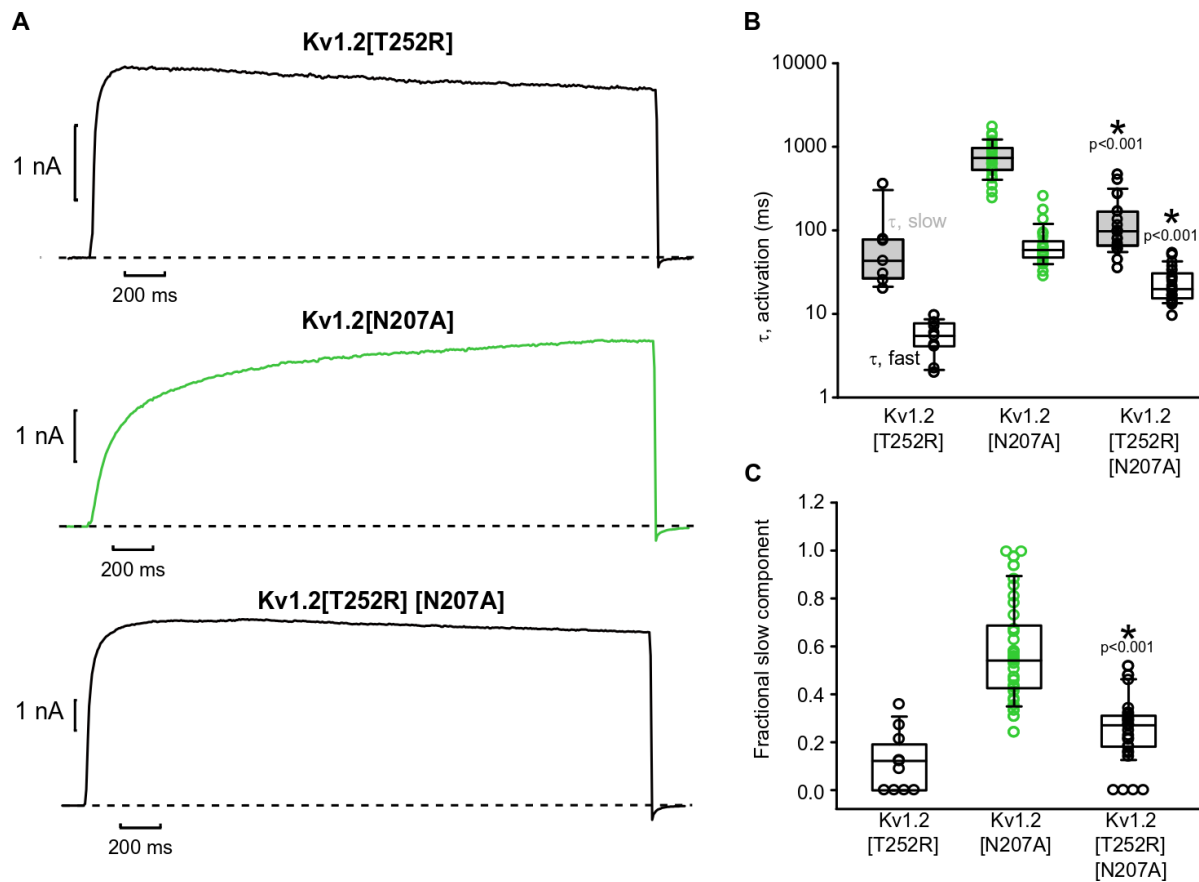


Figure 3.2: Slow gating of Kv1.2[N207A] channels is attenuated by the T252R mutation.

(A) Exemplar whole-cell current recordings of Kv1.2[T252R], Kv1.2[N207A], and Kv1.2[T252R][N207A] channels expressed in LM cells are shown (2 s depolarization to +10 mV, holding potential of -80 mV). (B) Slow (grey box plots; τ , slow) and fast (white box plots; τ , fast) activation time constants are shown for Kv1.2[T252R] (n=11), Kv1.2[N207A] (n=33), and Kv1.2[T252R][N207A] (n=24) channels, time constants were determined as described in Figure 3.1B. (C) The fractional contribution of the slow activation time constant was determined for each cell as described in Figure 3.1C (note that data for Kv1.2[N207A] has been duplicated to allow direct comparison). Kv1.2[T252R][N207A] and Kv1.2[N207A] gating parameters were compared with a Mann-Whitney U test (non-parametric). Significant differences are indicated by * with the associated P value shown.

3.2.4: Altered use-dependent activation properties in glycosylation deficient channels

The slow gating mode of Kv1.2 channels manifests as use-dependent increases in current magnitude during trains of brief repeated depolarizations, constructed to approximate the brief stimulations Kv1.2 channels may encounter *in vivo* (Baronas et al., 2015a). This phenomenon is termed use-dependent activation and occurs due to progressive rescue of channels from the

slow mode. It is exhibited by Kv1.2 containing channels in cell lines and primary neuronal cultures (Baronas et al., 2015a, 2015b). Use-dependent activation of Kv1.2 channels has previously been characterized using 20 Hz trains of 10 ms depolarizations to +60 mV and measured as the % increase between the 1st and peak pulse in a train (Baronas et al., 2017, 2015a). We utilized a similar protocol in our experiments, 200 sweeps of 10 ms depolarizations to +60 mV were applied to cells at a 20 Hz frequency, immediately followed by a 2 second pulse to +60 mV to confirm the true peak current magnitude at +60 mV was achieved during the 200 sweeps. For certain cells, especially cells expressing Kv1.2[N207A] channels, we found that the true peak current magnitude at +60 mV could not be achieved during the depolarization trains. Thus, % use-dependent activation was calculated as the % increase between the 1st pulse current in the +60 mV train and the true peak current magnitude at +60 mV, extracted from either the pulse train or the subsequent 2 second +60 mV depolarization. Kv1.2[N207A] channels show extreme use-dependent activation (Figure 3.3A&B). On a cell by cell basis, it is clear Kv1.2[N207A] channels show increased use-dependent activation compared to WT Kv1.2 channels (Figure 3.3B). Further confirming the role of slow gating regulation in the inhibition of the glycosylation mutants, introduction of the T252R mutation considerably diminishes their increased use-dependent activation (Figure 3.3A&B).

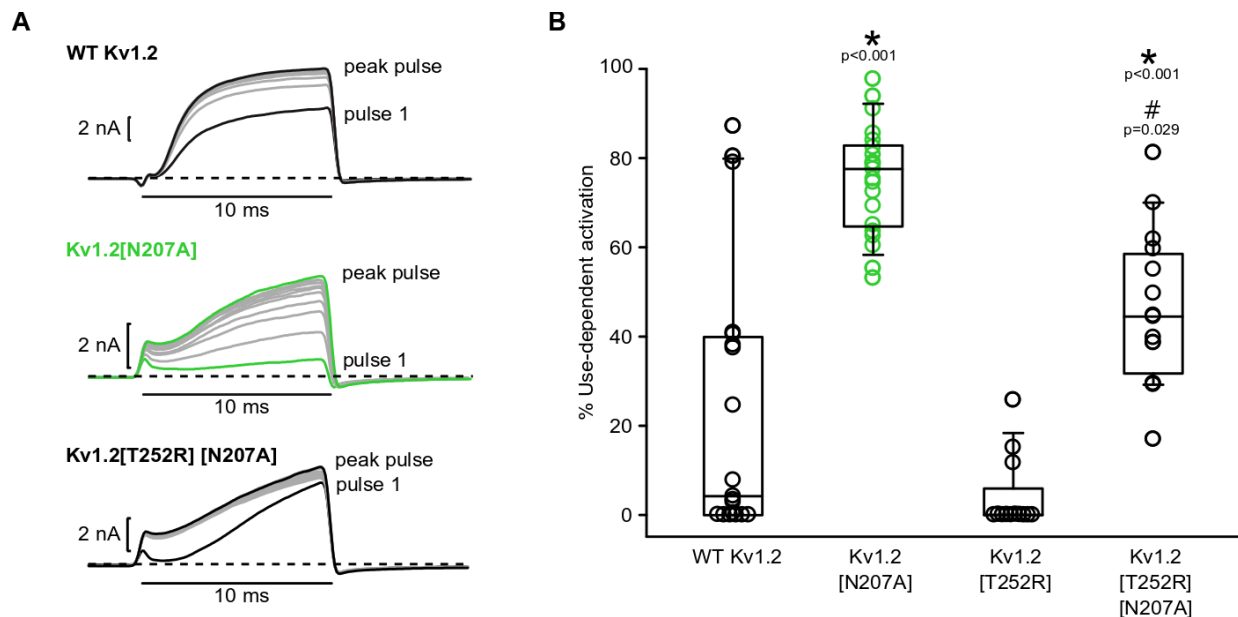


Figure 3.3: Enhanced use-dependent activation in Kv1.2[N207A] channels.

(A) Exemplar current traces from LM cells expressing WT Kv1.2, Kv1.2[N207A], and Kv1.2[T252R] [N207A] channels were elicited by 20 Hz trains of 10 ms depolarizations to +60 mV (holding potential of -80 mV). Every 20th pulse up to the peak pulse in the train is shown. Records illustrate increased use-dependence in Kv1.2[N207A] channels and attenuation of use-dependence by the T252R mutation. (B) Scatter/Box plots illustrate % use-dependent activation (1 - 1st pulse current magnitude/true peak current magnitude at +60 mV); WT Kv1.2 (n=19), Kv1.2[N207A] (n=21), Kv1.2[T252R] (n=12), and Kv1.2[T252R] [N207A] (n=15). * describes a significant difference between Kv1.2[N207A] and Kv1.2[T252R] [N207A] vs. WT Kv1.2 using a one-way ANOVA (Kruskal-Wallis non-parametric) followed by Dunn's post-hoc test comparing . # describes a significant difference between Kv1.2[N207A] and Kv1.2[T252R] [N207A] using a student's t-test.

3.2.5: Slow activation is not an intrinsic property of glycosylation deficient Kv1.2 channels

The activation kinetics of slow mode Kv1.2 channels can be accelerated by the application of strong prior depolarizations (i.e. prepulse potentiation), reflecting activity dependent relief of Kv1.2 inhibition by slow gating regulation (Baronas et al., 2015a; Rezazadeh et al., 2007). To demonstrate the plasticity and moment-to-moment regulation of Kv1.2[N207A] channel activation kinetics, we utilized a double pulse protocol similar to the previously referenced reports (Figure 3.4A). Channels were first depolarized to +30 mV for 2 s, repolarized to -100 mV

for 400 ms, then depolarized again to +30 mV for 2 s (Figure 3.4A). Due to the variable contribution of the fast and slow gating components from cell to cell, we used the 20%-80% rise time to generate single value quantifications of activation kinetics. WT Kv1.2 channels exhibit variable levels of slow activation kinetics, but frequently exhibit acceleration of activation during the second depolarizing step (Figure 3.4B). This effect is far more pronounced for Kv1.2[N207A] channels (Figure 3.4B). As expected, Kv1.2[N207A] channels activate very slowly in the first pulse relative to WT Kv1.2, however their activation kinetics are considerably accelerated in the second pulse (Figure 3.4B). This result indicates that the markedly slow activation kinetics of the glycosylation mutants are not an intrinsic property of the channel. Instead, the dramatic acceleration of Kv1.2[N207A] activation by activating prepulses (Figure 3.4) and the T252R mutation (Figure 3.2 & Figure 3.3) demonstrates that the slow activation kinetics of glycosylation deficient Kv1.2 channels are due to extreme sensitivity to slow gating regulation.

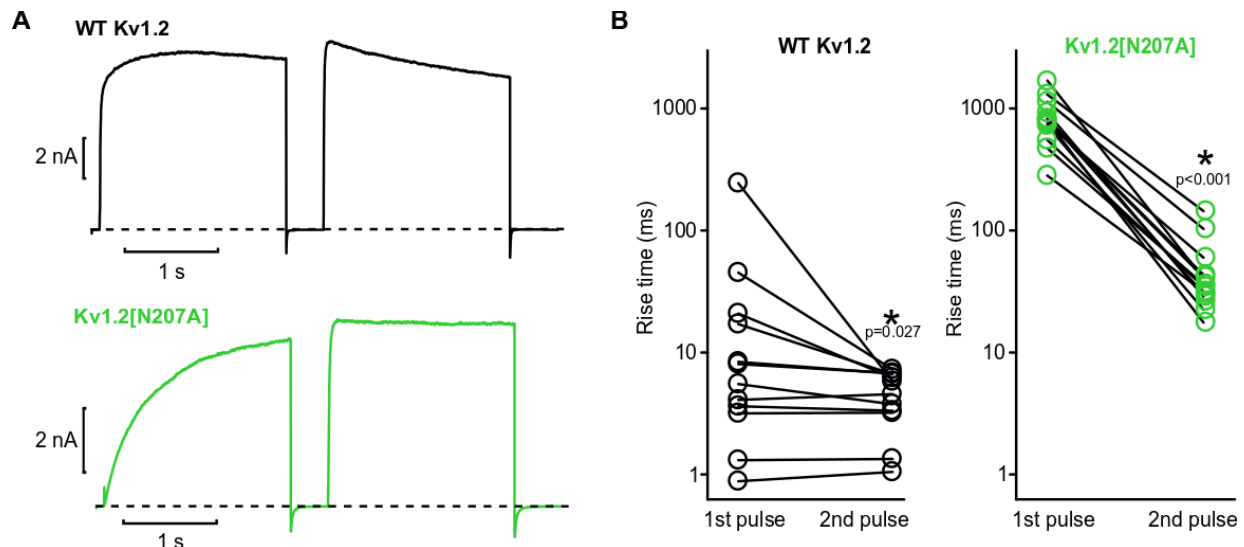


Figure 3.4: Pre-pulse potentiation of Kv1.2[N207A] channel activation.

(A) Currents from WT Kv1.2 and Kv1.2[N207A] expressing LM cells were elicited with two successive depolarizations to +30 mV (+30 mV for 2 s, -100 mV for 400 ms, +30 mV for 2 s). Exemplar current traces illustrate acceleration of activation kinetics in the second pulse compared to the first pulse, but with far more prominent slow gating of Kv1.2[N207A] during the first depolarization. (B) Activation rise times between 20%-80% of the first and second pulse currents were measured and plotted for WT Kv1.2 (n=12) and Kv1.2[N207A] (n=16) channels. Rise time in the 1st and 2nd pulses were compared with a paired student's t-test, and significant difference is indicated by * with the associated P value shown. Rapidly activating currents (rise time: 1-2 ms) may be contaminated by capacitive currents in this experiment. Based on whole cell voltage clamp compensation parameters, the largest voltage clamp time constant among analyzed cells was approximately 130 μ s.

3.2.6: Slc7a5 competes with slow gating regulation in Kv1.2 channels

The amino acid transporter Slc7a5 exerts powerful effects on the gating and expression of Kv1.2 channels (Baronas et al., 2018). Notably, Slc7a5 hyperpolarizes the activation half-voltage of Kv1.2 channels by ~50 mV (Figure 3.5) (Baronas et al., 2018). Our group observed WT Kv1.2 channels co-expressed with Slc7a5 did not exhibit markers of slow gating regulation (slow activation kinetics, depolarized conductance-voltage relationships, and use-dependence) in ambient redox conditions (Figure 3.5B). These markers of slow gating were partially rescued

by reducing agents such as DTT that enhance the slow gating mode (Figure 3.5B). The voltage-dependence of activation of WT Kv1.2 channels in DTT is shifted to depolarized voltages, indicating inhibition of channel activation (Figure 3.5A). In contrast to the hyperpolarized voltage-dependence of activation of WT Kv1.2 channels in ambient redox subjected to activating prepulses to relieve the slow gating mode (potentiated GV) (Figure 3.5A). When these experiments are repeated for Kv1.2 channels co-expressed with Slc7a5, there is a prominent dissociation of the conductance-voltage relationship in DTT (Figure 3.5B). Compared to the strongly hyperpolarized conductance-voltage relationships of Kv1.2 channels co-expressed with Slc7a5 in ambient redox (potentiated GV) (Figure 3.5B). Our rationalization for these observations is that Slc7a5 occludes the interaction of the slow gating regulatory molecule with Kv1.2 channels in ambient redox conditions, preventing its effects on channel gating (Figure 3.5B&F). In reducing conditions, the affinity of the protein mediating slow gating is increased and there is competition for binding to Kv1.2 between this protein and Slc7a5 (3.5F), underlying the biphasic conductance-voltage relationships of Kv1.2 channels co-expressed with Slc7a5 in DTT (Figure 3.5B). The conductance-voltage relationships of Kv1.2 channels co-expressed with Slc7a5 in DTT show a hyperpolarized activation component ($V_{1/2,a} = -53 \pm 2$ mV) corresponding to Slc7a5-regulated channels (Figure 3.5B). In addition to a depolarized activation component ($V_{1/2,b} = 44 \pm 4$ mV) corresponding to channels in the slow gating mode due to the application of DTT (Figure 3.5B).

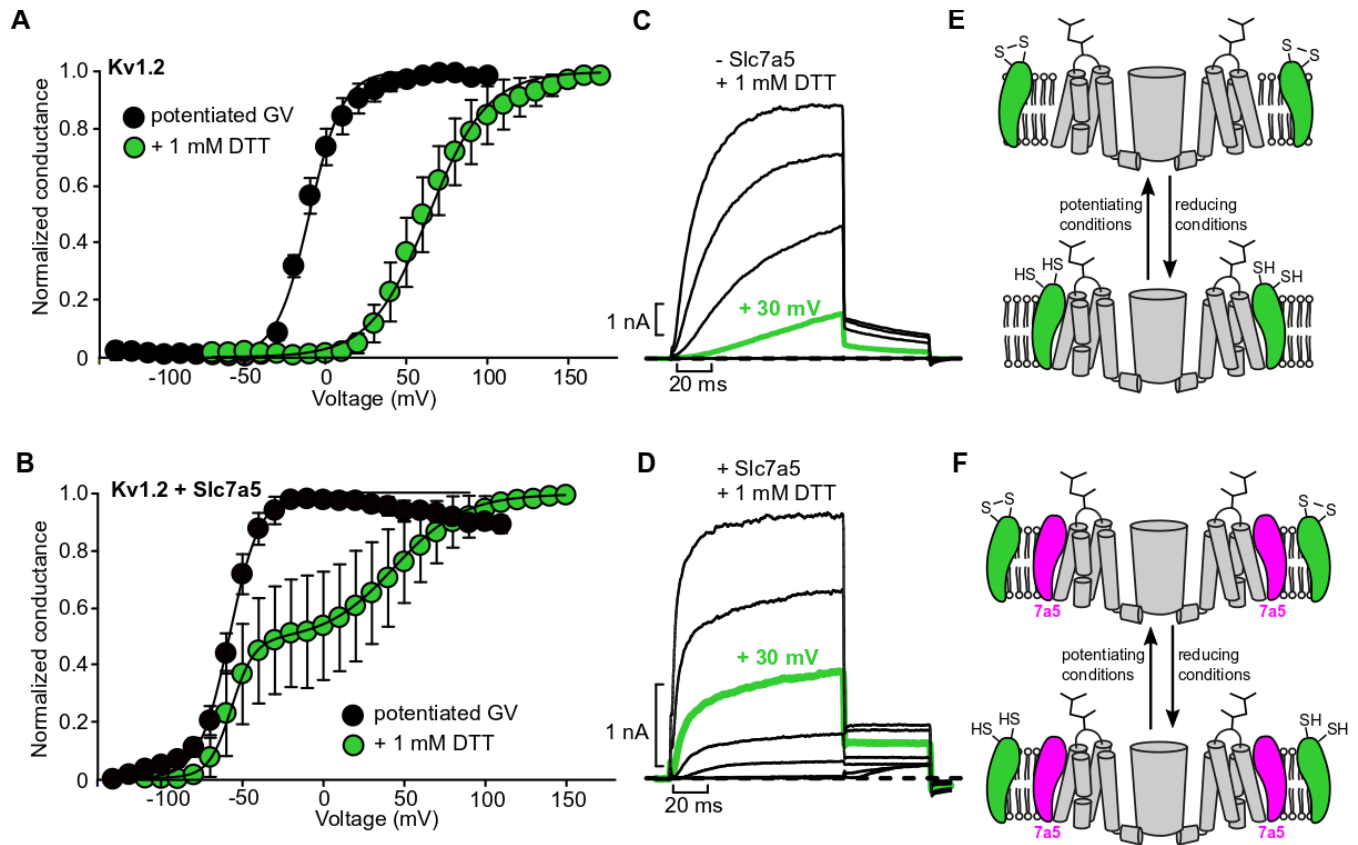


Figure 3.5: Slc7a5 competes with the slow gating mechanism in wild-type Kv1.2 channels.

(A,B) Conductance-voltage relationships were determined for Kv1.2 (\pm Slc7a5) in the indicated conditions. Cells were pulsed from a holding potential of -80 mV to voltages between -130 mV and $+150$ mV for 100 ms, followed by a -20 mV repolarization for tail current measurement. Tail currents were normalized to the peak tail current magnitude and fit with a Boltzmann (Equation 1), or the sum of two Boltzmann equations (for Kv1.2 + Slc7a5 + DTT, Equation 2). For generation of potentiated GV, test pulses were each preceded by a 500 ms depolarization to $+60$ mV, and a brief 400 ms repolarization to -120 mV to deactivate channels (Kv1.2: potentiated $V_{1/2} = -10 \pm 1$ mV; Kv1.2 + 1 mM DTT: $V_{1/2} = 64 \pm 4$ mV; Kv1.2 + Slc7a5: potentiated $V_{1/2} = -58 \pm 3$ mV; Kv1.2 + Slc7a5: + 1 mM DTT: $V_{1/2,a} = -53 \pm 2$ mV (39%) $V_{1/2,b} = 44 \pm 4$ mV (61%)). The proportion of the conductance-voltage relationship corresponding to the hyperpolarized activation component was obtained from the Boltzmann fit parameter “A” (Equation 2). The proportion corresponding to the depolarized activation component was calculated as $1-A$. (C,D) Exemplar current records for Kv1.2 + 1 mM DTT (top) and Kv1.2 + Slc7a5 + 1 mM DTT (bottom). Every 4th sweep beginning at -130 mV is depicted for clarity. Sweeps were delivered every 10 s. (E, F) Hypothetical mechanism underlying attenuation of slow gating by Slc7a5. A putative regulator of slow gating (green) can freely associate with Kv1.2 channels when Slc7a5 levels are low (panel E), but overexpression of Slc7a5 (magenta) is proposed to occlude association of the slow gating regulator with Kv1.2 (panel F).

Slc7a5 also powerfully alters slow gating behavior in glycosylation deficient channels (Figure 3.6). Cells co-expressing Slc7a5 and Kv1.2[N207A] channels had no significant currents, this was likely due to a combination of Slc7a5 suppression of total Kv1.2 channel expression (Baronas et al., 2018), and the reduced surface expression of Kv1.2 glycosylation deficient channels (Watanabe et al., 2007). To overcome this challenge, we used a chimeric channel comprising the N-terminus and T1 domain of Kv1.5, fused to the transmembrane domains and C-terminus of Kv1.2, which we have used previously to increase Kv1.2 expression (Baronas et al., 2018). The Kv1.5N/Kv1.2[N207A] chimera remained sensitive to the slow gating mode and permitted detection of functional currents in the presence of Slc7a5 (Figure 3.6A). These channels exhibit considerably depolarized conductance voltage relationships (Figure 3.6B) and slow activation time courses (Figure 3.6C) with a significant slow component of activation (Figure 3.6D). Co-expression with Slc7a5 strongly diminishes these markers of slow gating regulation in the chimera (Figure 3.6B-D). This effect is most apparent in the fractional contribution of the slow component (Figure 3.6D). The contribution of the slow activation component is significantly smaller in Kv1.5N/Kv1.2[N207A] + Slc7a5 currents compared to Kv1.5N/Kv1.2[N207A] currents (Figure 3.6D). The competition between slow gating regulation and Slc7a5 regulation is also evident in Figure 3.6B. Kv1.5N/Kv1.2[N207A] + Slc7a5 cells exhibit a biphasic conductance-voltage relationship (Figure 3.6B), reminiscent of conductance-voltage relationships of WT Kv1.2 + Slc7a5 cells in DTT (Figure 3.5B). A proportion of channels (23%) are under regulation by slow gating and exhibit the characteristic depolarized conductance-voltage relationship ($V_{1/2, a} = 61 \pm 8$ mV), while the rest of the channels (77%) are associated with Slc7a5 and exhibit a hyperpolarized conductance-voltage relationship ($V_{1/2, b} = -30 \pm 4$ mV) (Figure 3.6B). These results strengthen our hypothesis that occlusion of the slow gating regulator by Slc7a5 underlies the absence of slow gating in WT Kv1.2 channels co-expressed with Slc7a5 and further highlight the enhanced inhibition of glycosylation deficient Kv1.2 channels by slow gating regulation.

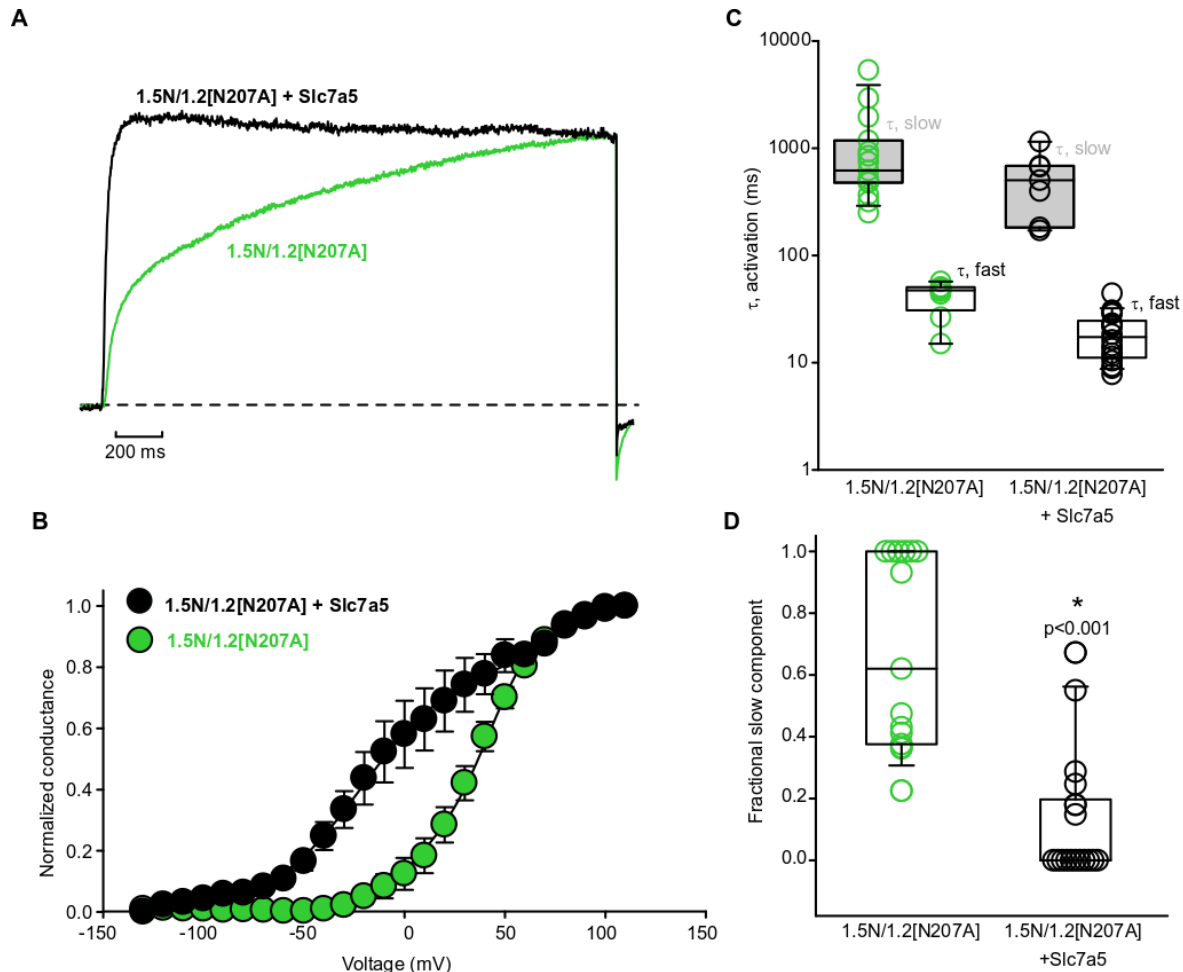


Figure 3.6: Slc7a5 antagonizes slow gating regulation of Kv1.2[N207A] channels.

(A) Exemplar currents elicited from Kv1.5N/Kv1.2[N207A] channels \pm Slc7a5 with a 2 s depolarization to +10 mV. (B) Conductance-voltage relationships were generated by stepping between -130 mV and +110 mV (100 ms in 10 mV steps, -100 mV holding potential), followed by a tail current voltage of -30 mV. Conductance-voltage relationships were obtained from the tail current amplitudes and fit with the sum of two Boltzmann functions (Equation 2) (Kv1.5N/Kv1.2[N207A]: $V_{1/2,a} = 38 \pm 3$ mV (92%), $V_{1/2,b} = -10 \pm 4$ mV (8%), $n = 7$; Kv1.5N/Kv1.2[N207A] + Slc7a5: $V_{1/2,a} = 61 \pm 8$ mV (23%), $V_{1/2,b} = -30 \pm 4$ mV (77%), $n = 4$). The proportion of the conductance-voltage relationship corresponding to the hyperpolarized activation component was obtained from the Boltzmann fit parameter “A” (Equation 2). The proportion corresponding to the depolarized activation component was calculated as 1-A. (C) Activation time constants for Kv1.5N/Kv1.2[N207A] ($n=16$) and Kv1.5N/Kv1.2[N207A] + Slc7a5 ($n=18$) channels were derived at +10 mV, as described in Figure 3.1. Activating current traces were elicited by a 2 s depolarization to +10 mV (-80 mV holding potential). (D) Fractional slow component for Kv1.5N/Kv1.2[N207A] ($n=16$) and Kv1.5N/Kv1.2[N207A] + Slc7a5 ($n=18$). Fractional slow components were compared using a Mann-Whitney U test (non-parametric), with the significance level indicated by *.

3.2.7: Reducing conditions attenuate Slc7a5 effects on glycosylation mutants

Similar experiments were conducted in the presence of DTT to further accentuate the slow gating mode (Figure 3.7). In DTT, Kv1.5N/Kv1.2[N207A] channels gate almost exclusively in the slow mode (Figure 3.7). The fast component made a significant contribution in only 3/12 cells (Figure 3.7C&D). In addition, these channels exhibited extremely depolarized conductance-voltage relationships ($V_{1/2,a} = 48 \pm 3$ mV (95%), $V_{1/2,b} = -2.3 \pm 2$ mV (5%)) (Figure 3.7B). Co-expression with Slc7a5 attenuated these effects, however Slc7a5 attenuation of slow gating is not as powerful as in ambient redox conditions (Figure 3.6 vs Figure 3.7). Slc7a5 still reduces the fractional contribution of the slow component (Figure 3.7D) and introduces a considerable hyperpolarized component to the GV relationships of Kv1.5N/Kv1.2[N207A] channels in DTT ($V_{1/2,a} = 51 \pm 2$ mV (51%), $V_{1/2,b} = -32 \pm 4$ mV (49%), $n = 8$), representing the Slc7a5 mediated activation component (Figure 3.7B). Overall, these results show that Slc7a5 occludes slow gating regulation of Kv1.2 channels. In addition, the competition between Slc7a5 regulation and slow gating regulation is influenced by factors that alter channel sensitivity to the slow gating mode, such as DTT.

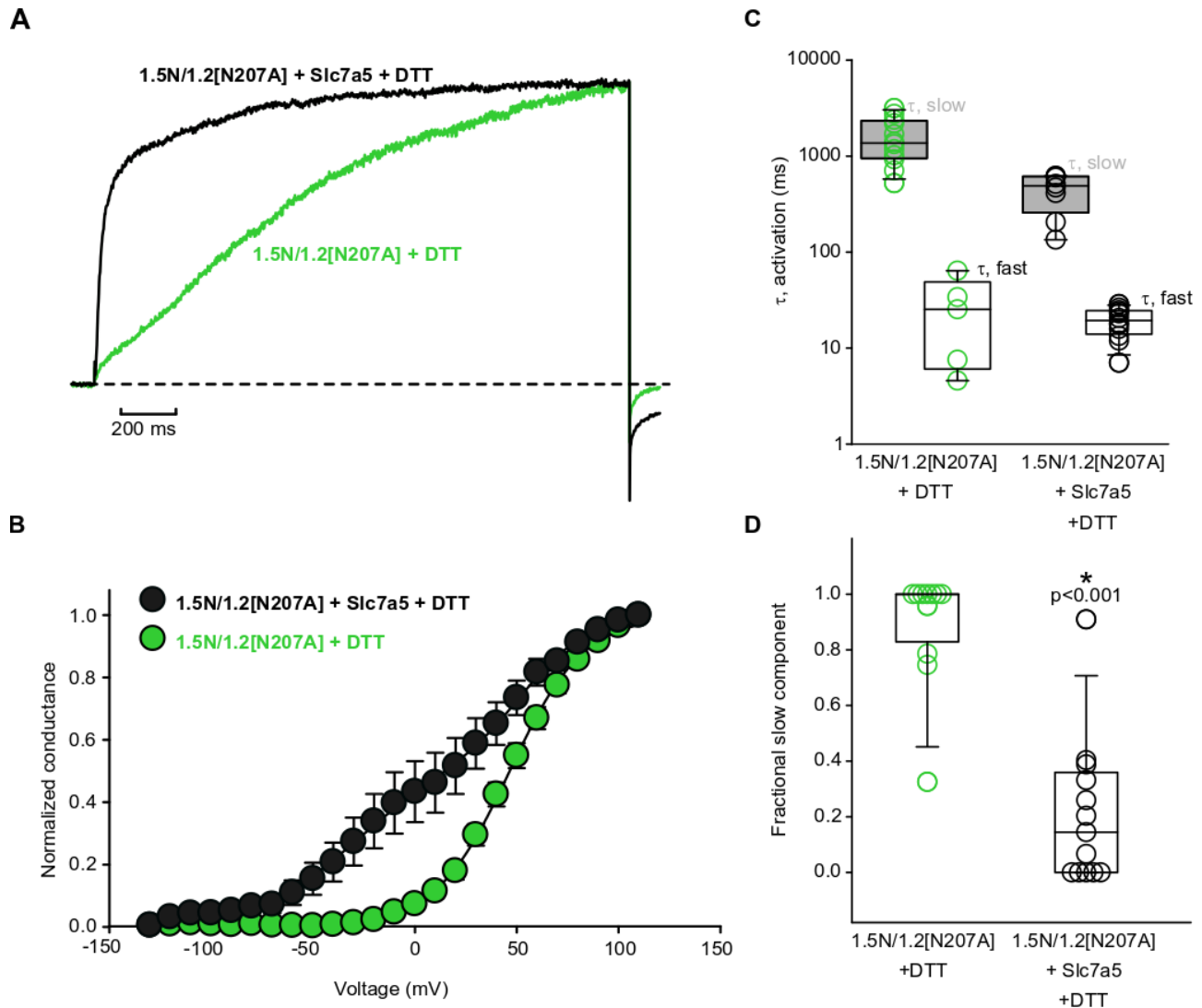


Figure 3.7: The Slc7a5 effect on Kv1.2 channels is diminished in reducing conditions.

(A) Exemplar current traces of Kv1.5N/Kv1.2[N207A] \pm Slc7a5 in the presence of DTT (400 μ M). Currents were elicited by a 2 s depolarization to +10 mV. (B) Conductance-voltage relationships were obtained as described in Figure 3.6B. Kv1.5N/Kv1.2[N207A] (+DTT): $V_{1/2,a} = 48 \pm 3$ mV (95%), $V_{1/2,b} = -2.3 \pm 2$ mV (5%), $n = 9$; Kv1.5N/Kv1.2[N207A] + Slc7a5 (+DTT) $V_{1/2,a} = 51 \pm 2$ mV (51%), $V_{1/2,b} = -32 \pm 4$ mV (49%), $n = 8$. The proportion of the conductance-voltage relationship corresponding to the hyperpolarized activation component was obtained from the Boltzmann fit parameter “A” (Equation 2). The proportion corresponding to the depolarized activation component was calculated as 1-A. (C) Activation time constants for Kv1.5N/Kv1.2[N207A] (+DTT) ($n=12$) and Kv1.5N/Kv1.2[N207A] + Slc7a5 (+DTT) ($n=10$). Activation time constants were determined as described in Figure 3.1B. (D) Fractional slow component for Kv1.5N/Kv1.2[N207A] (+DTT) ($n=12$) and Kv1.5N/Kv1.2[N207A] + Slc7a5 (+DTT) ($n=13$). Fractional slow components were compared using a Mann-Whitney U-test with significance level indicated by *.

3.2.8: Slow gating regulation is absent in *Xenopus laevis* oocytes

Finally, further supporting the hypothesis that increased sensitivity to slow gating regulation underlies the inhibited activation kinetics of glycosylation deficient Kv1.2 channels, we observed that in *X. laevis* oocytes, Kv1.2[N207A] channels exhibit similar activation kinetics to WT Kv1.2 and Kv1.2[T252R] channels (Figure 3.8A&B). This contrasts with the stark differences in activation properties between these channels described previously in this chapter (Figure 3.1&Figure 3.2). In fact, Kv1.2[N207A] channels activate ~40 fold faster in oocytes compared to LM cells. Kv1.2[N207A] median activation time constants in oocytes were 18 ms (τ , slow) and 3 ms (τ , fast) compared to 734 ms (τ , slow) and 58 ms (τ , fast) for Kv1.2[N207A] channels in LM cells (Figure 3.8B vs Figure 3.2B). These results provide additional evidence that slow activation kinetics is not an intrinsic property of glycosylation deficient Kv1.2 channels but is due to considerably increased sensitivity to slow gating regulation. We hypothesize that slow gating regulation is mediated by an extrinsic regulator (Figure 1.3), and our findings suggest that this regulator is present in LM cells but likely absent or significantly diminished in *X.laevis* oocytes, given the absence of slow gating behavior for all channels (Figure 3.8A&B).

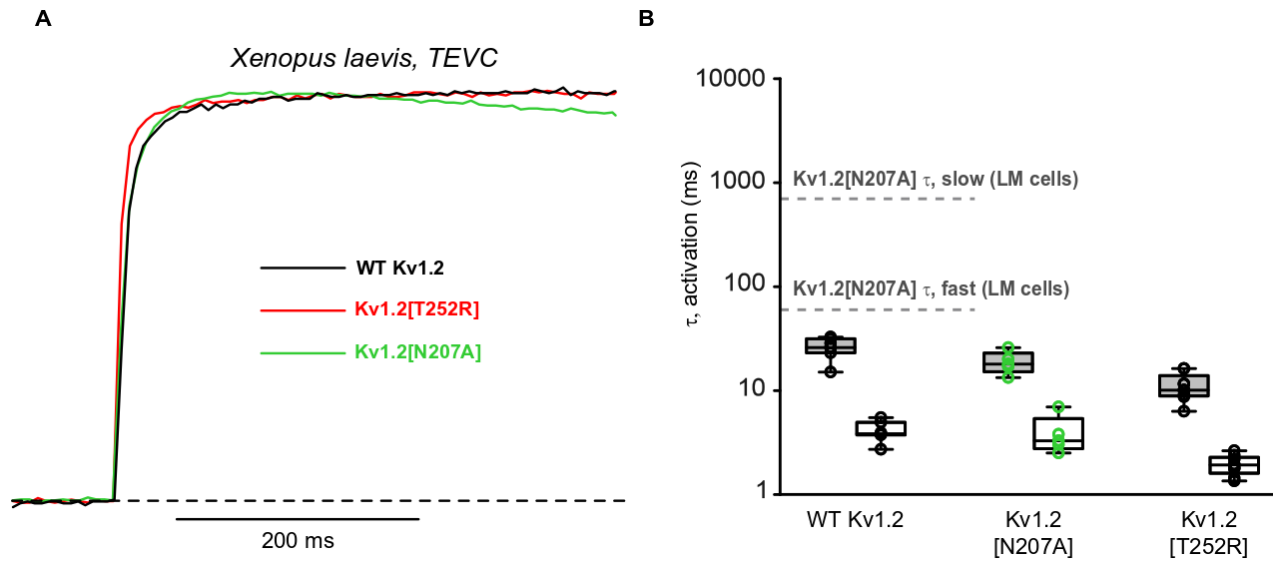


Figure 3.8: Slow gating of Kv1.2 channels is absent in *Xenopus laevis* oocytes.

(A) Superimposed representative traces illustrating the comparable activation kinetics of WT Kv1.2, Kv1.2[N207A], and Kv1.2[T252R] channels expressed in *Xenopus laevis* oocytes. Currents were elicited by a 2 s depolarization to +10 mV (holding voltage -80 mV) using two-electrode voltage clamp. (B) Activation time constants for WT Kv1.2 (n=7), Kv1.2[N207A] (n=5), and Kv1.2[T252R] channels (n=9). Activation time constants were generated as described in Figure 3.1. Dashed lines indicate the median slow and fast activation time constant values for Kv1.2[N207A] channels expressed in LM cells (see Figure 3.1).

3.2.9: Delayed deactivation kinetics of glycosylation deficient channels

Another noteworthy feature that we observed in these channels was significant deceleration of deactivation (Figure 3.9). This property was not sensitive to the T252R mutation and is likely due to an effect of glycosylation loss on the intrinsic biophysical properties of Kv1.2 (Figure 3.9B&D). This property resulted in incomplete closure of Kv1.2[N207A] channels in Figure 3.3A, producing a small instantaneous current observed at the beginning of each depolarization in the train.

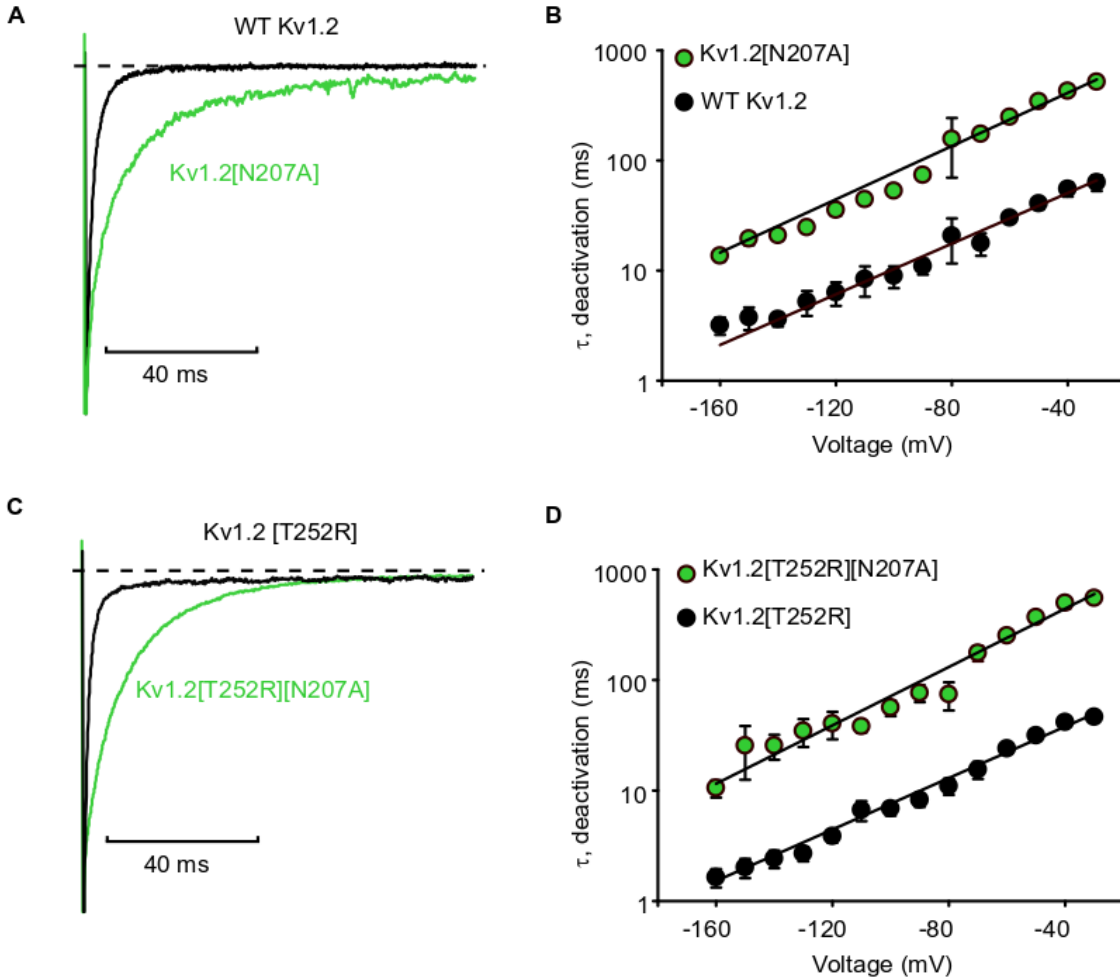


Figure 3.9: Glycosylation deficient Kv1.2 channels exhibit delayed deactivation kinetics.

(A&B) Superimposed representative current traces illustrating the slowed deactivation kinetics of Kv1.2[N207A] and Kv1.2[T252R] [N207A] channels compared to WT Kv1.2 and Kv1.2[T252R] respectively. Currents were obtained by a 1 s test pulse to -140 mV following a 2 s depolarization to 0 mV. (C) Deactivation time constants (τ , deactivation) in milliseconds as a function of voltage for Kv1.2[N207A] (n=20) and WT Kv1.2 (n=8) channels expressed in LM cells. Cells were subjected to 0 mV depolarizations for 2 s then stepped to the test pulses (-30 to -160 mV in 10 mV increments) for 1 s (holding voltage -100 mV). τ values were generated by fitting tail currents with a single exponential function (Equation 3). (D) Deactivation time constants (τ , deactivation) in milliseconds as a function of voltage for Kv1.2[T252R] (n=10) and Kv1.2[T252R] [N207A] (n=10) channels expressed in LM cells. The voltage protocol and τ value derivations are as described in C.

Section 3.3: Discussion

In this chapter, I have demonstrated that glycosylation loss increases the sensitivity of Kv1.2 channels to slow gating regulation, underlying the inhibited activation properties of glycosylation deficient Kv1.2 channels. Several pieces of data support this conclusion. Currents from Kv1.2[N207A] and Kv1.2[N207Q] channels, which are non-glycosylated due to mutation of the consensus Kv1.2 N207 glycosylation site, exhibited slow activation kinetics and a slow activation component that dominated the currents from most cells compared to WT Kv1.2 channels (Figure 3.1). Cell to cell variations are evident in the activation kinetics and fractional slow component (Figure 3.1), reminiscent of earlier descriptions of Kv1.2 slow gating regulation (Rezazadeh et al., 2007). Prior studies have demonstrated considerable attenuation of slow gating regulation following mutation of Threonine 252 in the S2-S3 linker of Kv1.2 (Baronas et al., 2015b, 2015a; Rezazadeh et al., 2007). Mutation of this residue to arginine in glycosylation deficient channels accelerated their activation kinetics and diminished the contribution of the slow activation component (Figure 3.2B&C), providing the first direct link between slow gating regulation and the inhibited activation of glycosylation deficient channels. The glycosylation deficient channels also exhibited prominent use-dependent activation compared to WT Kv1.2 channels (Figure 3.3B), reflecting progressive rescue of these channels from the slow gating mode (Baronas et al., 2015b, 2015a). The T252R mutation also attenuated the prominent use-dependent activation of glycosylation deficient channels (Figure 3.3B).

Furthermore, I have shown that the inhibited activation kinetics of glycosylation deficient channels are not intrinsic, supported by the observation that activating prepulses frequently generate an approximately 10 fold acceleration in their activation kinetics (Figure 3.4B). This pre-pulse potentiation effect has been described previously for WT Kv1.2 channels, and it is postulated to reflect the relief of Kv1.2 channels from slow gating inhibition by the opening of the

channel (Baronas et al., 2015a; Rezazadeh et al., 2007). The degree of disinhibition provided by potentiating pre-pulses to glycosylation deficient channels displays the considerable inhibition of these channels by slow gating regulation (Figure 3.4B). In addition, I have shown that Slc7a5 attenuates the depolarized conductance voltage relationships and slow activation kinetics of glycosylation deficient channels, indicating weakening of slow gating regulation by Slc7a5 (Figure 3.6&Figure 3.7). Finally, Kv1.2[N207A], WT Kv1.2, and Kv1.2[T252R] channels exhibit similar activation kinetics in *Xenopus laevis* oocytes (Figure 3.8), lending further support to our conclusion that increased sensitivity to slow gating regulation underlies the inhibited activation properties of glycosylation deficient channels.

3.3.1: Interaction between Slc7a5 and slow gating regulation

We have demonstrated functional interaction between slow gating and Slc7a5 regulation (Figure 3.6&Figure 3.7). These two regulatory mechanisms generate dramatically different outcomes on channel gating. Slc7a5 modulation hyperpolarizes the activation $V_{1/2}$ of WT Kv1.2 channels (Figure 3.5; Baronas et al., 2018) and glycosylation deficient channels (Figure 3.6&Figure 3.7). In contrast, regulation by slow gating produces depolarized shifts in the Kv1.2 activation $V_{1/2}$ (Baronas et al., 2015a; Rezazadeh et al., 2007). These regulation mechanisms are mutually exclusive and compete for binding to Kv1.2 channels. This is indicated by the biphasic conductance voltage relationships when both these mechanisms are present (Figure 3.5B; Figure 3.6B; Figure 3.7B). The extent of Slc7a5 competition can be altered by redox conditions (Figure 3.5B&Figure 3.7B). Our working hypothesis is that the molecular players in these regulatory processes likely occlude one another's interaction with Kv1.2, leading to distinct populations of channels with either prominent Slc7a5-mediated features, or prominent slow gating (Figure 3.5F).

3.3.2: Previously reported effects of glycosylation loss on Kv1.2 channels

Altered gating properties of Kv1.2 glycosylation deficient channels have been reported by Watanabe et al., (2007). Specifically, Kv1.2 glycosylation deficient channels showed a combination of slower activation and deactivation kinetics, and a hyperpolarized activation $V_{1/2}$ shift (~ 10 mV) in CHO cells (Watanabe et al., 2007). However, the effects of glycosylation loss reported by Watanabe et al., (2007) are far milder than those observed in my study. For example, the activation time constant for Kv1.2[N207Q] channels at 0 mV is 18.6 ms in the published report (Watanabe et al., 2007), compared to 903 ms (τ , slow) and 68 ms (τ , fast) for Kv1.2[N207Q] channels at +10 mV in my study (Figure 3.1). The authors proposed the altered properties were caused by changes in the Kv1.2 effective surface potential due to loss of negatively charged sialic acids in the Kv1.2 glycosylation tree (Watanabe et al., 2007). Based on my findings, it is also clear that glycosylation state alters sensitivity to slow gating, and this produces considerably greater effects on channel gating than the surface potential mechanism reported by Watanabe et al., (2007). We rationalize the results presented by Watanabe et al., (2007) by suggesting that the specific CHO cell lines used in this study may lack, or possess diminished amounts, of certain components required for slow gating. Previous reports have highlighted variability of slow gating between cell lines (Rezazadeh et al., 2007).

In summary, this study demonstrates that glycosylation is an important determinant of Kv1.2 sensitivity to the slow gating mode. The identification of glycosylation as an extracellular factor that impacts slow gating further supports the hypothesis that a transmembrane component mediates slow gating. Transmembrane communication is required for modulation of slow gating by both extracellular factors (glycosylation and extracellular redox) and intracellular factors (T252R mutation in the intracellular S2-S3 linker). We also demonstrate that multiple proteins, including Slc7a5, may compete for the regulation of Kv1.2 channels, generating a vast dynamic

range of voltages over which Kv1.2 gating can be modulated. Kv1.2 has played a central role in our understanding of the structural basis of voltage-dependent regulation of ion channels and could be a useful model to study extrinsic modulation of voltage-dependent gating.

Chapter 4: Propofol exerts contrasting functional effects on Kv1.2 channels and interacts with slow gating regulation

Section 4.1: Introduction

Propofol (2,6-diisopropylphenol) is an intravenous general anaesthetic widely used for the induction and maintenance of general anesthesia, a state characterized by immobility, sedation, analgesia, and loss of consciousness and memory (Hemmings et al., 2005; Rudolph and Antkowiak, 2004; Trapani et al., 2000). The exact mechanisms by which propofol and other general anaesthetics produce the components of general anesthesia are incompletely understood (Franks, 2008). Positive modulation of the chloride permeable ionotropic receptor GABA_A is the chief mechanism by which propofol is postulated to exert its anaesthetic effects (Trapani et al., 2000). Propofol potentiates the response of GABA_A receptors to GABA (γ -aminobutyric acid), the major inhibitory neurotransmitter in the brain and the endogenous ligand of GABA_A receptors, and directly activates GABA_A receptors without a requirement for GABA (Collins, 1988; Hales and Lambert, 1991; Hara et al., 1993; Trapani et al., 2000). Although it is evident GABA_A receptors play a key role in propofol-induced general anaesthesia, considering the physiological complexity of anaesthesia and the extensive molecular targets of propofol, it is unlikely that modulation of GABA_A receptors alone accounts for all the endpoints of propofol (Hemmings et al., 2005; Kojima et al., 2015; Nguyen et al., 2009; Ouyang et al., 2003; Trapani et al., 2000; Yang et al., 2015; Ying et al., 2006).

Kv1.2 channels are broadly expressed in the mammalian central nervous system where they act as crucial regulators of excitability. Mutations in Kv1.2 channels are associated with diseases of excitability such as epilepsies in humans, and deletion of Kv1.2 in mice leads to 100% lethality

(Coetzee et al., 1999; Masnada et al., 2017; Robbins and Tempel, 2012; Syrbe et al., 2015; Wang et al., 1994). These channels are appropriate candidates for investigation as molecular targets of propofol due to their localization and function in the central nervous system, and their demonstrated sensitivity to inhalation anaesthetics (Barber et al., 2012; Bu et al., 2018; Liang et al., 2015; Woll et al., 2017). Recent reports have demonstrated inhibition of Kv channels by propofol (Kojima et al., 2015; Yang et al., 2015). WT Kv1.2 channels are reported to be insensitive to propofol however propofol potentiates Kv1.2 G329T, a Kv1.2 channel mutant (Bu et al., 2018; Liang et al., 2015). This chapter demonstrates inhibition and potentiation of WT Kv1.2 channels by propofol, in contrast to previous reports, extending knowledge regarding the molecular targets of this anesthetic. In addition, Kv1.2 channels can occupy two distinct gating modes, a *fast gating mode* characterized by *fast activation kinetics and hyperpolarized GV relationships*, and a *slow gating mode* characterized by relatively *slow activation kinetics and depolarized GV relationships* (Rezazadeh et al., 2007) (see page 18). Kv1.2 inhibition by the slow gating mode is referred to as slow gating or slow gating regulation in this thesis. The results presented in this chapter indicate that propofol modulation of Kv1.2 channels is related to slow gating regulation, revealing interactions between slow gating and channel pharmacology. Overall, these results evince novel effects of propofol on Kv1.2 channels and demonstrate that slow gating regulation can influence the response of Kv1.2 channels to drugs, providing additional physiological and pharmacological relevance for this regulatory mechanism.

Section 4.2: Results

4.2.1: Kv1.2 currents progressively decay in propofol

To screen propofol for activity on Kv1.2, currents were recorded from LM cells expressing Kv1.2 channels in control conditions and after wash-in of 200 μ M propofol. Paired measurements were obtained for each cell in the study. Experiments were performed on cells expressing WT Kv1.2,

Kv1.2[N207A], and Kv1.2[T252R] channels to investigate potential effects of slow gating regulation on the response to propofol. Glycosylation deficient Kv1.2[N207A] channels exhibit increased sensitivity to slow gating regulation while Kv1.2[T252R] channels exhibit diminished sensitivity (Baronas et al., 2015a; Rezazadeh et al., 2007) (see chapter 3). In propofol, Kv1.2 channels exhibited a progressive decay in currents that was absent in control (Figure 4.1B,E-G). To investigate this effect, cells expressing WT Kv1.2, Kv1.2[N207A], and Kv1.2[T252R] channels were pulsed to +30 mV for 3 seconds in control solution and following perfusion of 200 μ M propofol into the bath 2-3 minutes (Figure 4.1). Cells were voltage clamped at -80 mV during propofol wash-in. The current amplitude at 1, 2, and 3 seconds into the pulse was determined for the control and propofol currents and expressed as a percentage of the peak current amplitude at +30 mV in each condition (% Residual current) (Figure 4.1 A&B). In control solution, currents from WT Kv1.2 and Kv1.2[N207A] channels decreased minimally from peak (Figure 4.1A). Residual current at 1 second into the pulse was approximately 99% of the peak current for WT Kv1.2 channels, and 98% of the peak current for Kv1.2[N207A] channels (Figure 4.1A). At the end of the pulse (3 seconds), the residual current magnitude was approximately 95% of the peak current for both channels (Figure 4.1A). The current decline in control solution was moderately greater for Kv1.2[T252R] channels, the residual current magnitude at 1 second into the pulse was approximately 88% of the peak current and declined to 76% of the peak at 3 seconds (Figure 4.1A).

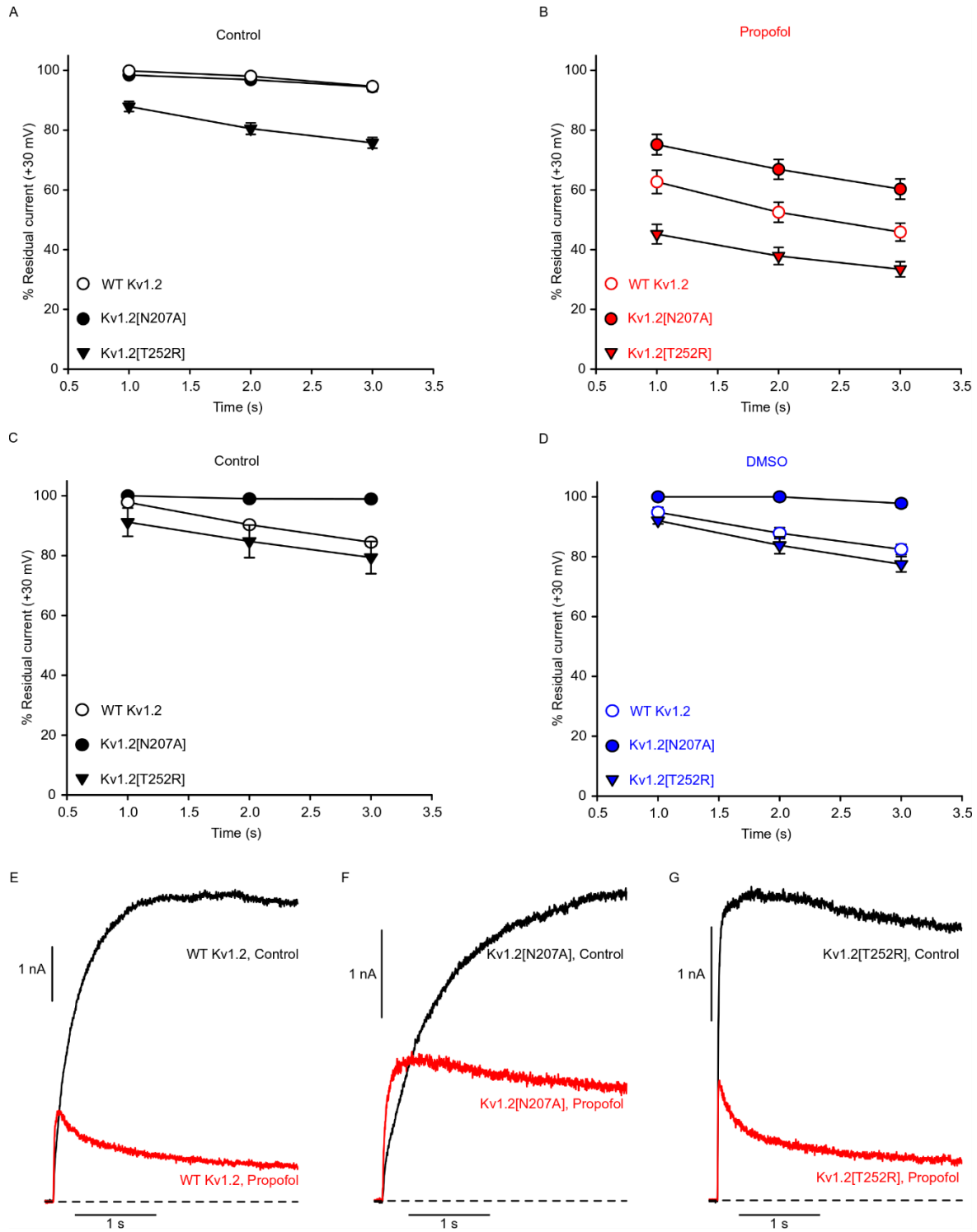


Figure 4.1: Kv1.2 channel currents progressively decay in propofol.

(A-B) % Residual current relative to peak (mean \pm S.E.M) at 1, 2, and 3 seconds into a 3 second depolarization to +30 mV (holding potential of -80 mV) for WT Kv1.2 (n=9), Kv1.2[N207A] (n=20), and Kv1.2[T252R] (n=21) channels in control solution (A) and 200 μ M propofol (B). (C-D) % Residual current

relative to peak (mean \pm S.E.M) at 1, 2, and 3 seconds into a 3 second depolarization to +30 mV (holding potential of -80 mV) for WT Kv1.2 (n=4), Kv1.2[N207A] (n=6), and Kv1.2[T252R] (n=3) channels in control solution (C) and 0.10% v/v DMSO (D). (E-F) Exemplar current traces from LM cells expressing WT Kv1.2, Kv1.2[N207A], and Kv1.2[T252R] channels \pm 200 μ M propofol as indicated (3 second depolarization to +30 mV, holding potential -80 mV). 200 μ M propofol or 0.10% v/v DMSO solution was perfused into the bath for 2-3 minutes after control recordings were obtained. Solutions were prepared as described in the materials and methods chapter (see page 27).

Following wash-in of 200 μ M propofol, currents exhibited more prominent time-dependent decay, and the magnitude of the current decay varied between the different Kv1.2 mutants (Figure 4.1B&E-G). At 1 second into the pulse in propofol, currents from WT Kv1.2, Kv1.2[N207A], and Kv1.2[T252R] channels had decayed to approximately 63%, 75%, and 45% of the peak, respectively (Figure 4.1B). Residual current at 3 seconds was approximately 45% of the peak for WT Kv1.2 channels, 60% for Kv1.2[N207A], and 33% for Kv1.2[T252R] (Figure 4.1B). Therefore, Kv1.2[N207A] channels were the least sensitive to the propofol-induced current decay, Kv1.2[T252R] channels were the most sensitive, and WT Kv1.2 channels exhibited intermediate sensitivity. As a vehicle control for DMSO which was used to prepare the propofol stock, identical experiments were performed following wash-in of 0.10% v/v DMSO solution for 2-3 minutes (Figure 4.1C&D). The current decay in 0.10% v/v DMSO solution did not differ considerably from control during the 3 second depolarization to +30 mV (Figure 4.1C&D). The current magnitude at 3 seconds in control solution was approximately 84% of the peak at +30 mV for WT Kv1.2 channels, 99% of the peak at +30 mV for Kv1.2[N207A] channels, and 79% of the peak at +30 mV for Kv1.2[T252R] channels (Figure 4.1C). The values in 0.10% v/v DMSO were nearly identical, the current magnitude at 3 seconds was 83% of the peak at +30 mV for WT Kv1.2 channels, 98% for Kv1.2[N207A] channels, and 78% for Kv1.2[T252R] channels (Figure 4.1D).

4.2.2: Propofol inhibits Kv1.2 channel peak currents

In addition to the current decay effect, propofol (200 μ M) also suppressed Kv1.2 channel peak currents (Figure 4.1E-G). To investigate this effect, cells expressing WT Kv1.2, Kv1.2[N207A], and Kv1.2[T252R] channels were pulsed for 300 ms to voltages between -130 mV and +70 mV in control solution and after perfusion of propofol (200 μ M) into the bath for 2-3 minutes (Figure 4.2A-C). Peak currents were measured in both conditions. Currents were normalized to the peak current magnitude at +70 mV in control conditions (Figure 4.2A-C). Propofol inhibited the peak currents from WT Kv1.2, Kv1.2[N207A], and Kv1.2[T252R] channels to a comparable extent in voltage ranges where channels were activated (Figure 4.2A-C). Overall, propofol exerts two inhibitory effects on Kv1.2 channels: suppression of peak currents (Figure 4.2), and time-dependent current decay resembling open channel block (Figure 4.1). We also performed a vehicle control of 0.10% v/v DMSO solution perfusion for 2-3 minutes (Figure 4.2D-F). The peak current magnitudes for all channels tested were largely unchanged from control following wash-in of 0.10% v/v DMSO solution (Figure 4.2D-F). Peak current amplitudes at +70 mV for WT Kv1.2, Kv1.2[N207A], and Kv1.2[T252R] channels in 0.10% v/v DMSO were 92%, 81%, and 91% respectively of the peak current at +70 mV in control solution (Figure 4.2D-F). The absence of Kv1.2 current inhibition by 0.10% v/v DMSO confirms the inhibitory effects of propofol on Kv1.2 channels.

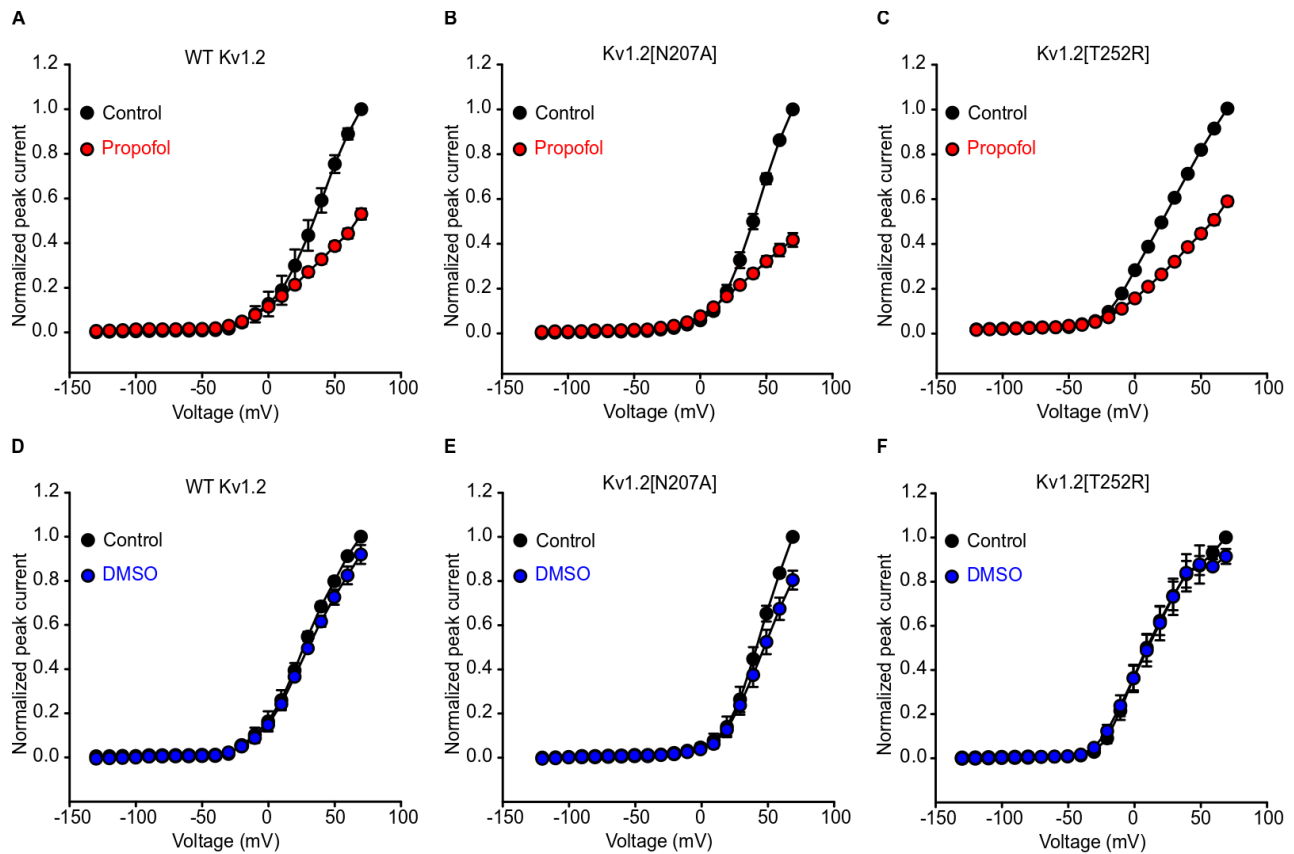


Figure 4.2: Propofol inhibits Kv1.2 channel peak currents.

(A-C) Mean current-voltage relationships (\pm S.E.M) for WT Kv1.2 (n=5), Kv1.2[N207A] (n=7), and Kv1.2[T252R] (n=5) channels in control solution and following wash-in of 200 μ M propofol. (D-E) Mean current-voltage relationships (\pm S.E.M) for WT Kv1.2 (n=5), Kv1.2[N207A] (n=5), and Kv1.2[T252R] (n=5) channels in control and following wash-in of 0.10% v/v DMSO. Currents were elicited by pulsing to voltages between -130 mV and +70 mV (300 ms in 10 mV steps, -100 mV holding potential) and normalized to the peak current magnitude at +70 mV in control conditions. 200 μ M propofol or 0.10% v/v DMSO solution was perfused into the bath for 2-3 minutes after control recordings. Solutions were prepared as described in the materials and methods chapter (page 27).

4.2.3: Propofol potentiates Kv1.2 channel activation

In addition to the current inhibition observed in the presence of propofol (Figure 4.1&Figure 4.2), Kv1.2 channel currents in propofol frequently exhibited accelerated activation kinetics. This effect of propofol is evident in the WT Kv1.2 and Kv1.2[N207A] sample traces presented in figure 4.1E&F and figure 4.3J&K. To investigate the basis of this effect, conductance-voltage relationships were obtained for cells expressing WT Kv1.2, Kv1.2[N207A], and Kv1.2[T252R]

channels in control solution and following wash-in of 200 μ M propofol (Figure 4.3A-C). Propofol induced a hyperpolarizing shift in the conductance-voltage relationships of WT Kv1.2, Kv1.2[N207A], and Kv1.2[T252R] channels (Figure 4.3&Figure 4.4), indicating propofol potentiates Kv1.2 voltage-dependent activation. The mean activation $V_{1/2}$ values in control conditions were +16.8 mV, +35.3 mV, and -4.2 mV for cells expressing WT Kv1.2, Kv1.2[N207A], and Kv1.2[T252R] channels, respectively (Figure 4.3A-C). In propofol, the activation $V_{1/2}$ values were -10.5 mV for WT Kv1.2 channels, +2.1 mV for Kv1.2[N207A], and -16.2 mV for Kv1.2[T252R] (Figure 4.3A-C). Thus, propofol hyperpolarized the activation $V_{1/2}$ of WT Kv1.2, Kv1.2[N207A], and Kv1.2[T252R] channels by approximately -27 mV, -33 mV, and -12 mV, respectively. Conductance-voltage relationships were also obtained for cells expressing WT Kv1.2, Kv1.2[N207A], and Kv1.2[T252R] channels with a vehicle control of 0.10% v/v DMSO solution (Figure 4.3D-F). The mean activation $V_{1/2}$ values of WT Kv1.2, Kv1.2[N207A], and Kv1.2[T252R] channels were similar in control and in 0.10% v/v DMSO (Figure 4.3D-F). The activation $V_{1/2}$ values for cells expressing WT Kv1.2, Kv1.2[N207A], and Kv1.2[T252R] channels in control solution were +9.8 mV, +38.1 mV, and -7.9 mV, respectively (Figure 4.3D-F), compared to +5.2 mV, +38.9 mV, and -10.3 mV in 0.10% v/v DMSO (Figure 4.3D-F). Thus, wash-in of 0.10% v/v DMSO solution did not appreciably shift the voltage-dependence of activation of Kv1.2 channels.

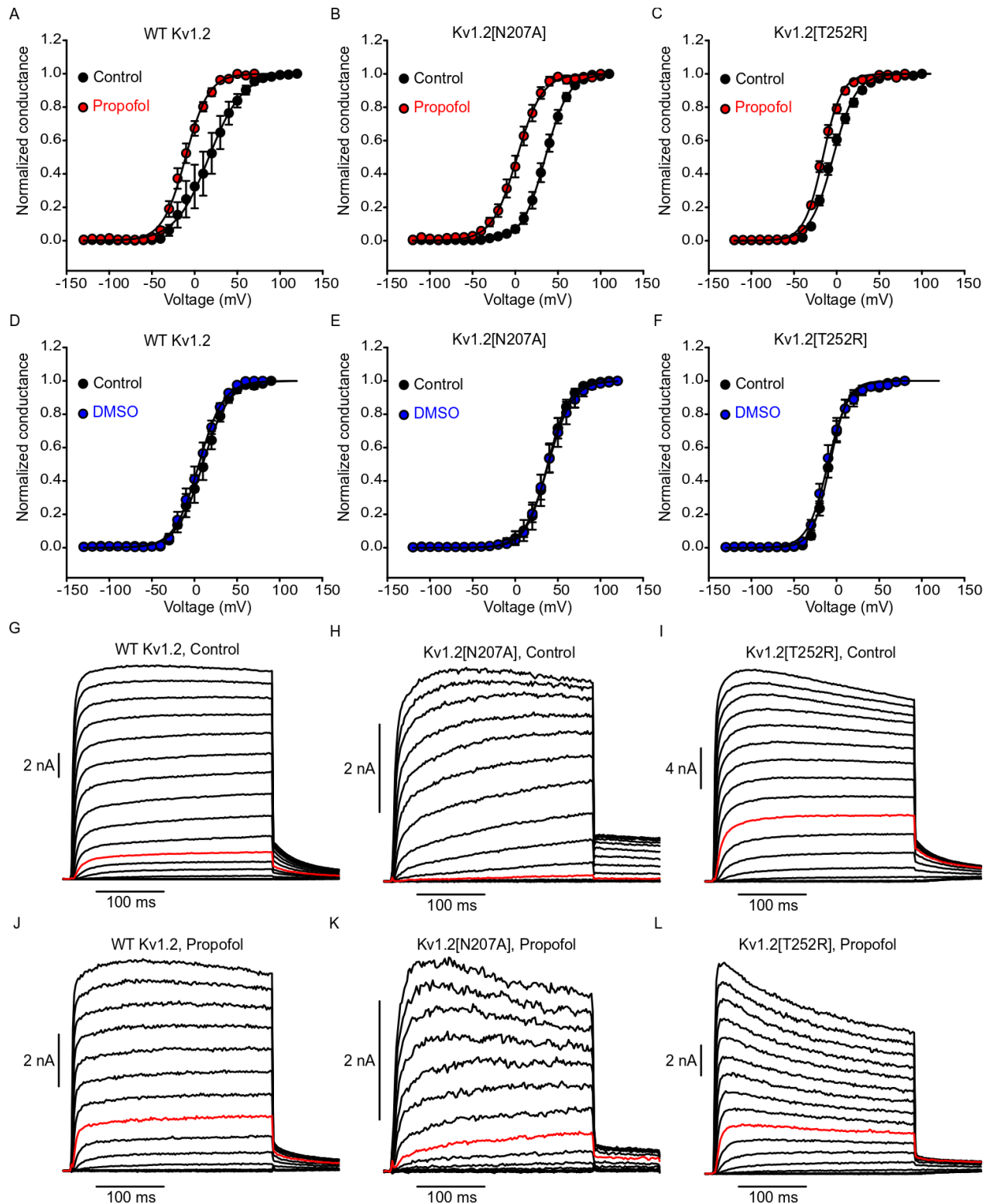


Figure 4.3: Propofol hyperpolarized the GV relationships of Kv1.2 channels.

(A-C) Conductance-voltage relationships (mean \pm S.E.M) for cells expressing WT Kv1.2 (n=6), Kv1.2[N207A] (n=7), and Kv1.2[T252R] (n=8) channels in control solution and after perfusion of 200 μ M

propofol. WT Kv1.2 $V_{1/2}$ (Control)= +16.8 mV, Kv1.2[N207A] $V_{1/2}$ (Control)= +35.3 mV, Kv1.2[T252R] $V_{1/2}$ (Control)= -4.2 mV. WT Kv1.2 $V_{1/2}$ (Propofol)= -10.5 mV, Kv1.2[N207A] $V_{1/2}$ (Propofol)= +2.1 mV, Kv1.2[T252R] $V_{1/2}$ (Propofol)= -16.2 mV. (D-F) Conductance-voltage relationships (mean \pm S.E.M) for cells expressing WT Kv1.2 (n=6), Kv1.2[N207A] (n=5), and Kv1.2[T252R] (n=6) channels in control and following wash-in of 0.10% v/v DMSO solution. WT Kv1.2 $V_{1/2}$ (Control)= +9.8 mV, Kv1.2[N207A] $V_{1/2}$ (Control)= +38.1 mV, Kv1.2[T252R] $V_{1/2}$ (Control)= -7.9 mV. WT Kv1.2 $V_{1/2}$ (DMSO)= +5.2 mV, Kv1.2[N207A] $V_{1/2}$ (DMSO)= +38.9 mV, Kv1.2[T252R] $V_{1/2}$ (DMSO)= -10.3 mV. (G-L) Exemplar current traces illustrating hyperpolarization of WT Kv1.2, Kv1.2[N207A], and Kv1.2[T252R] conductance-voltage relationships by 200 μ M propofol. Red traces represent a pulse to +10 mV. Conductance-voltage relationships were generated by stepping cells to voltages between -130 mV and +120 mV (300 ms in 10 mV steps, -100 mV holding potential), followed by a tail current voltage of -30 mV. Tail currents were normalized to the peak tail current magnitude and fit with a Boltzmann (Equation 1). Conductance-voltage relationships were obtained in control solution and after perfusion of 200 μ M propofol or 0.10% v/v DMSO solution into the bath for 2-3 minutes. Solutions were prepared as described in the materials and methods chapter (page 27).

Examination of the activation $V_{1/2}$ for individual cells revealed that propofol hyperpolarized the activation $V_{1/2}$ to some degree in all cells (Figure 4.4A-C). However, the degree of this shift varied from cell to cell, even for cells expressing the same Kv1.2 channel type (Figure 4.4A-C). The difference in the magnitude of the hyperpolarizing shift between WT Kv1.2, Kv1.2[N207A], and Kv1.2[T252R] channels (Figure 4.3A-C) reflects the differing responses of these channels to the potentiating effects of propofol. On a cell by cell basis, Kv1.2[N207A] channels typically exhibit large propofol-mediated $V_{1/2}$ shifts ranging from -25 mV to -43mV (Figure 4.4B). In contrast, Kv1.2[T252R] channels exhibited considerably smaller shifts, ranging from -6 mV to -19 mV (Figure 4.4C). The propofol response of WT Kv1.2 appeared segregated to two populations (Figure 4.4A). One population of cells exhibited large hyperpolarized shifts ranging from -25mV to -45 mV, similar to Kv1.2[N207A] channels, while the remaining cells exhibited smaller shifts of \sim -6 mV in magnitude, similar to the response of Kv1.2[T252R] channels (Figure 4.4A). Wash-in of 0.10% v/v DMSO solution did not have consistent effects on the voltage-dependence of activation (Figure 4.4D-F). The $V_{1/2}$ shifts following 0.10% v/v DMSO wash-in were not statistically significant; for the majority of the cells, the activation $V_{1/2}$ was shifted by <5 mV in either direction (Figure 4.4D-F). The $V_{1/2}$ shifts in 0.10% v/v DMSO were likely due to random variation or experimental error during the recording period.

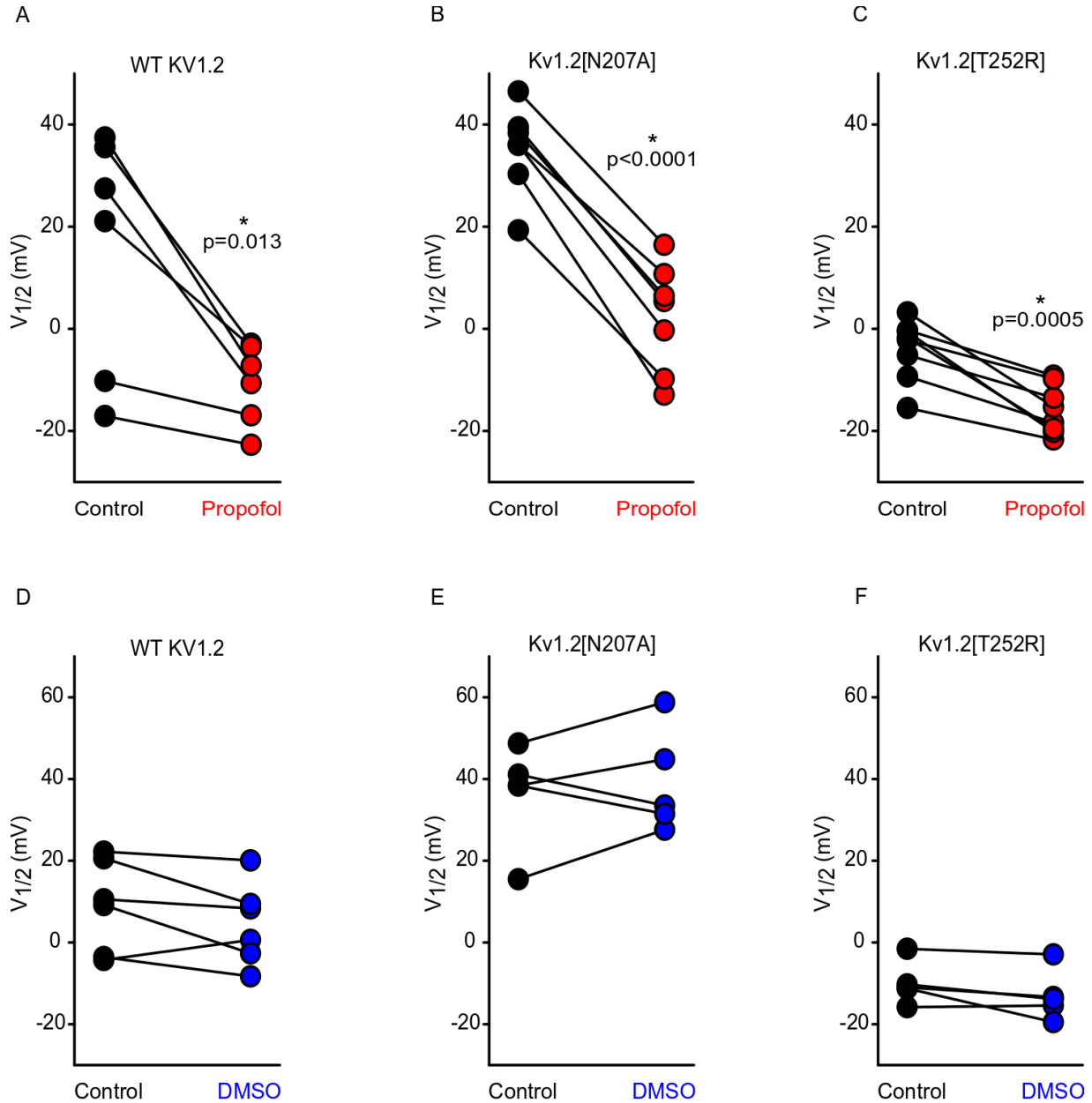


Figure 4.4: Propofol hyperpolarized the activation $V_{1/2}$ of all cells.

(A-C) Activation $V_{1/2}$ in control and following wash-in of 200 μ M propofol (paired measurements) for cells expressing WT Kv1.2 (n=6), Kv1.2[N207A] (n=7), and Kv1.2[T252R] (n=8) channels. The magnitude of the propofol-induced hyperpolarizing $V_{1/2}$ shift was variable from cell to cell. (D-E) Activation $V_{1/2}$ in control and following wash-in of 0.10% v/v DMSO solution (paired measurements) for cells expressing WT Kv1.2 (n=6), Kv1.2[N207A] (n=5), and Kv1.2[T252R] (n=6) channels. $V_{1/2}$ values were compared with a paired student's t-test, significant differences are indicated by * with the associated P value shown. Activation $V_{1/2}$ values were obtained for each cell by fitting conductance-voltage relationships with a Boltzmann (Equation 1). Conductance-voltage relationships were obtained as described in figure 4.3.

4.2.4: Propofol potentiates Kv1.2 channels by modifying slow gating regulation

The gating effects of propofol correlate with the sensitivity of the Kv1.2 mutants to slow gating regulation, leading us to suspect slow gating regulation was involved in this effect of propofol. The conductance-voltage relationships indicate Kv1.2[N207A] channels, which are highly sensitive to slow gating regulation, are potentiated strongly by propofol (Figure 4.3B&Figure 4.4B). Kv1.2[T252R] channels, which have diminished sensitivity to slow gating, exhibit modest hyperpolarized shifts in comparison (Figure 4.3C&Figure 4.4C). To determine a relationship between slow gating regulation and the potentiating effects of propofol, the activation $V_{1/2}$ in control, used as a measure of slow gating inhibition, was compared with the propofol-mediated gating shift on a cell-by-cell basis (Figure 4.5A). Kv1.2 channels gating in the slow mode exhibit relatively depolarized activation $V_{1/2}$ values, reflecting inhibition of voltage-dependent Kv1.2 activation by slow gating regulation (Baronas et al., 2015b, 2015b; Rezazadeh et al., 2007). Depolarized activation $V_{1/2}$ values in control conditions correlate with a large propofol induced hyperpolarizing gating shift (Figure 4.5A). Kv1.2[N207A] and slow mode WT Kv1.2 channels (activation $V_{1/2} > +10$ mV) exhibited hyperpolarized shifts ranging from -25 mV to -45 mV (Figure 4.5A), and an acceleration of their activation kinetics (Figure 4.5B&C). On the other hand, Kv1.2[T252R] channels and fast mode WT Kv1.2 channels (activation $V_{1/2} < +10$ mV) exhibited smaller shifts, with most cells in this range exhibiting a hyperpolarized shift less than -10 mV in magnitude (Figure 4.5A). In addition, Kv1.2[T252R] channels and fast mode WT Kv1.2 channels exhibited little or no acceleration of activation kinetics in propofol (Figure 4.5D&E). This result demonstrates that the magnitude of the hyperpolarizing shift in propofol varies with the degree of slow gating inhibition in control. Kv1.2[N207A] and slow mode WT Kv1.2 channels, which are prominently inhibited by slow gating regulation, are strongly potentiated by propofol (Figure 4.5). While fast mode WT Kv1.2 and Kv1.2[T252R] channels, which are weakly inhibited by slow

gating regulation, are modestly potentiated in comparison (Figure 4.5). Overall, these results indicate that propofol potentiates Kv1.2 channels by interfering with slow gating regulation.

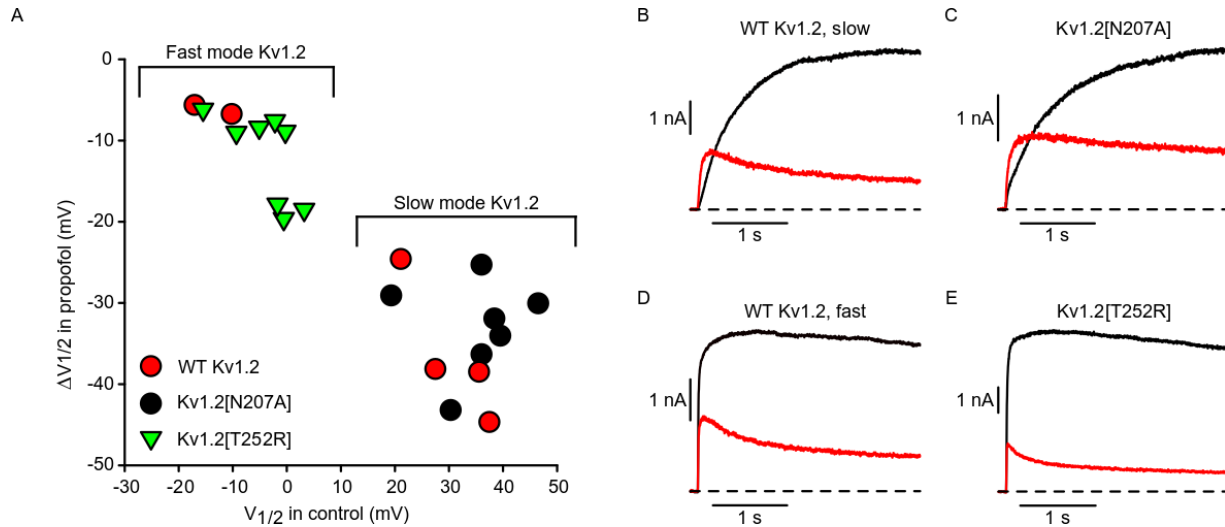


Figure 4.5: Depolarized activation $V_{1/2}$ values in control correlate with large $V_{1/2}$ shifts in propofol.

(A) Graph compares the activation $V_{1/2}$ in control solution to the activation $V_{1/2}$ change ($\Delta V_{1/2}$) following wash-in of 200 μ M propofol. WT Kv1.2 ($n=6$), Kv1.2[N207A] ($n=7$), and Kv1.2[T252R] ($n=8$). Each data point represents a single cell. The activation $V_{1/2}$ change for each cell was calculated as: activation $V_{1/2}$ in control – activation $V_{1/2}$ in propofol. Activation $V_{1/2}$ values were obtained from the individual Boltzmann fit parameters of the cells in figure 4.4A-C. (B-E) Exemplar current traces illustrating acceleration of the activation kinetics of “slow” mode WT Kv1.2 (B) and Kv1.2[N207A] (C) channels in 200 μ M propofol. The activation kinetics of “fast” mode WT Kv1.2 (D) and Kv1.2[T252R] channels (E) exhibit minimal acceleration in propofol. Currents were elicited by a 3 s pulse to + 30 mV (holding potential of -80 mV).

Section 4.3: Discussion

In this chapter, Kv1.2 channel regulation by propofol was investigated. Using channel mutants with varying sensitivity to slow gating (WT Kv1.2, Kv1.2[N207A], and Kv1.2[T252R]), we examined the interaction between slow gating and the Kv1.2 response to propofol. These findings revealed current inhibition of Kv1.2, together with a potentiating gating effect, demonstrating previously unreported effects of propofol on Kv1.2. Additionally, the results indicate Kv1.2 modulation by slow gating regulation considerably influences the response of Kv1.2 channels to propofol, and thus could alter the response of Kv1.2 channels to other drugs.

4.3.1: Propofol inhibition of Kv1.2 channels

Propofol (200 μ M) provoked a time-dependent decay of Kv1.2 channel currents (Figure 4.1) and suppressed Kv1.2 channel peak currents (Figure 4.2). Remarkably, the Kv1.2 channel mutants tested were differentially sensitive to propofol inhibition. Kv1.2[T252R] channels exhibited the greatest sensitivity to the propofol-induced current decay, followed by WT Kv1.2 channels, and Kv1.2[N207A] channels which were the least sensitive (Figure 4.1). Propofol inhibited the peak currents of WT Kv1.2, Kv1.2[N207A], and Kv1.2[T252R] channels to a comparable extent (Figure 4.2).

4.3.2: Propofol inhibits Kv1.2 channels by an open channel block mechanism

An open channel block mechanism likely underlies the inhibitory effects of propofol on Kv1.2 channels. Propofol inhibits another Shaker family channel, Kv1.5, via an open channel block mechanism (Kojima et al., 2015; Yang et al., 2015). Thus, it is reasonable to hypothesize propofol inhibits Kv1.2 channels via a similar mechanism. Supporting this hypothesis, a variety of compounds that inhibit Kv1.2 channels via an open channel block mechanism provoke a reduction in the peak currents combined with increased current decay (Brock et al., 2001; Poling et al., 1996; Russell et al., 1994; Sprunger et al., 1996; Yamagishi et al., 1995), similar to the action of propofol on Kv1.2 currents (Figure 4.1&Figure 4.2). The progressive decay of Kv1.2 channel currents in propofol once the current peak is achieved (Figure 4.1) is consistent with propofol interacting with and blocking open state Kv1.2 channels. The peak current inhibition effect (Figure 4.2) possibly reflects a fast phase of open channel block by propofol, as has been suggested for 4-aminopyridine which exerts similar effects as propofol on Kv1.2 currents (Russell et al., 1994). The recovery of the peak current between voltage pulses in propofol (Figure 4.2A-C&Figure 4.3J-L) indicates propofol unbinding occurs between pulses when channels are closed.

Furthermore, the differing sensitivities of WT Kv1.2, Kv1.2[N207A], and Kv1.2[T252R] channels to the inhibitory effects of propofol can be rationalized with an open channel block mechanism for propofol. Propofol inhibits Kv1.2[T252R] peak currents over a broader range of voltages (-40 mV to +70 mV) compared to WT Kv1.2 peak currents (-10 mV to +70 mV) and Kv1.2[N207A] peak currents (+20 mV to +70 mV) (Figure 4.2). This can be rationalized by increased availability of open state Kv1.2[T252R] channels within the voltage ranges tested due to their activation at relatively hyperpolarized potentials ($V_{1/2}$ (Control)= -4.2 mV; $V_{1/2}$ (Propofol)= -16.2 mV) compared to WT Kv1.2 channels ($V_{1/2}$ (Control)= +16.8 mV; $V_{1/2}$ (Propofol)= -10.5 mV) and Kv1.2[N207A] channels ($V_{1/2}$ (Control)= +35.3 mV; $V_{1/2}$ (Propofol)= +2.1 mV) (Figure 4.3&Figure 4.4). The difference in the predicted ratio of open channels at +30 mV for Kv1.2[T252R], WT Kv1.2, and Kv1.2[N207A] channels possibly underlies the difference in the rate of current decay (Figure 4.1). At +30 mV, Kv1.2[T252R] channels are at a near maximal open probability, whereas Kv1.2[N207A] are near the $V_{1/2}$ of activation (~50% open probability). This would account partially for the faster decay of current from activated Kv1.2[T252R] channels.

4.3.3: Modification of slow gating regulation by propofol

Propofol (200 μ M) induced a hyperpolarizing shift in the activation $V_{1/2}$ of Kv1.2 channels (Figure 4.3&Figure 4.4) and accelerated their activation kinetics (Figure 4.5B&C). The potentiation of Kv1.2 channel activation by propofol appears related to slow gating regulation. Previous reports have demonstrated hyperpolarized shifts in the activation $V_{1/2}$ of Kv1.2 channels following the application of strong depolarizing pre-pulses (Baronas et al., 2015b, 2015a; Rezazadeh et al., 2007). This prepulse potentiation effect reflects activity dependent relief of Kv1.2 channels from slow gating inhibition (Baronas et al., 2015b, 2015a; Rezazadeh et al., 2007). Kv1.2 channels inhibited by slow gating ("slow" mode Kv1.2 channels) were considerably potentiated by prepulses while fast mode Kv1.2 channels, which are weakly inhibited by slow gating regulation, showed minimal potentiation (Baronas et al., 2015a; Rezazadeh et al., 2007). The propofol-

induced potentiation of Kv1.2 activation bears similarity to the pre-pulse potentiation effect. In this study, propofol robustly potentiated the activation of Kv1.2 channels prominently inhibited by slow gating regulation (i.e. Kv1.2[N207A] channels) (Figure 4.3&Figure 4.4), and the magnitude of the hyperpolarizing $V_{1/2}$ shift in propofol increased with the degree of slow gating inhibition in control (Figure 4.5). These results, together with previous studies of slow gating, indicate that propofol potentiates the activation of Kv1.2 channels by facilitating relief from slow gating regulation. Kv1.2 channels strongly inhibited by slow gating (“slow” mode WT Kv1.2 and Kv1.2[N207A] channels) likely experience significant disinhibition from slow gating regulation in propofol, underlying their substantial hyperpolarized $V_{1/2}$ shifts in propofol (Figure 4.3&Figure 4.4). In comparison, Kv1.2 channels weakly inhibited by slow gating regulation (“fast mode” WT Kv1.2 and Kv1.2[T252R] channels) likely experience minimal disinhibition from slow gating in propofol, underlying the smaller hyperpolarized $V_{1/2}$ shifts of these channels (Figure 4.3&Figure 4.4). An alternative explanation for the effects of propofol is that propofol disrupts membrane lipids such as PIP₂ that influence Kv1.2 function (Rodriguez-Menchaca et al., 2012; Tsuchiya and Mizogami, 2013; Urban, 2002). However, PIP₂ depletion slows the deactivation kinetics of Kv1.2 channels (Rodriguez-Menchaca et al., 2012), and propofol exposure does not produce this effect.

4.3.4: Previously reported effects of propofol on Kv1.2 channels

Previous studies examining the effects of propofol on WT Kv1.2 channels in *Xenopus laevis* oocytes did not report inhibitory or potentiating effects of propofol (Bu et al., 2018; Liang et al., 2015). The absence of propofol inhibition of Kv1.2 channels in these studies could be due to the propofol concentrations used. These studies utilized propofol concentrations of 30 uM (Bu et al., 2018) and 60 uM (Liang et al., 2015), compared to the 200 uM propofol concentration utilized in this chapter. However, inhibitory effects of propofol on Kv1.2 channel currents were observed with 100 uM propofol in our experiments (data not shown). Although propofol did not potentiate

WT Kv1.2 channels in previous studies, propofol increased the maximum conductance and hyperpolarized the activation $V_{1/2}$ of Kv1.2 channels with a G329T mutation in their S4-S5 linker (Bu et al., 2018; Liang et al., 2015). The G329T mutation is hypothesized to alter the energetics of Kv1.2 channel gating in a manner that improves functional transduction of propofol's effects upon binding to Kv1.2 (Bu et al., 2018). In this study, propofol hyperpolarized the activation $V_{1/2}$ of Kv1.2 channels without an increase in the maximum conductance. Therefore, it is likely that the potentiation of WT Kv1.2 channels by propofol in this study, and the potentiation of Kv1.2 G329T channels by propofol in previous studies (Bu et al., 2018; Liang et al., 2015), occur through separate mechanisms. The inability of propofol to potentiate the activation of WT Kv1.2 channels in previous studies can be rationalized by the absence of slow gating regulation in *Xenopus laevis* oocytes, demonstrated in figure 3.8.

4.3.5: Exploring roles for Kv1.2 channels in anesthesia.

The results presented in this chapter demonstrate inhibition of Kv1.2 currents and potentiation of Kv1.2 activation by propofol. Kv1.2 channels are valid anaesthetic targets due to their broad localization in the central nervous system and roles in regulating excitability (Coleman et al., 2002; Dodson et al., 2003; Robbins and Tempel, 2012; Wang et al., 1994). Supporting roles for Kv1.2 channels in general anaesthesia, blockade of Kv1.2 channels in the central medial thalamic nucleus, a region of the brain involved in arousal and sleep, reverses loss of consciousness in anaesthetized rats (Lioudyno et al., 2013). Although the propofol concentration utilized in this study (200 μ M) is higher than the plasma propofol concentrations required to achieve anaesthesia (1-4 μ M) (Rudolph and Antkowiak, 2004, 2004; Sall et al., 2012). It is possible the effects of propofol on Kv1.2 channels occur *in-vivo* due to the fact that propofol is highly lipophilic, and thus, the concentration of propofol in the brain could be substantially greater than in plasma (Sall et al., 2012). Establishing a relationship between the

effects of propofol on Kv1.2 channels demonstrated in this study and the endpoints of propofol-mediated anaesthesia would require *in-vivo* studies.

In summary, this chapter reports novel inhibitory and potentiating effects of propofol on Kv1.2 channels. The results presented in this chapter indicate propofol inhibits Kv1.2 channels via an open channel block mechanism and potentiates Kv1.2 channels by facilitating disinhibition from slow gating regulation. These results demonstrate modification of slow gating regulation as a potential mechanism of action for drugs targeting Kv1.2 channels and the ability of slow gating regulation to alter Kv1.2 channel pharmacology.

Chapter 5: General discussion & Conclusion

Kv1.2 channel activity is modulated by a regulatory mechanism described in this thesis as “slow gating regulation” or “slow gating”. Kv1.2 channels in the slow gating mode exhibit prominent use-dependent activation, slowed activation kinetics, and depolarized GV relationships (Baronas et al., 2015a; Rezazadeh et al., 2007). The molecular players mediating slow gating regulation are unidentified, and the factors that tune the modulation of Kv1.2 channels by slow gating have not been fully elucidated. A summary of the identified factors is provided in Figure 5.1. Current evidence indicates slow gating regulation is mediated by an extrinsic, redox-sensitive, transmembrane protein (Baronas et al., 2017, 2015b) (see page 18). In this thesis, I aimed to identify novel factors modulating slow gating regulation of Kv1.2 channels. Additionally, I investigated the impact of slow gating regulation on Kv1.2 pharmacology. The findings in this thesis broaden the understanding of ion channel regulation by accessory subunits and its pharmacological consequences.

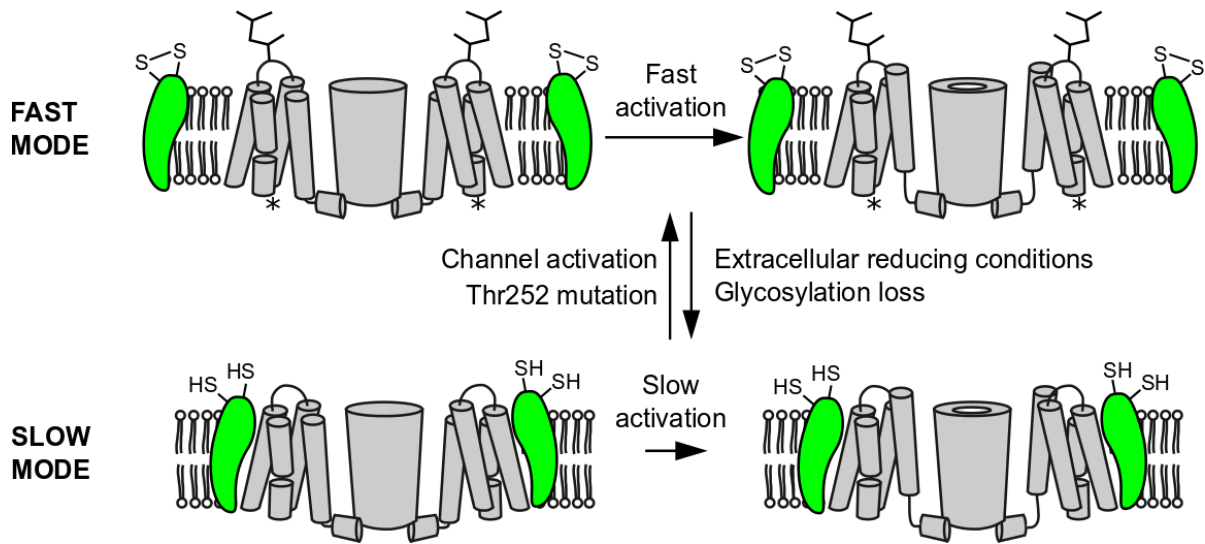


Figure 5.1: Factors modulating occupancy of the fast and slow gating modes.

Kv1.2 channels exhibit variable occupancy of a “fast” uninhibited gating mode and a “slow” inhibited gating mode. Kv1.2 channels bound to the putative regulatory protein (green) are in the slow gating mode. Extracellular reducing conditions strongly favour the slow gating mode, we hypothesize extracellular reducing agents modify a disulfide bond in the regulatory protein and increases its affinity for Kv1.2. Prior channel activation promotes the fast gating mode. We hypothesize this occurs by triggering dissociation of the regulatory protein from Kv1.2 channels. The mutation of Thr252, indicated by the asterisk, is posited to promote occupancy of the fast gating mode by disrupting the regulatory protein binding site in Kv1.2 (Baronas et al., 2017, 2015b). Glycosylation loss is demonstrated to promote occupancy of the slow gating mode in this thesis (Chapter 3).

5.1.1: Glycosylation loss promotes slow gating inhibition

In Chapter 3, I demonstrated that glycosylation loss increased the inhibition of Kv1.2 channels by slow gating regulation. I found that glycosylation deficient Kv1.2 channels exhibited enhanced use-dependence and extremely slow activation kinetics compared to WT Kv1.2 channels (Figure 3.1 & Figure 3.3). Additionally, I demonstrated the markedly depolarized conductance-voltage relationships of glycosylation deficient Kv1.2 channels (Figure 3.6B). The inhibited activation properties of glycosylation deficient Kv1.2 channels were relieved by manipulations previously shown to attenuate slow gating regulation. The T252R mutation, shown to weaken slow gating regulation in WT Kv1.2 channels, dramatically accelerated the activation kinetics of glycosylation deficient Kv1.2 channels (Figure 3.2) and attenuated their

enhanced use-dependent activation (Figure 3.3). I also found that activating pre-pulses produced remarkable acceleration of the activation kinetics of glycosylation deficient Kv1.2 channels (Figure 3.4). Additionally, Slc7a5, a protein that eliminates slow gating behavior in WT Kv1.2 channels (Figure 3.5), rescues the inhibited activation of glycosylation deficient channels (Figure 3.6 & Figure 3.7). Finally, I found that the activation kinetics of WT Kv1.2 and glycosylation deficient Kv1.2 channels expressed in *Xenopus laevis* oocytes are indistinguishable (Figure 3.8), compared to the striking differences in the activation kinetics of these channels when expressed in LM cells (Figure 3.1). The interpretation of this result is that the protein mediating slow gating regulation is expressed sparsely in *Xenopus laevis* oocytes. These findings demonstrate glycosylation state as a factor that modulates the sensitivity of Kv1.2 channels to slow gating (Figure 5.1), underlying the apparently large activation barrier of glycosylation deficient Kv1.2 channels. It is possible glycosylation is involved in the modulation of other ion channels by extrinsic regulatory mechanisms.

5.1.2: Modification of ion channel glycosylation *in-vivo*

Glycosylation is thought to alter the gating properties of ion channels by effects on their intrinsic biophysical properties (Baycin-Hizal et al., 2014; Jaeken, 2011). Modification of ion channel glycosylation may then present a mechanism by which ion channel gating properties are altered to meet excitability demands *in-vivo* (Scott and Panin, 2014). Studies have reported location dependent variations in the glycosylation of mammalian ion channels. This variation in glycosylation is observed in Kv3.1, Kv3.3, and Kv3.4 channels, which express dissimilar glycan structures in different regions of the adult rat central nervous system (Schwalbe et al., 2008). Changes in the glycan structure of ion channels also occur in biological development. Nav1.9 channels in the rat dorsal root ganglion show reduced glycosylation in neonates compared to adults (Tyrrell et al., 2001). These alterations in glycosylation are also accompanied by changes in the gating properties of Nav1.9 (Tyrrell et al., 2001). Alterations in glycosylation are also

observed in congenital disorders of glycosylation. Interestingly, congenital disorders of glycosylation are associated with severe neurological disorders in humans such as epilepsies, motor defects, and intellectual disabilities (Baycin-Hizal et al., 2014; Jaeken, 2011). These neurological disorders are also apparent in conditions that arise due to defects in ion channel function (Baycin-Hizal et al., 2014; Felix, 2000; Kullmann and Waxman, 2010). Considering the results in chapter 3, physiological changes in glycosylation may control ion channel function by altering sensitivity to extrinsic regulatory mechanisms, in addition to intrinsic biophysical effects.

5.1.3: Biophysical effects of glycosylation on voltage-gated ion channels

Glycosylation influences the gating of voltage-gated sodium (Bennett et al., 1997a; Zhang et al., 1999), potassium (Baycin-Hizal et al., 2014), and calcium channels (Liu et al., 2019; Park et al., 2015). The influence of glycosylation on the gating of voltage-gated ion channels is typically attributed to electrostatic effects of glycan sialic acids on their gating machinery (Baycin-Hizal et al., 2014; Lazniewska and Weiss, 2014). In the Golgi apparatus, the glycans of N- and O-glycosylated voltage-gated ion channels undergo processing that includes the addition of sialic acids (Lazniewska and Weiss, 2014; Reily et al., 2019). Sialic acids are nine carbon monosaccharides that possess a carboxylate moiety which is negatively charged at physiological pH (Baycin-Hizal et al., 2014). The presence of sialic acids on the extracellular surface of the membrane contributes negative charges to the extracellular surface potential (Baycin-Hizal et al., 2014; Bennett et al., 1997b; Schwetz et al., 2011). An increase in the negativity of the extracellular surface potential is proposed to depolarize the membrane electric field detected by the voltage sensors of ion channels through an electrostatic mechanism (Hille et al., 1975; Ji et al., 1993; Schwetz et al., 2011), consequently lowering the magnitude of depolarization required for channel activation (Hille et al., 1975; Ji et al., 1993; Schwetz et al., 2011). This effect of surface charges on the gating of ion channels is referred to as the surface potential theory (Hille et al., 1975). Based on this theory, the presence of sialic acids in the

glycans of voltage-gated ion channels will potentiate channel activation, and loss of glycan sialic acids will produce the opposite effect (Watanabe et al., 2007). In addition to the surface potential effect, glycosylation loss is posited to induce conformational changes that can alter the gating properties of voltage-gated ion channels (Watanabe et al., 2007, 2003). The inhibited activation of glycosylation deficient Kv1.2 channels has previously been attributed to the surface potential mechanism described above (Watanabe et al., 2007).

5.1.4: Inhibited activation of glycosylation deficient Kv1.2 channels is not consistent with an intrinsic biophysical mechanism

Mechanisms that describe alterations to intrinsic biophysical properties, such as the surface potential mechanism, cannot wholly explain the activation properties of glycosylation deficient Kv1.2 channels described in this thesis. The modification of intrinsic biophysical properties by glycosylation loss would produce consistent effects on the activation properties of glycosylation deficient Kv1.2 channels. I have demonstrated that the activation kinetics of glycosylation deficient Kv1.2 channels are variable from cell-to-cell (Figure 3.1B). Additionally, I have shown that activating pre-pulses accelerate the activation kinetics of glycosylation deficient Kv1.2 channels, indicating their slow activation kinetics can be modulated, and depend on prior activity (Figure 3.4). Both these observations are inconsistent with an intrinsic biophysical mechanism underlying the inhibited activation of glycosylation deficient channels. While intrinsic biophysical mechanisms may contribute to the inhibited activation of these channels, I have presented evidence of increased inhibition of glycosylation deficient Kv1.2 channels by slow gating regulation. I have also presented evidence demonstrating powerful relief of their inhibited activation properties by manipulations that target slow gating. These results indicate increased sensitivity to slow gating is likely the primary mechanism underlying the inhibited activation of glycosylation deficient Kv1.2 channels in the cell systems used in our study. In addition to altered activation properties, I also observed slowed deactivation kinetics of glycosylation

deficient Kv1.2 channels compared to WT Kv1.2 channels (Figure 3.9). This effect of glycosylation loss was insensitive to the T252R mutation (Figure 3.9). The slowed deactivation kinetics of glycosylation deficient Kv1.2 channels have been attributed to altered gating conformations following glycosylation removal (Watanabe et al., 2007).

5.1.5: Mechanism of increased slow gating inhibition in glycosylation deficient channels

At this time, I have not identified the exact mechanisms by which glycosylation loss increases sensitivity to slow gating regulation. Glycosylation has not been reported to alter the modulation of voltage-gated ion channels by extrinsic regulatory mechanisms such as slow gating regulation. Thus, the results in this thesis are novel in that regard. Previous studies of slow gating regulation presented evidence indicating it is mediated by an extrinsic regulatory factor, likely an unidentified accessory protein of Kv1.2 (Figure 5.1) (Baronas et al., 2017, 2015b). The Kv1.2 glycan may be involved in the binding of this extrinsic regulatory factor with Kv1.2 channels. Alternatively, glycosylation loss may initiate regulatory signals that lead to increased inhibition of Kv1.2 channels by the regulatory factor. Additional studies will be required to provide a definitive answer. Interestingly, efforts in our lab to determine the protein mediating slow gating regulation have led to the identification of LMAN2, a glycan-binding protein posited to be involved in the secretory pathway (Hauri et al., 2000; Kwon et al., 2016). The effects of this protein on Kv1.2 gating are being examined in our lab. The results presented in this thesis indicate glycosylation may play a role in the regulation of ion channels by extrinsic regulatory mechanisms. Future studies on glycosylation and ion channel function should consider a role for extrinsic regulators in addition to intrinsic biophysical mechanisms.

5.1.6: Novel effects of propofol on Kv1.2 channels

In Chapter 4, I reported previously unknown potentiating and inhibitory effects of the general anaesthetic propofol on Kv1.2 channels. I observed two inhibitory effects of propofol on Kv1.2. A 200 μM concentration of propofol decreased the peak currents of WT Kv1.2, Kv1.2[N207A], and Kv1.2[T252R] channels (Figure 4.2A-C & Figure 4.1E-G), and produced an additional time-dependent current decay resembling open channel block (Figure 4.1A-B & E-G). I found that the Kv1.2 channel mutants exhibited distinct sensitivities to the time-dependent current decay in propofol. The time-dependent current decay was most apparent in Kv1.2[T252R] channels, followed by WT Kv1.2 channels, and Kv1.2[N207A] channels which were the least sensitive (Figure 4.1A&B). The inhibitory effects of propofol are likely the result of open channel block. In addition to these inhibitory effects, I observed facilitated activation of Kv1.2 in propofol. This was apparent in effects on voltage-dependence and kinetics of activation. 200 μM propofol hyperpolarized the activation $V_{1/2}$ of WT Kv1.2, Kv1.2[N207A], and Kv1.2[T252R] channels (Figure 4.3A-C & Figure 4.4A-C), leading to channel activation at more negative voltages (Figure 4.3G-I vs J-L). Propofol also led to accelerated activation kinetics of these channels, with particularly prominent effects in Kv1.2[N207A] (Figure 4.5B-E).

One potential model to explain the effects of propofol in diverse Kv1.2 mutants is that propofol influences channel sensitivity to the slow gating mechanism. That is, propofol appears to potentiate Kv1.2 activation by facilitating relief from slow gating inhibition. Findings supporting this model are that propofol hyperpolarized the activation $V_{1/2}$ of Kv1.2[N207A] channels and WT Kv1.2 channels to a greater degree than predominantly fast Kv1.2[T252R] channels (Figure 4.3A-C & Figure 4.4A-C). Slow gating regulation prominently inhibits Kv1.2[N207A] and slow mode WT Kv1.2 channels (Figure 5.1), and these are the channel types that exhibit the most prominent gating effects in response to propofol (accelerated activation and prominent hyperpolarized shift of voltage-dependence) (Figure 4.5). In contrast, fast mode WT Kv1.2

channels and Kv1.2[T252R] channels exhibit less baseline modulation by slow gating (Figure 5.1), and consequently exhibit smaller responses to propofol (Figure 4.5). An important feature of slow gating regulation of Kv1.2 channels is that it exhibits marked cell to cell variability, likely due to variable expression of one or more regulatory players involved (Baronas et al., 2017, 2015b, 2015a; Rezazadeh et al., 2007). Consistent with this, I observed cell-to-cell variation in the magnitude of the propofol-mediated hyperpolarizing shift (Figure 4.4A-C). Especially for WT Kv1.2 which exhibits far more variability than Kv1.2[N207A] and Kv1.2[T252R] channels (Figure 4.4A-C). Finally, propofol-mediated potentiation of Kv1.2 channels and prepulse potentiation share similar properties (Baronas et al., 2015a; Rezazadeh et al., 2007), which indicates they likely occur through similar mechanisms. A model for propofol potentiation of Kv1.2 channels based on these results is illustrated schematically in Figure 5.2. In this model, propofol and the slow gating regulator (green structure) compete for interaction with Kv1.2 channels. In conditions that favor fast mode behavior, the interaction with the slow gating regulator (green) is weak. This allows for rapid activation of Kv1.2 channels and rapid time-dependent inhibition (open channel block) of Kv1.2 channels by propofol (red P). In conditions that favor slow mode behavior, association with the slow gating regulator (green) is more prominent and Kv1.2 channel inhibition is increased. As propofol competes with the slow gating regulator for association with Kv1.2, propofol facilitates activation and attenuates the slow activation kinetics that would be observed otherwise (Figure 5.2).

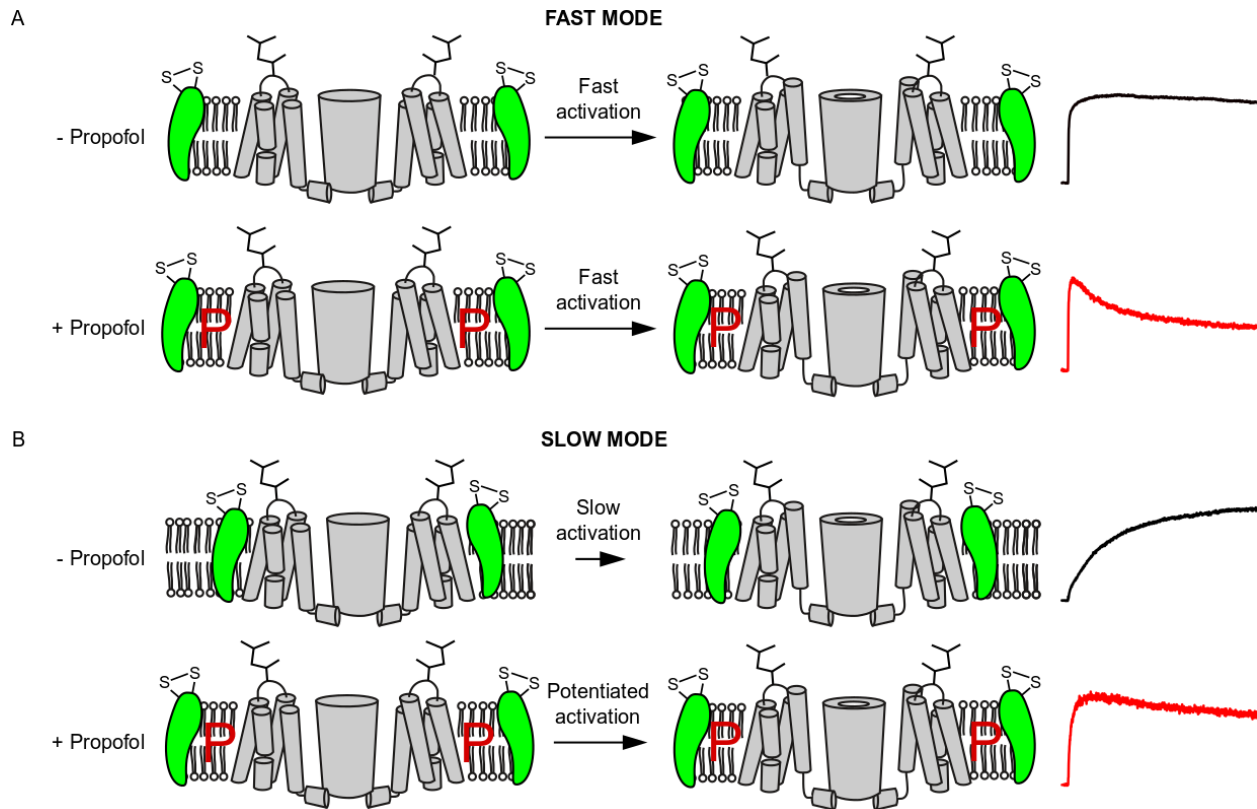


Figure 5.2: Model of Kv1.2 potentiation by propofol.

Kv1.2 activation is modulated by slow gating. This regulatory mechanism is likely mediated by an extrinsic transmembrane protein (green). Kv1.2 channels are either bound to the slow gating regulator in the “slow” mode or unbound from the regulator in the “fast” mode. In the absence of propofol (- Propofol), the activation of “fast” mode Kv1.2 channels is uninhibited while the activation of “slow” mode Kv1.2 channels is inhibited by the regulator. Propofol (depicted by “P”) likely binds to a site in Kv1.2 that disrupts the interaction of the regulator with Kv1.2 channels. In propofol (+ Propofol), the interaction between the regulator and “slow” mode Kv1.2 channels is disrupted, and their activation is potentiated. “Fast” mode Kv1.2 channels are initially unbound from the regulator in the absence of propofol (- Propofol) thus are not potentiated in propofol (+ Propofol).

Overall, I have shown that propofol inhibits Kv1.2 channels by open channel block and potentiates Kv1.2 channel activation by facilitating disinhibition from slow gating regulation.

Thus, propofol may predominantly potentiate or inhibit Kv1.2 channels depending on the degree of slow gating regulation and the magnitude and time scale of applied depolarizations.

Potentiation of Kv1.2 channels by propofol *in-vivo* could produce CNS hypoexcitability that may contribute to propofol mediated general anaesthesia.

5.1.7: Impact of slow gating regulation on Kv1.2 pharmacology

The results presented in chapter 4 reveal implications of slow gating regulation on Kv1.2 pharmacology. Specifically, my findings demonstrate that propofol can potentiate Kv1.2 channels in certain contexts where slow gating regulation is prominent. Propofol may accomplish this by binding near a site where the regulatory protein mediating slow gating regulation interacts with Kv1.2 channels (Figure 5.2). This would disrupt the interaction between the regulator and Kv1.2, resulting in disinhibition from slow gating (Figure 5.2). This is a likely mechanism given that anaesthetics such as propofol can bind to multiple sites in ion channels, including protein-protein interfaces, and can also bind to the interface between ion channels and the lipid bilayer (Urban, 2002). Although propofol appears to target many protein types, this is a valuable first step for our group as it is the first small molecule we have identified that can manipulate the Kv1.2 slow gating regulatory mechanism. Identification of propofol binding sites in Kv1.2 could allow for the design of drug molecules targeting slow gating regulation. Targeting physical contacts between interacting proteins has been explored in drug design, however, only a few compounds acting through this mechanism have been developed (Arkin and Wells, 2004; Chen et al., 2011; Wilson, 2009).

These results also reveal slow gating regulation can influence the response of Kv1.2 channels to drugs that require pore access. I have described evidence indicating propofol inhibits Kv1.2 channels by open channel block. The state model: $C \rightleftharpoons O \rightleftharpoons OB$ describes the state-dependence of open channel blockers, where C, O, and OB represent the closed, open, and open-blocked state of the channel, respectively (Bett and Rasmusson, 2008). In models of this form, channels must reach the open state before open channel block occurs. In chapter 4, I found that Kv1.2[T252R] currents decayed at a faster rate than Kv1.2[N207A] channels in propofol (Figure 4.1A-B). Additionally, propofol inhibited Kv1.2[T252R] peak currents over a broader voltage

range compared to Kv1.2[N207A] channel peak currents (Figure 4.2A-C). The open probability of Kv1.2[N207A] channels is low compared to Kv1.2[T252R] due to their increased inhibition by slow gating regulation. This would account for the apparent differences in the response of these channels to open state inhibition by propofol. Similarly, slow gating regulation could alter the response of Kv1.2 channels to other pore binding drugs. Kv1.2 channels under increased inhibition by slow gating regulation may exhibit reduced sensitivity to drugs that bind in the pore.

5.1.8: Conclusion

Extrinsic regulatory mechanisms considerably influence voltage-gated ion channel gating. The findings in this thesis advance the understanding of factors that modulate extrinsic ion channel regulatory mechanisms and the physiological roles of glycosylation. In addition, the findings in this thesis further show that extrinsic regulatory mechanisms should be important considerations for ion channel drug design, given the significant influence they can exert on ion channel pharmacology.

BIBLIOGRAPHY

- Abraham, M.J., Fleming, K.L., Raymond, S., Wong, A.Y.C., Bergeron, R., 2019. The sigma-1 receptor behaves as an atypical auxiliary subunit to modulate the functional characteristics of Kv1.2 channels expressed in HEK293 cells. *Physiol. Rep.* 7. <https://doi.org/10.14814/phy2.14147>
- Accili, E.A., Kiehn, J., Yang, Q., Wang, Z., Brown, A.M., Wible, B.A., 1997. Separable Kvbeta subunit domains alter expression and gating of potassium channels. *J. Biol. Chem.* 272, 25824–25831. <https://doi.org/10.1074/jbc.272.41.25824>
- Arancibia-Carcamo, I.L., Attwell, D., 2014. The node of Ranvier in CNS pathology. *Acta Neuropathol. (Berl.)* 128, 161–175. <https://doi.org/10.1007/s00401-014-1305-z>
- Arkin, M.R., Wells, J.A., 2004. Small-molecule inhibitors of protein–protein interactions: progressing towards the dream. *Nat. Rev. Drug Discov.* 3, 301–317. <https://doi.org/10.1038/nrd1343>
- Armstrong, C.M., 2003. Voltage-Gated K Channels. *Sci. STKE* 2003, re10–re10. <https://doi.org/10.1126/stke.2003.188.re10>
- Avdonin, V., Nolan, B., Sabatier, J.-M., De Waard, M., Hoshi, T., 2000. Mechanisms of Maurotoxin Action on Shaker Potassium Channels. *Biophys. J.* 79, 776–787. [https://doi.org/10.1016/S0006-3495\(00\)76335-1](https://doi.org/10.1016/S0006-3495(00)76335-1)
- Bähring, R., Vardanyan, V., Pongs, O., 2004. Differential modulation of Kv1 channel-mediated currents by co-expression of Kvβ3 subunit in a mammalian cell-line. *Mol. Membr. Biol.* 21, 19–25. <https://doi.org/10.1080/09687680310001597749>
- Barber, A.F., Liang, Q., Covarrubias, M., 2012. Novel Activation of Voltage-gated K⁺ Channels by Sevoflurane. *J. Biol. Chem.* 287, 40425–40432. <https://doi.org/10.1074/jbc.M112.405787>
- Baronas, V.A., McGuinness, B.R., Brigidi, G.S., Kolisko, R.N.G., Vilin, Y.Y., Kim, R.Y., Lynn, F.C., Bamji, S.X., Yang, R., Kurata, H.T., 2015a. Use-Dependent Activation of Neuronal Kv1.2 Channel Complexes. *J. Neurosci.* 35, 3515–3524. <https://doi.org/10.1523/JNEUROSCI.4518-13.2015>
- Baronas, V.A., Yang, R., Vilin, Y.Y., Kurata, H.T., 2015b. Determinants of frequency-dependent regulation of Kv1.2-containing potassium channels. *Channels* 10, 158–166. <https://doi.org/10.1080/19336950.2015.1120390>
- Baronas, V.A., Yang, R.Y., Kurata, H.T., 2017. Extracellular redox sensitivity of Kv1.2 potassium channels. *Sci. Rep.* 7, 9142. <https://doi.org/10.1038/s41598-017-08718-z>
- Baronas, V.A., Yang, R.Y., Morales, L.C., Sipione, S., Kurata, H.T., 2018. Slc7a5 regulates Kv1.2 channels and modifies functional outcomes of epilepsy-linked channel mutations. *Nat. Commun.* 9, 1–15. <https://doi.org/10.1038/s41467-018-06859-x>
- Barros, F., Pardo, L.A., Domínguez, P., Sierra, L.M., de la Peña, P., 2019. New Structures and Gating of Voltage-Dependent Potassium (Kv) Channels and Their Relatives: A Multi-Domain and Dynamic Question. *Int. J. Mol. Sci.* 20. <https://doi.org/10.3390/ijms20020248>
- Barski, O.A., Tipparaju, S.M., Bhatnagar, A., 2008. The Aldo-Keto Reductase Superfamily and its Role in Drug Metabolism and Detoxification. *Drug Metab. Rev.* 40, 553–624. <https://doi.org/10.1080/03602530802431439>
- Baukrowitz, T., Yellen, G., 1996. Use-Dependent Blockers and Exit Rate of the Last Ion from the Multi-Ion Pore of a K⁺ Channel. *Science* 271, 653–656. <https://doi.org/10.1126/science.271.5249.653>
- Baukrowitz, T., Yellen, G., 1995. Modulation of K⁺ current by frequency and external [K⁺]: A tale of two inactivation mechanisms. *Neuron* 15, 951–960. [https://doi.org/10.1016/0896-6273\(95\)90185-X](https://doi.org/10.1016/0896-6273(95)90185-X)

- Baycin-Hizal, D., Gottschalk, A., Jacobson, E., Mai, S., Wolozny, D., Zhang, H., Krag, S.S., Betenbaugh, M.J., 2014. Physiologic and pathophysiologic consequences of altered sialylation and glycosylation on ion channel function. *Biochem. Biophys. Res. Commun.* 453, 243–253. <https://doi.org/10.1016/j.bbrc.2014.06.067>
- Bennett, E., Urcan, M.S., Tinkle, S.S., Koszowski, A.G., Levinson, S.R., 1997a. Contribution of Sialic Acid to the Voltage Dependence of Sodium Channel Gating A Possible Electrostatic Mechanism. *J. Gen. Physiol.* 109, 327–343. <https://doi.org/10.1085/jgp.109.3.327>
- Bennett, E., Urcan, M.S., Tinkle, S.S., Koszowski, A.G., Levinson, S.R., 1997b. Contribution of Sialic Acid to the Voltage Dependence of Sodium Channel Gating A Possible Electrostatic Mechanism. *J. Gen. Physiol.* 109, 327–343. <https://doi.org/10.1085/jgp.109.3.327>
- Bett, G.C.L., Rasmusson, R.L., 2008. Modification of K⁺ channel–drug interactions by ancillary subunits. *J. Physiol.* 586, 929–950. <https://doi.org/10.1113/jphysiol.2007.139279>
- Blight, A.R., 2011. Treatment of walking impairment in multiple sclerosis with dalfampridine. *Ther. Adv. Neurol. Disord.* 4, 99–109. <https://doi.org/10.1177/1756285611403960>
- Blight, A.R., 1989. Effect of 4-aminopyridine on axonal conduction-block in chronic spinal cord injury. *Brain Res. Bull., Spinal Cord-Recent Work on Trauma and Recovery* 22, 47–52. [https://doi.org/10.1016/0361-9230\(89\)90126-3](https://doi.org/10.1016/0361-9230(89)90126-3)
- Blunck, R., Batulan, Z., 2012. Mechanism of Electromechanical Coupling in Voltage-Gated Potassium Channels. *Front. Pharmacol.* 3. <https://doi.org/10.3389/fphar.2012.00166>
- Bou-Abboud, E., Nerbonne, J.M., 1999. Molecular correlates of the calcium-independent, depolarization-activated K⁺ currents in rat atrial myocytes. *J. Physiol.* 517, 407–420. <https://doi.org/10.1111/j.1469-7793.1999.0407t.x>
- Brock, M.W., Mathes, C., Gilly, W.F., 2001. Selective Open-Channel Block of Shaker (Kv1) Potassium Channels by S-Nitrosodithiothreitol (Sndtt). *J. Gen. Physiol.* 118, 113–134.
- Bu, W., Liang, Q., Zhi, L., Maciunas, L., Loll, P.J., Eckenhoff, R.G., Covarrubias, M., 2018. Sites and Functional Consequence of Alkylphenol Anesthetic Binding to Kv1.2 Channels. *Mol. Neurobiol.* 55, 1692–1702. <https://doi.org/10.1007/s12035-017-0437-2>
- Buraei, Z., Yang, J., 2010. The β Subunit of Voltage-Gated Ca²⁺ Channels. *Physiol. Rev.* 90, 1461–1506. <https://doi.org/10.1152/physrev.00057.2009>
- Cachero, T.G., Morielli, A.D., Peralta, E.G., 1998. The Small GTP-Binding Protein RhoA Regulates a Delayed Rectifier Potassium Channel. *Cell* 93, 1077–1085. [https://doi.org/10.1016/S0092-8674\(00\)81212-X](https://doi.org/10.1016/S0092-8674(00)81212-X)
- Calhoun, J.D., Isom, L.L., 2014. The Role of Non-pore-Forming β Subunits in Physiology and Pathophysiology of Voltage-Gated Sodium Channels, in: Ruben, P.C. (Ed.), *Voltage Gated Sodium Channels, Handbook of Experimental Pharmacology*. Springer, Berlin, Heidelberg, pp. 51–89. https://doi.org/10.1007/978-3-642-41588-3_4
- Castle, N.A., London, D.O., Creech, C., Fajloun, Z., Stocker, J.W., Sabatier, J.-M., 2003. Maurotoxin: A Potent Inhibitor of Intermediate Conductance Ca²⁺-Activated Potassium Channels. *Mol. Pharmacol.* 63, 409–418. <https://doi.org/10.1124/mol.63.2.409>
- Catterall, W.A., 2010. Ion Channel Voltage Sensors: Structure, Function, and Pathophysiology. *Neuron* 67, 915–928. <https://doi.org/10.1016/j.neuron.2010.08.021>
- Chanda, B., Asamoah, O.K., Blunck, R., Roux, B., Bezanilla, F., 2005. Gating charge displacement in voltage-gated ion channels involves limited transmembrane movement. *Nature* 436, 852–856. <https://doi.org/10.1038/nature03888>
- Chandy, K.G., Wulff, H., Beeton, C., Pennington, M., Gutman, G.A., Cahalan, M.D., 2004. K⁺ channels as targets for specific immunomodulation. *Trends Pharmacol. Sci.* 25, 280–289. <https://doi.org/10.1016/j.tips.2004.03.010>
- Chen, J., Jin, S., Abraham, V., Huang, X., Liu, B., Mitten, M.J., Nimmer, P., Lin, X., Smith, M., Shen, Y., Shoemaker, A.R., Tahir, S.K., Zhang, H., Ackler, S.L., Rosenberg, S.H.,

- Maecker, H., Sampath, D., Levenson, J.D., Tse, C., Elmore, S.W., 2011. The Bcl-2/Bcl-XL/Bcl-w Inhibitor, Navitoclax, Enhances the Activity of Chemotherapeutic Agents In Vitro and In Vivo. *Mol. Cancer Ther.* 10, 2340–2349. <https://doi.org/10.1158/1535-7163.MCT-11-0415>
- Chen, X., Johnston, D., 2004. Properties of single voltage-dependent K⁺ channels in dendrites of CA1 pyramidal neurones of rat hippocampus. *J. Physiol.* 559, 187–203. <https://doi.org/10.1113/jphysiol.2004.068114>
- Chen, X., Wang, Q., Ni, F., Ma, J., 2010. Structure of the full-length Shaker potassium channel Kv1.2 by normal-mode-based X-ray crystallographic refinement. *Proc. Natl. Acad. Sci.* 107, 11352. <https://doi.org/10.1073/pnas.1000142107>
- Christie, M.J., North, R.A., Osborne, P.B., Douglass, J., Adelman, J.P., 1990. Heteropolymeric potassium channels expressed in xenopus oocytes from cloned subunits. *Neuron* 4, 405–411. [https://doi.org/10.1016/0896-6273\(90\)90052-H](https://doi.org/10.1016/0896-6273(90)90052-H)
- Coetzee, W.A., Amarillo, Y., Chiu, J., Chow, A., Lau, D., McCORMACK, T., Morena, H., Nadal, M.S., Ozaita, A., Pountney, D., Saganich, M., De Miera, E.V.-S., Rudy, B., 1999. Molecular Diversity of K⁺ Channels. *Ann. N. Y. Acad. Sci.* 868, 233–255. <https://doi.org/10.1111/j.1749-6632.1999.tb11293.x>
- Coleman, S.K., Newcombe, J., Pryke, J., Dolly, J.O., 2002. Subunit Composition of Kv1 Channels in Human CNS. *J. Neurochem.* 73, 849–858. <https://doi.org/10.1046/j.1471-4159.1999.0730849.x>
- Collins, G.G., 1988. Effects of the anaesthetic 2,6-diisopropylphenol on synaptic transmission in the rat olfactory cortex slice. *Br. J. Pharmacol.* 95, 939–949.
- Corbett, M.A., Bellows, S.T., Li, M., Carroll, R., Micallef, S., Carvill, G.L., Myers, C.T., Howell, K.B., Maljevic, S., Lerche, H., Gazina, E.V., Mefford, H.C., Bahlo, M., Berkovic, S.F., Petrou, S., Scheffer, I.E., Gecz, J., 2016. Dominant KCNA2 mutation causes episodic ataxia and pharmacoresponsive epilepsy. *Neurology* 87, 1975–1984. <https://doi.org/10.1212/WNL.0000000000003309>
- Covarrubias, M., Wei, A., Salkoff, L., 1991. Shaker, Shal, Shab, and Shaw express independent K⁺ current systems. *Neuron* 7, 763–773. [https://doi.org/10.1016/0896-6273\(91\)90279-9](https://doi.org/10.1016/0896-6273(91)90279-9)
- Davies, A., Hendrich, J., Van Minh, A.T., Wratten, J., Douglas, L., Dolphin, A.C., 2007. Functional biology of the $\alpha 2\delta$ subunits of voltage-gated calcium channels. *Trends Pharmacol. Sci.* 28, 220–228. <https://doi.org/10.1016/j.tips.2007.03.005>
- del Camino, D., Yellen, G., 2001. Tight Steric Closure at the Intracellular Activation Gate of a Voltage-Gated K⁺ Channel. *Neuron* 32, 649–656. [https://doi.org/10.1016/S0896-6273\(01\)00487-1](https://doi.org/10.1016/S0896-6273(01)00487-1)
- Delint-Ramirez, I., Garcia-Oscos, F., Segev, A., Kourrich, S., 2020. Cocaine engages a non-canonical, dopamine-independent, mechanism that controls neuronal excitability in the nucleus accumbens. *Mol. Psychiatry* 25, 680–691. <https://doi.org/10.1038/s41380-018-0092-7>
- Dodson, P.D., Barker, M.C., Forsythe, I.D., 2002. Two Heteromeric Kv1 Potassium Channels Differentially Regulate Action Potential Firing. *J. Neurosci.* 22, 6953–6961. <https://doi.org/10.1523/JNEUROSCI.22-16-06953.2002>
- Dodson, P.D., Billups, B., Rusznák, Z., Szûcs, G., Barker, M.C., Forsythe, I.D., 2003. Presynaptic rat Kv1.2 channels suppress synaptic terminal hyperexcitability following action potential invasion. *J. Physiol.* 550, 27–33. <https://doi.org/10.1113/jphysiol.2003.046250>
- Dodson, P.D., Forsythe, I.D., 2004. Presynaptic K⁺ channels: electrifying regulators of synaptic terminal excitability. *Trends Neurosci.* 27, 210–217. <https://doi.org/10.1016/j.tins.2004.02.012>
- Doyle, D.A., Cabral, J.M., Pfuetzner, R.A., Kuo, A., Gulbis, J.M., Cohen, S.L., Chait, B.T., MacKinnon, R., 1998. The Structure of the Potassium Channel: Molecular Basis of K⁺

- Conduction and Selectivity. *Science* 280, 69–77.
<https://doi.org/10.1126/science.280.5360.69>
- Fan, L., Guan, X., Wang, W., Zhao, J.-Y., Zhang, H., Tiwari, V., Hoffman, P.N., Li, M., Tao, Y.-X., 2014. Impaired neuropathic pain and preserved acute pain in rats overexpressing voltage-gated potassium channel subunit Kv1.2 in primary afferent neurons. *Mol. Pain* 10, 8. <https://doi.org/10.1186/1744-8069-10-8>
- Fan, Z., Ji, X., Fu, M., Zhang, W., Zhang, D., Xiao, Z., 2012. Electrostatic interaction between inactivation ball and T1–S1 linker region of Kv1.4 channel. *Biochim. Biophys. Acta BBA - Biomembr.* 1818, 55–63. <https://doi.org/10.1016/j.bbamem.2011.09.028>
- Felix, R., 2000. Channelopathies: ion channel defects linked to heritable clinical disorders. *J. Med. Genet.* 37, 729–740. <https://doi.org/10.1136/jmg.37.10.729>
- Frances, P., Johnson Rosalyn, Kerr Paul, Wiehler William, Thorneloe Kevin, Ishii Kuniaki, Chen Tim, Cole William, 2005. Heteromultimeric Kv1 Channels Contribute to Myogenic Control of Arterial Diameter. *Circ. Res.* 96, 216–224.
<https://doi.org/10.1161/01.RES.0000154070.06421.25>
- Franks, N.P., 2008. General anaesthesia: from molecular targets to neuronal pathways of sleep and arousal. *Nat. Rev. Neurosci.* 9, 370–386. <https://doi.org/10.1038/nrn2372>
- Gulbis, J.M., Mann, S., MacKinnon, R., 1999. Structure of a Voltage-Dependent K⁺ Channel β Subunit. *Cell* 97, 943–952. [https://doi.org/10.1016/S0092-8674\(00\)80805-3](https://doi.org/10.1016/S0092-8674(00)80805-3)
- Gulbis, J.M., Zhou, M., Mann, S., MacKinnon, R., 2000. Structure of the Cytoplasmic β Subunit--T1 Assembly of Voltage-Dependent K⁺ Channels. *Science* 289, 123–127.
<https://doi.org/10.1126/science.289.5476.123>
- Haddad, G.A., Blunck, R., 2011. Mode shift of the voltage sensors in Shaker K⁺ channels is caused by energetic coupling to the pore domain. *J. Gen. Physiol.* 137, 455–472.
<https://doi.org/10.1085/jgp.201010573>
- Hales, T.G., Lambert, J.J., 1991. The actions of propofol on inhibitory amino acid receptors of bovine adrenomedullary chromaffin cells and rodent central neurones. *Br. J. Pharmacol.* 104, 619–628.
- Hara, M., Kai, Y., Ikemoto, Y., 1993. Propofol activates GABAA receptor-chloride ionophore complex in dissociated hippocampal pyramidal neurons of the rat. *Anesthesiology* 79, 781–788. <https://doi.org/10.1097/00000542-199310000-00021>
- Hart, P.J., Overturf, K.E., Russell, S.N., Carl, A., Hume, J.R., Sanders, K.M., Horowitz, B., 1993. Cloning and expression of a Kv1.2 class delayed rectifier K⁺ channel from canine colonic smooth muscle. *Proc. Natl. Acad. Sci. U. S. A.* 90, 9659–9663.
- Harvey, A.L., 1997. Recent studies on dendrotoxins and potassium ion channels. *Gen. Pharmacol. Vasc. Syst.* 28, 7–12. [https://doi.org/10.1016/S0306-3623\(96\)00173-5](https://doi.org/10.1016/S0306-3623(96)00173-5)
- Hattan, D., Nesti, E., Cachero, T.G., Morielli, A.D., 2002. Tyrosine Phosphorylation of Kv1.2 Modulates Its Interaction with the Actin-binding Protein Cortactin. *J. Biol. Chem.* 277, 38596–38606. <https://doi.org/10.1074/jbc.M205005200>
- Hauri, H.-P., Appenzeller, C., Kuhn, F., Nufer, O., 2000. Lectins and traffic in the secretory pathway. *FEBS Lett.* 476, 32–37. [https://doi.org/10.1016/S0014-5793\(00\)01665-3](https://doi.org/10.1016/S0014-5793(00)01665-3)
- Heginbotham, L., Lu, Z., Abramson, T., MacKinnon, R., 1994. Mutations in the K⁺ channel signature sequence. *Biophys. J.* 66, 1061–1067.
- Hemmings, H.C., Akabas, M.H., Goldstein, P.A., Trudell, J.R., Orser, B.A., Harrison, N.L., 2005. Emerging molecular mechanisms of general anesthetic action. *Trends Pharmacol. Sci.* 26, 503–510. <https://doi.org/10.1016/j.tips.2005.08.006>
- Hille, B., Woodhull, M., Shapiro, B.I., Thomas, R.C., Keynes, R.D., 1975. Negative surface charge near sodium channels of nerve: divalent ions, monovalent ions, and pH. *Philos. Trans. R. Soc. Lond. B Biol. Sci.* 270, 301–318. <https://doi.org/10.1098/rstb.1975.0011>
- Hopkins, W.F., Allen, M.L., Houamed, K.M., Tempel, B.L., 1994. Properties of voltage-gated K⁺ currents expressed in *Xenopus* oocytes by mKv1.1, mKv1.2 and their heteromultimers

- as revealed by mutagenesis of the dendrotoxin-binding site in mKv1.1. *Pflüg. Arch.* 428, 382–390. <https://doi.org/10.1007/BF00724522>
- Huang, X.-Y., Morielli, A.D., Peralta, E.G., 1993. Tyrosine kinase-dependent suppression of a potassium channel by the G protein-coupled m1 muscarinic acetylcholine receptor. *Cell* 75, 1145–1156. [https://doi.org/10.1016/0092-8674\(93\)90324-J](https://doi.org/10.1016/0092-8674(93)90324-J)
- Hundallah, K., Alenizi, A., AlHashem, A., Tabarki, B., 2016. Severe early-onset epileptic encephalopathy due to mutations in the KCNA2 gene: Expansion of the genotypic and phenotypic spectrum. *Eur. J. Paediatr. Neurol. EJPJN Off. J. Eur. Paediatr. Neurol. Soc.* 20, 657–660. <https://doi.org/10.1016/j.ejpn.2016.03.011>
- Hurst, R.S., Busch, A.E., Kavanaugh, M.P., Osborne, P.B., North, R.A., Adelman, J.P., 1991. Identification of amino acid residues involved in dendrotoxin block of rat voltage-dependent potassium channels. *Mol. Pharmacol.* 40, 572–576.
- Hyun, J.H., Eom, K., Lee, K.-H., Ho, W.-K., Lee, S.-H., 2013. Activity-dependent downregulation of D-type K⁺ channel subunit Kv1.2 in rat hippocampal CA3 pyramidal neurons. *J. Physiol.* 591, 5525–5540. <https://doi.org/10.1113/jphysiol.2013.259002>
- Ishikawa, T., Nakamura, Y., Saitoh, N., Li, W.-B., Iwasaki, S., Takahashi, T., 2003. Distinct Roles of Kv1 and Kv3 Potassium Channels at the Calyx of Held Presynaptic Terminal. *J. Neurosci.* 23, 10445–10453. <https://doi.org/10.1523/JNEUROSCI.23-32-10445.2003>
- Iwakura, A., Uchigashima, M., Miyazaki, T., Yamasaki, M., Watanabe, M., 2012. Lack of Molecular–Anatomical Evidence for GABAergic Influence on Axon Initial Segment of Cerebellar Purkinje Cells by the Pinceau Formation. *J. Neurosci.* 32, 9438–9448. <https://doi.org/10.1523/JNEUROSCI.1651-12.2012>
- Jaeken, J., 2011. Congenital disorders of glycosylation (CDG): it's (nearly) all in it! *J. Inherit. Metab. Dis.* 34, 853–858. <https://doi.org/10.1007/s10545-011-9299-3>
- Jensen, M.Ø., Jogini, V., Borhani, D.W., Leffler, A.E., Dror, R.O., Shaw, D.E., 2012. Mechanism of Voltage Gating in Potassium Channels. *Science* 336, 229–233. <https://doi.org/10.1126/science.1216533>
- Ji, S., Weiss, J.N., Langer, G.A., 1993. Modulation of voltage-dependent sodium and potassium currents by charged amphiphiles in cardiac ventricular myocytes. Effects via modification of surface potential. *J. Gen. Physiol.* 101, 355–375. <https://doi.org/10.1085/jgp.101.3.355>
- Jiang, Y., Lee, A., Chen, J., Ruta, V., Cadene, M., Chait, B.T., MacKinnon, R., 2003a. X-ray structure of a voltage-dependent K⁺ channel. *Nature* 423, 33–41. <https://doi.org/10.1038/nature01580>
- Jiang, Y., Ruta, V., Chen, J., Lee, A., MacKinnon, R., 2003b. The principle of gating charge movement in a voltage-dependent K⁺ channel. *Nature* 423, 42–48. <https://doi.org/10.1038/nature01581>
- Katz, E., Stoler, O., Scheller, A., Khrapunsky, Y., Goebbels, S., Kirchhoff, F., Gutnick, M.J., Wolf, F., Fleidervish, I.A., 2018. Role of sodium channel subtype in action potential generation by neocortical pyramidal neurons. *Proc. Natl. Acad. Sci. U. S. A.* 115, E7184–E7192. <https://doi.org/10.1073/pnas.1720493115>
- Kerr, P.M., Clément-Chomienne Odile, Thorneloe Kevin S., Chen Tim T., Ishii Kuniaki, Sontag David P., Walsh Michael P., Cole William C., 2001. Heteromultimeric Kv1.2-Kv1.5 Channels Underlie 4-Aminopyridine-Sensitive Delayed Rectifier K⁺ Current of Rabbit Vascular Myocytes. *Circ. Res.* 89, 1038–1044. <https://doi.org/10.1161/hh2301.100803>
- Khavandgar, S., Walter, J.T., Sageser, K., Khodakhah, K., 2005. Kv1 channels selectively prevent dendritic hyperexcitability in rat Purkinje cells. *J. Physiol.* 569, 545–557. <https://doi.org/10.1113/jphysiol.2005.098053>
- Kim, D.M., Nimigean, C.M., 2016. Voltage-Gated Potassium Channels: A Structural Examination of Selectivity and Gating. *Cold Spring Harb. Perspect. Biol.* 8. <https://doi.org/10.1101/cshperspect.a029231>

- Kim, D.S., Choi, J.O., Rim, H.D., Cho, H.J., 2002. Downregulation of voltage-gated potassium channel α gene expression in dorsal root ganglia following chronic constriction injury of the rat sciatic nerve. *Mol. Brain Res.* 105, 146–152. [https://doi.org/10.1016/S0169-328X\(02\)00388-1](https://doi.org/10.1016/S0169-328X(02)00388-1)
- Knot, H.J., Nelson, M.T., 1995. Regulation of membrane potential and diameter by voltage-dependent K⁺ channels in rabbit myogenic cerebral arteries. *Am. J. Physiol.-Heart Circ. Physiol.* <https://doi.org/10.1152/ajpheart.1995.269.1.H348>
- Koch, R.O., Wanner, S.G., Koschak, A., Hanner, M., Schwarzer, C., Kaczorowski, G.J., Slaughter, R.S., Garcia, M.L., Knaus, H.G., 1997. Complex subunit assembly of neuronal voltage-gated K⁺ channels. Basis for high-affinity toxin interactions and pharmacology. *J. Biol. Chem.* 272, 27577–27581. <https://doi.org/10.1074/jbc.272.44.27577>
- Kojima, A., Ito, Y., Ding, W.-G., Kitagawa, H., Matsuura, H., 2015. Interaction of propofol with voltage-gated human Kv1.5 channel through specific amino acids within the pore region. *Eur. J. Pharmacol.* 764, 622–632. <https://doi.org/10.1016/j.ejphar.2015.08.007>
- Kole, M.H.P., Letzkus, J.J., Stuart, G.J., 2007. Axon Initial Segment Kv1 Channels Control Axonal Action Potential Waveform and Synaptic Efficacy. *Neuron* 55, 633–647. <https://doi.org/10.1016/j.neuron.2007.07.031>
- Kole, M.J., Qian, J., Waase, M.P., Klassen, T.L., Chen, T.T., Augustine, G.J., Noebels, J.L., 2015. Selective Loss of Presynaptic Potassium Channel Clusters at the Cerebellar Basket Cell Terminal Pinceau in Adam11 Mutants Reveals Their Role in Ephaptic Control of Purkinje Cell Firing. *J. Neurosci.* 35, 11433–11444. <https://doi.org/10.1523/JNEUROSCI.1346-15.2015>
- Kopp-Scheinflug, C., Tolnai, S., Malmierca, M.S., Rübtsamen, R., 2008. The medial nucleus of the trapezoid body: Comparative physiology. *Neuroscience, From Cochlea to Cortex: Recent Advances in Auditory Neuroscience* 154, 160–170. <https://doi.org/10.1016/j.neuroscience.2008.01.088>
- Kourrich, S., Hayashi, T., Chuang, J.-Y., Tsai, S.-Y., Su, T.-P., Bonci, A., 2013. Sigma-1R and Kv1.2: A Dynamic Interaction Shaping Neuronal and Behavioral Response to Cocaine. *Cell* 152, 236–247. <https://doi.org/10.1016/j.cell.2012.12.004>
- Kourrich, S., Su, T.-P., Fujimoto, M., Bonci, A., 2012. The sigma-1 receptor: roles in neuronal plasticity and disease. *Trends Neurosci.* 35, 762–771. <https://doi.org/10.1016/j.tins.2012.09.007>
- Kruse, M., Hille, B., 2013. The phosphoinositide sensitivity of the KV channel family. *Channels* 7, 530–536. <https://doi.org/10.4161/chan.25816>
- Kuang, Q., Purhonen, P., Hebert, H., 2015. Structure of potassium channels. *Cell. Mol. Life Sci. CMLS* 72, 3677–3693. <https://doi.org/10.1007/s00018-015-1948-5>
- Kullmann, D.M., Waxman, S.G., 2010. Neurological channelopathies: new insights into disease mechanisms and ion channel function. *J. Physiol.* 588, 1823–1827. <https://doi.org/10.1113/jphysiol.2010.190652>
- Kurata, H.T., Fedida, D., 2006. A structural interpretation of voltage-gated potassium channel inactivation. *Prog. Biophys. Mol. Biol.* 92, 185–208. <https://doi.org/10.1016/j.pbiomolbio.2005.10.001>
- Kwon, S.-H., Oh, S., Nacke, M., Mostov, K.E., Lipschutz, J.H., 2016. Adaptor Protein CD2AP and L-type Lectin LMAN2 Regulate Exosome Cargo Protein Trafficking through the Golgi Complex. *J. Biol. Chem.* 291, 25462–25475. <https://doi.org/10.1074/jbc.M116.729202>
- Labro, A.J., Raes, A.L., Bellens, I., Ottschytch, N., Snyders, D.J., 2003. Gating of Shaker-type Channels Requires the Flexibility of S6 Caused by Prolines. *J. Biol. Chem.* 278, 50724–50731. <https://doi.org/10.1074/jbc.M306097200>

- Labro, A.J., Snyders, D.J., 2012. Being Flexible: The Voltage-Controllable Activation Gate of Kv Channels. *Front. Pharmacol.* 3. <https://doi.org/10.3389/fphar.2012.00168>
- Lazniewska, J., Weiss, N., 2014. The “Sweet” Side of Ion Channels, in: Nilius, B., Gudermann, T., Jahn, R., Lill, R., Offermanns, S., Petersen, O.H. (Eds.), *Reviews of Physiology, Biochemistry and Pharmacology*, Vol. 167, *Reviews of Physiology, Biochemistry and Pharmacology*. Springer International Publishing, Cham, pp. 67–114. https://doi.org/10.1007/112_2014_20
- Li, M., Jan, Y., Jan, L., 1992. Specification of subunit assembly by the hydrophilic amino-terminal domain of the Shaker potassium channel. *Science* 257, 1225. <https://doi.org/10.1126/science.1519059>
- Li, Y., Xu, J., Xu, Y., Zhao, X.-Y., Liu, Y., Wang, J., Wang, G.-M., Lv, Y.-T., Tang, Q.-Y., Zhang, Z., 2018. Regulatory Effect of General Anesthetics on Activity of Potassium Channels. *Neurosci. Bull.* 34, 887–900. <https://doi.org/10.1007/s12264-018-0239-1>
- Liang, Q., Anderson, W.D., Jones, S.T., Souza, C.S., Hosoume, J.M., Treptow, W., Covarrubias, M., 2015. Positive Allosteric Modulation of Kv Channels by Sevoflurane: Insights into the Structural Basis of Inhaled Anesthetic Action. *PLoS ONE* 10. <https://doi.org/10.1371/journal.pone.0143363>
- Lioudyno, M.I., Birch, A.M., Tanaka, B.S., Sokolov, Y., Goldin, A.L., Chandy, K.G., Hall, J.E., Alkire, M.T., 2013. Shaker-Related Potassium Channels in the Central Medial Nucleus of the Thalamus Are Important Molecular Targets for Arousal Suppression by Volatile General Anesthetics. *J. Neurosci.* 33, 16310–16322. <https://doi.org/10.1523/JNEUROSCI.0344-13.2013>
- Liu, Y., Wang, P., Ma, F., Zheng, M., Liu, G., Kume, S., Kurokawa, T., Ono, K., 2019. Asparagine-linked glycosylation modifies voltage-dependent gating properties of CaV3.1-T-type Ca²⁺ channel. *J. Physiol. Sci.* 69, 335–343. <https://doi.org/10.1007/s12576-018-0650-4>
- Long, S.B., Campbell, E.B., MacKinnon, R., 2005a. Crystal Structure of a Mammalian Voltage-Dependent Shaker Family K⁺ Channel. *Science* 309, 897–903. <https://doi.org/10.1126/science.1116269>
- Long, S.B., Campbell, E.B., MacKinnon, R., 2005b. Voltage Sensor of Kv1.2: Structural Basis of Electromechanical Coupling. *Science* 309, 903–908. <https://doi.org/10.1126/science.1116270>
- Long, S.B., Tao, X., Campbell, E.B., MacKinnon, R., 2007. Atomic structure of a voltage-dependent K⁺ channel in a lipid membrane-like environment. *Nature* 450, 376–382. <https://doi.org/10.1038/nature06265>
- Lorincz, A., Nusser, Z., 2008. Cell-Type-Dependent Molecular Composition of the Axon Initial Segment. *J. Neurosci.* 28, 14329–14340. <https://doi.org/10.1523/JNEUROSCI.4833-08.2008>
- Lu, Z., Klem, A.M., Ramu, Y., 2002. Coupling between Voltage Sensors and Activation Gate in Voltage-gated K⁺ Channels. *J. Gen. Physiol.* 120, 663–676. <https://doi.org/10.1085/jgp.20028696>
- MacKinnon, R., 1991. Determination of the subunit stoichiometry of a voltage-activated potassium channel. *Nature* 350, 232–235. <https://doi.org/10.1038/350232a0>
- MacKinnon, R., Miller, C., 1989. Mutant potassium channels with altered binding of charybdotoxin, a pore-blocking peptide inhibitor. *Science* 245, 1382–1385. <https://doi.org/10.1126/science.2476850>
- MacKinnon, R., Miller, C., 1988. Mechanism of charybdotoxin block of the high-conductance, Ca²⁺-activated K⁺ channel. *J. Gen. Physiol.* 91, 335–349. <https://doi.org/10.1085/jgp.91.3.335>

- Majumder, K., Biasi, M.D., Wang, Z., Wible, B.A., 1995. Molecular cloning and functional expression of a novel potassium channel β -subunit from human atrium. *FEBS Lett.* 361, 13–16. [https://doi.org/10.1016/0014-5793\(95\)00120-X](https://doi.org/10.1016/0014-5793(95)00120-X)
- Masnada, S., Hedrich, U.B.S., Gardella, E., Schubert, J., Kaiwar, C., Klee, E.W., Lanpher, B.C., Gavrilova, R.H., Synofzik, M., Bast, T., Gorman, K., King, M.D., Allen, N.M., Conroy, J., Ben Zeev, B., Tzadok, M., Korff, C., Dubois, F., Ramsey, K., Narayanan, V., Serratos, J.M., Giraldez, B.G., Helbig, I., Marsh, E., O'Brien, M., Bergqvist, C.A., Binelli, A., Porter, B., Zaeyen, E., Horovitz, D.D., Wolff, M., Marjanovic, D., Caglayan, H.S., Arslan, M., Pena, S.D.J., Sisodiya, S.M., Balestrini, S., Syrbe, S., Veggiotti, P., Lemke, J.R., Møller, R.S., Lerche, H., Rubboli, G., 2017. Clinical spectrum and genotype–phenotype associations of KCNA2-related encephalopathies. *Brain* 140, 2337–2354. <https://doi.org/10.1093/brain/awx184>
- McCormack, T., McCormack, K., 1994. Shaker K⁺ channel beta subunits belong to an NAD(P)H-dependent oxidoreductase superfamily. *Cell* 79, 1133–1135. [https://doi.org/10.1016/0092-8674\(94\)90004-3](https://doi.org/10.1016/0092-8674(94)90004-3)
- McKay, B.E., Molineux, M.L., Mehaffey, W.H., Turner, R.W., 2005. Kv1 K⁺ Channels Control Purkinje Cell Output to Facilitate Postsynaptic Rebound Discharge in Deep Cerebellar Neurons. *J. Neurosci.* 25, 1481–1492. <https://doi.org/10.1523/JNEUROSCI.3523-04.2005>
- Metz, A.E., Spruston, N., Martina, M., 2007. Dendritic D-type potassium currents inhibit the spike afterdepolarization in rat hippocampal CA1 pyramidal neurons. *J. Physiol.* 581, 175–187. <https://doi.org/10.1113/jphysiol.2006.127068>
- Miller, C., 1995. The charybdotoxin family of K⁺ channel-blocking peptides. *Neuron* 15, 5–10. [https://doi.org/10.1016/0896-6273\(95\)90057-8](https://doi.org/10.1016/0896-6273(95)90057-8)
- Monaghan, M.M., Trimmer, J.S., Rhodes, K.J., 2001. Experimental Localization of Kv1 Family Voltage-Gated K⁺ Channel α and β Subunits in Rat Hippocampal Formation. *J. Neurosci.* 21, 5973–5983. <https://doi.org/10.1523/JNEUROSCI.21-16-05973.2001>
- Moremen, K.W., Tiemeyer, M., Nairn, A.V., 2012. Vertebrate protein glycosylation: diversity, synthesis and function. *Nat. Rev. Mol. Cell Biol.* 13, 448–462. <https://doi.org/10.1038/nrm3383>
- Mu, P., Moyer, J.T., Ishikawa, M., Zhang, Y., Panksepp, J., Sorg, B.A., Schlüter, O.M., Dong, Y., 2010. Exposure to Cocaine Dynamically Regulates the Intrinsic Membrane Excitability of Nucleus Accumbens Neurons. *J. Neurosci.* 30, 3689–3699. <https://doi.org/10.1523/JNEUROSCI.4063-09.2010>
- Nakahira, K., Shi, G., Rhodes, K.J., Trimmer, J.S., 1996. Selective Interaction of Voltage-gated K Channel α -Subunits with β -Subunits. *J. Biol. Chem.* 271, 7084–7089. <https://doi.org/10.1074/jbc.271.12.7084>
- Napp, J., Monje, F., Stühmer, W., Pardo, L.A., 2005. Glycosylation of Eag1 (Kv10.1) Potassium Channels INTRACELLULAR TRAFFICKING AND FUNCTIONAL CONSEQUENCES. *J. Biol. Chem.* 280, 29506–29512. <https://doi.org/10.1074/jbc.M504228200>
- Nerbonne, J.M., 2000. Molecular basis of functional voltage-gated K⁺ channel diversity in the mammalian myocardium. *J. Physiol.* 525, 285–298. <https://doi.org/10.1111/j.1469-7793.2000.t01-1-00285.x>
- Nesti, E., Everill, B., Morielli, A.D., 2004. Endocytosis as a Mechanism for Tyrosine Kinase-dependent Suppression of a Voltage-gated Potassium Channel. *Mol. Biol. Cell* 15, 4073–4088. <https://doi.org/10.1091/mbc.e03-11-0788>
- Nguyen, H.T., Li, K., daGraca, R.L., Delphin, E., Xiong, M., Ye, J.H., 2009. Behavior and Cellular Evidence for Propofol-induced Hypnosis Involving Brain Glycine Receptors. *Anesthesiol. J. Am. Soc. Anesthesiol.* 110, 326–332. <https://doi.org/10.1097/ALN.0b013e3181942b5b>

- Ogawa, Y., Horresh, I., Trimmer, J.S., Bredt, D.S., Peles, E., Rasband, M.N., 2008. Postsynaptic Density-93 Clusters Kv1 Channels at Axon Initial Segments Independently of Caspr2. *J. Neurosci.* 28, 5731–5739. <https://doi.org/10.1523/JNEUROSCI.4431-07.2008>
- Osteen, J.D., Barro-Soria, R., Robey, S., Sampson, K.J., Kass, R.S., Larsson, H.P., 2012. Allosteric gating mechanism underlies the flexible gating of KCNQ1 potassium channels. *Proc. Natl. Acad. Sci. U. S. A.* 109, 7103–7108. <https://doi.org/10.1073/pnas.1201582109>
- Ouyang, W., Wang, G., Hemmings, H.C., 2003. Isoflurane and Propofol Inhibit Voltage-Gated Sodium Channels in Isolated Rat Neurohypophysial Nerve Terminals. *Mol. Pharmacol.* 64, 373–381. <https://doi.org/10.1124/mol.64.2.373>
- Park, H.-J., Min, S.-H., Won, Y.-J., Lee, J.-H., 2015. Asn-Linked Glycosylation Contributes to Surface Expression and Voltage-Dependent Gating of Cav1.2 Ca²⁺ Channel. *J. Microbiol. Biotechnol.* 25, 1371–1379. <https://doi.org/10.4014/jmb.1501.01066>
- Pena, S.D.J., Coimbra, R.L.M., 2015. Ataxia and myoclonic epilepsy due to a heterozygous new mutation in *KCNA2*: proposal for a new channelopathy: Ataxia and myoclonic epilepsy due to a heterozygous new mutation. *Clin. Genet.* 87, e1–e3. <https://doi.org/10.1111/cge.12542>
- Peters, C.J., Vaid, M., Horne, A.J., Fedida, D., Accili, E.A., 2009. The molecular basis for the actions of KVbeta1.2 on the opening and closing of the KV1.2 delayed rectifier channel. *Channels Austin Tex* 3, 314–322. <https://doi.org/10.4161/chan.3.5.9558>
- Petrecca, K., Atanasiu, R., Akhavan, A., Shrier, A., 1999. N-linked glycosylation sites determine HERG channel surface membrane expression. *J. Physiol.* 515, 41–48. <https://doi.org/10.1111/j.1469-7793.1999.041ad.x>
- Plane, F., Johnson Rosalyn, Kerr Paul, Wiehler William, Thorneloe Kevin, Ishii Kuniaki, Chen Tim, Cole William, 2005. Heteromultimeric Kv1 Channels Contribute to Myogenic Control of Arterial Diameter. *Circ. Res.* 96, 216–224. <https://doi.org/10.1161/01.RES.0000154070.06421.25>
- Poliak, S., Salomon, D., Elhanany, H., Sabanay, H., Kiernan, B., Pevny, L., Stewart, C.L., Xu, X., Chiu, S.-Y., Shrager, P., Furley, A.J.W., Peles, E., 2003. Juxtaparanodal clustering of Shaker-like K⁺ channels in myelinated axons depends on Caspr2 and TAG-1. *J. Cell Biol.* 162, 1149–1160. <https://doi.org/10.1083/jcb.200305018>
- Poling, J.S., Rogawski, M.A., Salem, N., Vicini, S., 1996. Anandamide, an Endogenous Cannabinoid, Inhibits Shaker-related Voltage-gated K⁺ Channels. *Neuropharmacology* 35, 983–991. [https://doi.org/10.1016/0028-3908\(96\)00130-X](https://doi.org/10.1016/0028-3908(96)00130-X)
- Pongs, O., Schwarz, J.R., 2010. Ancillary Subunits Associated With Voltage-Dependent K⁺ Channels. *Physiol. Rev.* 90, 755–796. <https://doi.org/10.1152/physrev.00020.2009>
- Ranjan, R., Logette, E., Marani, M., Herzog, M., Tâche, V., Scantamburlo, E., Buchillier, V., Markram, H., 2019. A Kinetic Map of the Homomeric Voltage-Gated Potassium Channel (Kv) Family. *Front. Cell. Neurosci.* 13, 358. <https://doi.org/10.3389/fncel.2019.00358>
- Rasband, M.N., Park, E.W., Vanderah, T.W., Lai, J., Porreca, F., Trimmer, J.S., 2001. Distinct potassium channels on pain-sensing neurons. *Proc. Natl. Acad. Sci. U. S. A.* 98, 13373–13378. <https://doi.org/10.1073/pnas.231376298>
- Rasmusson, R.L., Morales Michael J., Wang Shimin, Liu Shuguang, Campbell Donald L., Brahmajothi Mulugu V., Strauss Harold C., 1998. Inactivation of Voltage-Gated Cardiac K⁺ Channels. *Circ. Res.* 82, 739–750. <https://doi.org/10.1161/01.RES.82.7.739>
- Reily, C., Stewart, T.J., Renfrow, M.B., Novak, J., 2019. Glycosylation in health and disease. *Nat. Rev. Nephrol.* 15, 346–366. <https://doi.org/10.1038/s41581-019-0129-4>
- Rettig, J., Heinemann, S.H., Wunder, F., Lorra, C., Parcej, D.N., Dolly, J.O., Pongs, O., 1994. Inactivation properties of voltage-gated K⁺ channels altered by presence of β -subunit. *Nature* 369, 289–294. <https://doi.org/10.1038/369289a0>

- Rettig, J., Wunder, F., Stocker, M., Lichtinghagen, R., Mastiaux, F., Beckh, S., Kues, W., Pedarzani, P., Schröter, K. h., Ruppertsberg, J. p., 1992. Characterization of a Shaw-related potassium channel family in rat brain. *EMBO J.* 11, 2473–2486. <https://doi.org/10.1002/j.1460-2075.1992.tb05312.x>
- Rezazadeh, S., Kurata, H.T., Claydon, T.W., Kehl, S.J., Fedida, D., 2007. An Activation Gating Switch in Kv1.2 Is Localized to a Threonine Residue in the S2-S3 Linker. *Biophys. J.* 93, 4173–4186. <https://doi.org/10.1529/biophysj.107.116160>
- Rhodes, K.J., Keilbaugh, S.A., Barrezueta, N.X., Lopez, K.L., Trimmer, J.S., 1995. Association and colocalization of K⁺ channel alpha- and beta-subunit polypeptides in rat brain. *J. Neurosci.* 15, 5360–5371. <https://doi.org/10.1523/JNEUROSCI.15-07-05360.1995>
- Robbins, C.A., Tempel, B.L., 2012. Kv1.1 and Kv1.2: Similar channels, different seizure models. *Epilepsia* 53, 134–141. <https://doi.org/10.1111/j.1528-1167.2012.03484.x>
- Roberds, S.L., Tamkun, M.M., 1991. Cloning and tissue-specific expression of five voltage-gated potassium channel cDNAs expressed in rat heart. *Proc. Natl. Acad. Sci. U. S. A.* 88, 1798–1802.
- Robertson, B., 1996. Novel effects of dendrotoxin homologues on subtypes of mammalian Kvl potassium channels expressed in *Xenopus* oocytes. *FEBS Lett.* 5.
- Rodriguez-Menchaca, A.A., Adney, S.K., Tang, Q.-Y., Meng, X.-Y., Rosenhouse-Dantsker, A., Cui, M., Logothetis, D.E., 2012. PIP2 controls voltage-sensor movement and pore opening of Kv channels through the S4–S5 linker. *Proc. Natl. Acad. Sci.* 109, E2399–E2408. <https://doi.org/10.1073/pnas.1207901109>
- Rodríguez de la Vega, R.C., Merino, E., Becerril, B., Possani, L.D., 2003. Novel interactions between K⁺ channels and scorpion toxins. *Trends Pharmacol. Sci.* 24, 222–227. [https://doi.org/10.1016/S0165-6147\(03\)00080-4](https://doi.org/10.1016/S0165-6147(03)00080-4)
- Rudolph, U., Antkowiak, B., 2004. Molecular and neuronal substrates for general anaesthetics. *trapan* 5, 709–720. <https://doi.org/10.1038/nrn1496>
- Russell, S.N., Publicover, N.G., Hart, P.J., Carl, A., Hume, J.R., Sanders, K.M., Horowitz, B., 1994. Block by 4-aminopyridine of a Kv1.2 delayed rectifier K⁺ current expressed in *Xenopus* oocytes. *J. Physiol.* 481, 571–584.
- Sall, J.W., Stratmann, G., Leong, J., Woodward, E., Bickler, P.E., 2012. Propofol at Clinically Relevant Concentrations Increases Neuronal Differentiation But Is Not Toxic to Hippocampal Neural Precursor Cells In Vitro. *Anesthesiol. J. Am. Soc. Anesthesiol.* 117, 1080–1090. <https://doi.org/10.1097/ALN.0b013e31826f8d86>
- Sands, Z., Grottesi, A., Sansom, M.S.P., 2005. Voltage-gated ion channels. *Curr. Biol.* 15, R44–R47. <https://doi.org/10.1016/j.cub.2004.12.050>
- Schwalbe, R.A., Corey, M.J., Cartwright, T.A., 2008. Novel Kv3 glycoforms differentially expressed in adult mammalian brain contain sialylated N-glycans. *Biochem. Cell Biol.* 86, 21–30. <https://doi.org/10.1139/O07-152>
- Schwetz, T.A., Norring, S.A., Ednie, A.R., Bennett, E.S., 2011. Sialic Acids Attached to O-Glycans Modulate Voltage-gated Potassium Channel Gating. *J. Biol. Chem.* 286, 4123–4132. <https://doi.org/10.1074/jbc.M110.171322>
- Scott, H., Panin, V.M., 2014. The role of protein N-glycosylation in neural transmission. *Glycobiology* 24, 407–417. <https://doi.org/10.1093/glycob/cwu015>
- Scott, V.E., Parcej, D.N., Keen, J.N., Findlay, J.B., Dolly, J.O., 1990. Alpha-dendrotoxin acceptor from bovine brain is a K⁺ channel protein. Evidence from the N-terminal sequence of its larger subunit. *J. Biol. Chem.* 265, 20094–20097.
- Segal, J.L., Pathak, M.S., Hernandez, J.P., Hember, P.L., Brunneemann, S.R., Charter, R.S., 1999. Safety and Efficacy of 4-Aminopyridine in Humans with Spinal Cord Injury: A Long-Term, Controlled Trial. *Pharmacother. J. Hum. Pharmacol. Drug Ther.* 19, 713–723. <https://doi.org/10.1592/phco.19.9.713.31540>

- Shamotienko, O.G., Parcej, D.N., Dolly, J.O., 1997. Subunit Combinations Defined for K⁺ Channel Kv1 Subtypes in Synaptic Membranes from Bovine Brain. *Biochemistry* 36, 8195–8201. <https://doi.org/10.1021/bi970237g>
- Sharmin, N., Lamothe, S.M., Baronas, V.A., Silver, G., Hao, Y., Kurata, H.T., 2020. Control of Slc7a5 sensitivity by the voltage-sensing domain of Kv1 channels. *bioRxiv* 2020.01.17.910059. <https://doi.org/10.1101/2020.01.17.910059>
- Shen, N.V., Pfaffinger, P.J., 1995. Molecular recognition and assembly sequences involved in the subfamily-specific assembly of voltage-gated K⁺ channel subunit proteins. *Neuron* 14, 625–633. [https://doi.org/10.1016/0896-6273\(95\)90319-4](https://doi.org/10.1016/0896-6273(95)90319-4)
- Shen, V.N., Chen, X., Boyer, M.M., Pfaffinger, P.J., 1993. Deletion analysis of K⁺ channel assembly. *Neuron* 11, 67–76. [https://doi.org/10.1016/0896-6273\(93\)90271-R](https://doi.org/10.1016/0896-6273(93)90271-R)
- Sheng, M., Jan, Y.N., Jan, L., 1995. Chapter 8 The molecular organization of voltage-dependent K⁺ channels in vivo, in: Yu, A.C.H., Eng, L.F., McMahan, U.J., Schulman, H., Shooter, E.M., Stadlin, A. (Eds.), *Progress in Brain Research*. Elsevier, pp. 87–93. [https://doi.org/10.1016/S0079-6123\(08\)63286-0](https://doi.org/10.1016/S0079-6123(08)63286-0)
- Sheng, M., Tsaur, M., Jan, Y., Jan, L., 1994. Contrasting subcellular localization of the Kv1.2 K⁺ channel subunit in different neurons of rat brain. *J. Neurosci.* 14, 2408–2417. <https://doi.org/10.1523/JNEUROSCI.14-04-02408.1994>
- Shi, G., Nakahira, K., Hammond, S., Rhodes, K.J., Schechter, L.E., Trimmer, J.S., 1996. β Subunits Promote K⁺ Channel Surface Expression through Effects Early in Biosynthesis. *Neuron* 16, 843–852. [https://doi.org/10.1016/S0896-6273\(00\)80104-X](https://doi.org/10.1016/S0896-6273(00)80104-X)
- Shi, G., Trimmer, J.S., 1999. Differential Asparagine-Linked Glycosylation of Voltage-Gated K⁺ Channels in Mammalian Brain and in Transfected Cells. *J. Membr. Biol.* 168, 265–273. <https://doi.org/10.1007/s002329900515>
- Shu, Y., Yu, Y., Yang, J., McCormick, D.A., 2007. Selective control of cortical axonal spikes by a slowly inactivating K⁺ current. *Proc. Natl. Acad. Sci.* 104, 11453–11458. <https://doi.org/10.1073/pnas.0702041104>
- Smith, K.E., Browne, L., Selwood, D.L., McAlpine, D., Jagger, D.J., 2015. Phosphoinositide Modulation of Heteromeric Kv1 Channels Adjusts Output of Spiral Ganglion Neurons from Hearing Mice. *J. Neurosci.* 35, 11221–11232. <https://doi.org/10.1523/JNEUROSCI.0496-15.2015>
- Southan, A.P., Robertson, B., 1998. Patch-Clamp Recordings from Cerebellar Basket Cell Bodies and Their Presynaptic Terminals Reveal an Asymmetric Distribution of Voltage-Gated Potassium Channels. *J. Neurosci.* 18, 948–955. <https://doi.org/10.1523/JNEUROSCI.18-03-00948.1998>
- Spiro, R.G., 2002. Protein glycosylation: nature, distribution, enzymatic formation, and disease implications of glycopeptide bonds. *Glycobiology* 12, 43R–56R. <https://doi.org/10.1093/glycob/12.4.43R>
- Sprunger, L.K., Stewig, N.J., O'Grady, S.M., 1996. Effects of charybdotoxin on K⁺ channel (Kv1.2) deactivation and inactivation kinetics. *Eur. J. Pharmacol.* 314, 357–364. [https://doi.org/10.1016/S0014-2999\(96\)00556-0](https://doi.org/10.1016/S0014-2999(96)00556-0)
- Stirling, L., Williams, M.R., Morielli, A.D., 2009. Dual Roles for RHOA/RHO-Kinase In the Regulated Trafficking of a Voltage-sensitive Potassium Channel. *Mol. Biol. Cell* 20, 2991–3002. <https://doi.org/10.1091/mbc.E08-10-1074>
- Stühmer, W., Ruppersberg, J.P., Schröter, K.H., Sakmann, B., Stocker, M., Giese, K.P., Perschke, A., Baumann, A., Pongs, O., 1989. Molecular basis of functional diversity of voltage-gated potassium channels in mammalian brain. *EMBO J.* 8, 3235–3244.
- Su, T.-P., Hayashi, T., Maurice, T., Buch, S., Ruoho, A.E., 2010. The sigma-1 receptor chaperone as an inter-organellar signaling modulator. *Trends Pharmacol. Sci.* 31, 557–566. <https://doi.org/10.1016/j.tips.2010.08.007>

- Swanson, R., Marshall, J., Smith, J.S., Williams, J.B., Boyle, M.B., Folander, K., Luneau, C.J., Antanavage, J., Oliva, C., Buhrow, S.A., Bennet, C., Stein, R.B., Kaczmarek, L.K., 1990. Cloning and expression of cDNA and genomic clones encoding three delayed rectifier potassium channels in rat brain. *Neuron* 4, 929–939. [https://doi.org/10.1016/0896-6273\(90\)90146-7](https://doi.org/10.1016/0896-6273(90)90146-7)
- Swartz, K.J., 2008. Sensing voltage across lipid membranes. *Nature* 456, 891–897. <https://doi.org/10.1038/nature07620>
- Syrbe, S., Hedrich, U.B.S., Riesch, E., Djémié, T., Müller, S., Møller, R.S., Maher, B., Hernandez-Hernandez, L., Synofzik, M., Caglayan, H.S., Arslan, M., Serratosa, J.M., Nothnagel, M., May, P., Krause, R., Löffler, H., Detert, K., Dorn, T., Vogt, H., Krämer, G., Schöls, L., Mullis, P.E., Linnankivi, T., Lehesjoki, A.-E., Sterbova, K., Craiu, D.C., Hoffman-Zacharska, D., Korff, C.M., Weber, Y.G., Steinlin, M., Gallati, S., Bertsche, A., Bernhard, M.K., Merckenschlager, A., Kiess, W., Balling, R., Barisic, N., Baulac, S., Caglayan, H.S., Craiu, D.C., De Jonghe, P., Depienne, C., Gormley, P., Guerrini, R., Helbig, I., Hjalgrim, H., Hoffman-Zacharska, D., Jähn, J., Klein, K.M., Koeleman, B.P.C., Komarek, V., Krause, R., LeGuern, E., Lehesjoki, A.-E., Lemke, J.R., Lerche, H., Marini, C., May, P., Møller, R.S., Muhle, H., Palotie, A., Pal, D., Rosenow, F., Selmer, K., Serratosa, J.M., Sisodiya, S.M., Stephani, U., Sterbova, K., Striano, P., Suls, A., Talvik, T., von Spiczak, S., G Weber, Y., Weckhuysen, S., Zara, F., Gonzalez, M., Züchner, S., Palotie, A., Suls, A., De Jonghe, P., Helbig, I., Biskup, S., Wolff, M., Maljevic, S., Schüle, R., Sisodiya, S.M., Weckhuysen, S., Lerche, H., Lemke, J.R., EuroEPINOMICS RES, 2015. De novo loss- or gain-of-function mutations in KCNA2 cause epileptic encephalopathy. *Nat. Genet.* 47, 393–399. <https://doi.org/10.1038/ng.3239>
- Tärlungeanu, D.C., Deliu, E., Dotter, C.P., Kara, M., Janiesch, P.C., Scalise, M., Galluccio, M., Tesulov, M., Morelli, E., Sonmez, F.M., Bilguvar, K., Ohgaki, R., Kanai, Y., Johansen, A., Esharif, S., Ben-Omran, T., Topcu, M., Schlessinger, A., Indiveri, C., Duncan, K.E., Caglayan, A.O., Gunel, M., Gleeson, J.G., Novarino, G., 2016. Impaired Amino Acid Transport at the Blood Brain Barrier Is a Cause of Autism Spectrum Disorder. *Cell* 167, 1481–1494.e18. <https://doi.org/10.1016/j.cell.2016.11.013>
- Thayer, D.A., Yang, S., Jan, Y.N., Jan, L.Y., 2016. N-linked glycosylation of Kv1.2 voltage-gated potassium channel facilitates cell surface expression and enhances the stability of internalized channels. *J. Physiol.* 594, 6701–6713. <https://doi.org/10.1113/JP272394>
- Tipparaaju, S.M., Liu, S.-Q., Barski, O., Bhatnagar, A., 2007. NADPH Binding to β -Subunit Regulates Inactivation of Voltage-Gated K⁺ Channels. *Biochem. Biophys. Res. Commun.* 359, 269–276. <https://doi.org/10.1016/j.bbrc.2007.05.102>
- Torres, Y.P., Morera, F.J., Carvacho, I., Latorre, R., 2007. A Marriage of Convenience: β -Subunits and Voltage-dependent K⁺ Channels. *J. Biol. Chem.* 282, 24485–24489. <https://doi.org/10.1074/jbc.R700022200>
- Traka, M., Goutebroze, L., Denisenko, N., Bessa, M., Nifli, A., Havaki, S., Iwakura, Y., Fukamauchi, F., Watanabe, K., Soliven, B., Girault, J.-A., Karagogeos, D., 2003. Association of TAG-1 with Caspr2 is essential for the molecular organization of juxtaparanodal regions of myelinated fibers. *J. Cell Biol.* 162, 1161–1172. <https://doi.org/10.1083/jcb.200305078>
- Trapani, G.M., Altomare, C., Sanna, E., Liso, G.B. and G., 2000. Propofol in Anesthesia. Mechanism of Action, Structure-Activity Relationships, and Drug Delivery [WWW Document]. *Curr. Med. Chem.* URL <http://www.eurekaselect.com/65739/article> (accessed 5.11.20).
- Tsuchiya, H., Mizogami, M., 2013. Interaction of Local Anesthetics with Biomembranes Consisting of Phospholipids and Cholesterol: Mechanistic and Clinical Implications for Anesthetic and Cardiotoxic Effects [WWW Document]. *Anesthesiol. Res. Pract.* <https://doi.org/10.1155/2013/297141>

- Tyrrell, L., Renganathan, M., Dib-Hajj, S.D., Waxman, S.G., 2001. Glycosylation Alters Steady-State Inactivation of Sodium Channel Nav1.9/NaN in Dorsal Root Ganglion Neurons and Is Developmentally Regulated. *J. Neurosci.* 21, 9629–9637. <https://doi.org/10.1523/JNEUROSCI.21-24-09629.2001>
- Tytgat, J., Debont, T., Carmeliet, E., Daenens, P., 1995. The α -Dendrotoxin Footprint on a Mammalian Potassium Channel. *J. Biol. Chem.* 270, 24776–24781. <https://doi.org/10.1074/jbc.270.42.24776>
- Urban, B.W., 2002. Current assessment of targets and theories of anaesthesia. *Br. J. Anaesth.* 89, 167–183. <https://doi.org/10.1093/bja/aef165>
- Vallon, V., Grahammer, F., Volkl, H., Sandu, C.D., Richter, K., Rexhepaj, R., Gerlach, U., Rong, Q., Pfeifer, K., Lang, F., 2005. KCNQ1-dependent transport in renal and gastrointestinal epithelia. *Proc. Natl. Acad. Sci. U. S. A.* 102, 17864–17869. <https://doi.org/10.1073/pnas.0505860102>
- Vardanyan, V., Pongs, O., 2012. Coupling of Voltage-Sensors to the Channel Pore: A Comparative View. *Front. Pharmacol.* 3. <https://doi.org/10.3389/fphar.2012.00145>
- Vargas, E., Bezanilla, F., Roux, B., 2011. In search of a consensus model of the resting state of a voltage-sensing domain. *Neuron* 72, 713–720. <https://doi.org/10.1016/j.neuron.2011.09.024>
- Visan, V., Fajloun, Z., Sabatier, J.-M., Grissmer, S., 2004. Mapping of Maurotoxin Binding Sites on hKv1.2, hKv1.3, and hKCa1 Channels. *Mol. Pharmacol.* 66, 1103–1112. <https://doi.org/10.1124/mol.104.002774>
- Wang, F.C., Parcej, D.N., Dolly, J.O., 1999. α Subunit compositions of Kv1.1-containing K⁺ channel subtypes fractionated from rat brain using dendrotoxins. *Eur. J. Biochem.* 263, 230–237. <https://doi.org/10.1046/j.1432-1327.1999.00493.x>
- Wang, H., Kunkel, D.D., Martin, T.M., Schwartzkroin, P.A., Tempel, B.L., 1993. Heteromultimeric K⁺ channels in terminal and juxtaparanodal regions of neurons. *Nature* 365, 75–79. <https://doi.org/10.1038/365075a0>
- Wang, H., Kunkel, D.D., Schwartzkroin, P.A., Tempel, B.L., 1994. Localization of Kv1.1 and Kv1.2, two K channel proteins, to synaptic terminals, somata, and dendrites in the mouse brain. *J. Neurosci. Off. J. Soc. Neurosci.* 14, 4588–4599. <https://doi.org/10.1523/JNEUROSCI.14-08-04588.1994>
- Watanabe, I., Wang, H.-G., Sutachan, J.J., Zhu, J., Recio-Pinto, E., Thornhill, W.B., 2003. Glycosylation Affects Rat Kv1.1 Potassium Channel Gating by a Combined Surface Potential and Cooperative Subunit Interaction Mechanism. *J. Physiol.* 550, 51–66. <https://doi.org/10.1113/jphysiol.2003.040337>
- Watanabe, I., Zhu, J., Recio-Pinto, E., Thornhill, W.B., 2015. The degree of N-glycosylation affects the trafficking and cell surface expression levels of Kv1.4 potassium channels. *J. Membr. Biol.* 248, 187–196. <https://doi.org/10.1007/s00232-014-9756-7>
- Watanabe, I., Zhu, J., Sutachan, J.J., Gottschalk, A., Recio-Pinto, E., Thornhill, W.B., 2007. The glycosylation state of Kv1.2 potassium channels affects trafficking, gating, and simulated action potentials. *Brain Res.* 1144, 1–18. <https://doi.org/10.1016/j.brainres.2007.01.092>
- Weng, J., Cao, Y., Moss, N., Zhou, M., 2006. Modulation of voltage-dependent Shaker family potassium channels by an aldo-keto reductase. *J. Biol. Chem.* 281, 15194–15200. <https://doi.org/10.1074/jbc.M513809200>
- Werkman, T.R., Gustafson, T.A., Rogowski, R.S., Blaustein, M.P., Rogawski, M.A., 1993. Tityustoxin-K alpha, a structurally novel and highly potent K⁺ channel peptide toxin, interacts with the alpha-dendrotoxin binding site on the cloned Kv1.2 K⁺ channel. *Mol. Pharmacol.* 44, 430–436.
- Werkman, T.R., Kawamura, T., Yokoyama, S., Higashida, H., Rogawski, M.A., 1992. Charybdotoxin, dendrotoxin and mast cell degranulating peptide block the voltage-activated K⁺ current of fibroblast cells stably transfected with NGK1 (Kv1.2) K⁺ channel

- complementary DNA. *Neuroscience* 50, 935–946. [https://doi.org/10.1016/0306-4522\(92\)90216-O](https://doi.org/10.1016/0306-4522(92)90216-O)
- Westhoff, M., Eldstrom, J., Murray, C.I., Thompson, E., Fedida, D., 2019. IKs ion-channel pore conductance can result from individual voltage sensor movements. *Proc. Natl. Acad. Sci.* 116, 7879–7888. <https://doi.org/10.1073/pnas.1811623116>
- Willis, M., Leitner, I., Seppi, K., Trieb, M., Wietzorrek, G., Marksteiner, J., Knaus, H.-G., 2018. Shaker-related voltage-gated potassium channels Kv1 in human hippocampus. *Brain Struct. Funct.* 223, 2663–2671. <https://doi.org/10.1007/s00429-018-1653-x>
- Wilson, A.J., 2009. Inhibition of protein–protein interactions using designed molecules. *Chem. Soc. Rev.* 38, 3289–3300. <https://doi.org/10.1039/B807197G>
- Woll, K.A., Peng, W., Liang, Q., Zhi, L., Jacobs, J.A., Maciunas, L., Bhanu, N., Garcia, B.A., Covarrubias, M., Loll, P.J., Dailey, W.P., Eckenhoff, R.G., 2017. Photoaffinity Ligand for the Inhalational Anesthetic Sevoflurane Allows Mechanistic Insight into Potassium Channel Modulation. *ACS Chem. Biol.* 12, 1353–1362. <https://doi.org/10.1021/acscchembio.7b00222>
- Wulff, H., Castle, N.A., Pardo, L.A., 2009. Voltage-gated Potassium Channels as Therapeutic Drug Targets. *Nat. Rev. Drug Discov.* 8, 982–1001. <https://doi.org/10.1038/nrd2983>
- Yamagishi, T., Ishii, K., Taira, N., 1995. Antiarrhythmic and bradycardic drugs inhibit currents of cloned K⁺ channels, KV1.2 and KV1.4. *Eur. J. Pharmacol.* 281, 151–159. [https://doi.org/10.1016/0014-2999\(95\)00240-L](https://doi.org/10.1016/0014-2999(95)00240-L)
- Yang, J., H, V., Ks, P., E, C., Js, T., 2007. Trafficking-dependent phosphorylation of Kv1.2 regulates voltage-gated potassium channel cell surface expression. *Proc. Natl. Acad. Sci. U. S. A.* 104, 20055–20060. <https://doi.org/10.1073/pnas.0708574104>
- Yang, L., Liu, H., Sun, H.-Y., Li, G.-R., 2015. Intravenous Anesthetic Propofol Inhibits Multiple Human Cardiac Potassium Channels. *Anesthesiol. J. Am. Soc. Anesthesiol.* 122, 571–584. <https://doi.org/10.1097/ALN.0000000000000495>
- Yarov-Yarovoy, V., Baker, D., Catterall, W.A., 2006. Voltage sensor conformations in the open and closed states in rosetta structural models of K⁺ channels. *Proc. Natl. Acad. Sci. U. S. A.* 103, 7292–7297. <https://doi.org/10.1073/pnas.0602350103>
- Yellen, G., 1998. The moving parts of voltage-gated ion channels. *Q. Rev. Biophys.* 31, 239–295. <https://doi.org/10.1017/S0033583598003448>
- Ying, S.-W., Abbas, S.Y., Harrison, N.L., Goldstein, P.A., 2006. Propofol block of Ih contributes to the suppression of neuronal excitability and rhythmic burst firing in thalamocortical neurons. *Eur. J. Neurosci.* 23, 465–480. <https://doi.org/10.1111/j.1460-9568.2005.04587.x>
- Yuan, X.-J., Wang, J., Juhaszova, M., Golovina, V.A., Rubin, L.J., 1998. Molecular basis and function of voltage-gated K⁺ channels in pulmonary arterial smooth muscle cells. *Am. J. Physiol.-Lung Cell. Mol. Physiol.* 274, L621–L635. <https://doi.org/10.1152/ajplung.1998.274.4.L621>
- Zagotta, W., Hoshi, T., Aldrich, R., 1990. Restoration of inactivation in mutants of Shaker potassium channels by a peptide derived from ShB. *Science* 250, 568–571. <https://doi.org/10.1126/science.2122520>
- Zhang, Y., Hartmann, H.A., Satin, J., 1999. Glycosylation Influences Voltage-Dependent Gating of Cardiac and Skeletal Muscle Sodium Channels. *J. Membr. Biol.* 171, 195–207. <https://doi.org/10.1007/s002329900571>
- Zhao, J.-Y., Liang, L., Gu, X., Li, Z., Wu, S., Sun, L., Atianjoh, F.E., Feng, J., Mo, K., Jia, S., Lutz, B.M., Bekker, A., Nestler, E.J., Tao, Y.-X., 2017. DNA methyltransferase DNMT3a contributes to neuropathic pain by repressing Kcna2 in primary afferent neurons. *Nat. Commun.* 8. <https://doi.org/10.1038/ncomms14712>
- Zhao, X., Tang, Z., Zhang, H., Atianjoh, F.E., Zhao, J.-Y., Liang, L., Wang, W., Guan, X., Kao, S.-C., Tiwari, V., Gao, Y.-J., Hoffman, P.N., Cui, H., Li, M., Dong, X., Tao, Y.-X., 2013. A

long noncoding RNA contributes to neuropathic pain by silencing *Kcna2* in primary afferent neurons. *Nat. Neurosci.* 16, 1024–1031. <https://doi.org/10.1038/nn.3438>

Zhou, Y., Morais-Cabral, J.H., Kaufman, A., MacKinnon, R., 2001. Chemistry of ion coordination and hydration revealed by a K⁺ channel–Fab complex at 2.0 Å resolution. *Nature* 414, 43–48. <https://doi.org/10.1038/35102009>

Zhu, J., Recio-Pinto, E., Hartwig, T., Sellers, W., Yan, J., Thornhill, W.B., 2009. The Kv1.2 potassium channel: The position of an N-glycan on the extracellular linkers affects its protein expression and function. *Brain Res.* 1251, 16–29. <https://doi.org/10.1016/j.brainres.2008.11.033>